The Pennsylvania State University

The Graduate School

Department of Kinesiology

INFLUENCE OF THE FOOT ON ANKLE JOINT FUNCTION DURING RUNNING

A Dissertation in

Kinesiology

by

Justin C. Wager

Submitted in Partial Fulfillment
of the Requirements
for the Degree of

Doctor of Philosophy

August 2019

The dissertation of Justin C. Wager was reviewed and approved* by the following:

John H. Challis
Professor of Kinesiology
Dissertation Advisor
Chair of Committee

Jonas Rubenson
Associate Professor of Kinesiology

H.J. Sommer III
Professor of Mechanical and Nuclear Engineering

Robert B. Eckhardt
Professor of Developmental Genetics and Evolutionary Morphology

Stephen J. Piazza
Professor of Kinesiology, Mechanical Engineering, and Orthopaedics & Rehabilitation
Kinesiology Graduate Program Director

*Signatures are on file in the Graduate School

ABSTRACT

The human foot is a complex structure comprising bones and soft tissues which collectively exhibit substantial mobility. However, biomechanical analyses typically model the foot as a single rigid segment, which omits this mobility and its potential effects on surrounding muscles and joints. Recent studies have utilized multisegment foot models, which represent the foot using a system of linked rigid segments. Utilizing these models to analyze walking has shown that ankle joint kinematics and power during push-off differ from those found with traditional single segment foot models. However, multisegment foot models have yet to be used to study ankle joint function during running. In addition, omitting foot mobility from biomechanical models prohibits the study of the interactions between the mobility of the foot and the adjacent joints and tissues. These interactions may arise due to muscles and soft tissues that span both the joints of the foot and the ankle, but there is little work investigating whether these interactions are important to locomotion mechanics. The purpose of the three studies in this dissertation were to 1) compare ankle joint kinematics and kinetics computed using a multisegment foot model and a single segment foot model, 2) determine if foot model topology affects models of the ankle plantarflexor muscles by comparing results of simulations using the multisegment and single segment foot models, and 3) explore the interactions between the metatarsophalangeal and ankle plantarflexor muscles to better understand how foot mobility can influence locomotion mechanics. In Study 1, a multisegment foot model and a single segment foot model were used to compute ankle joint kinematics and kinetics of seven subjects during running. Similar to previous studies on walking, the multisegment foot model produced lower ankle joint excursion over the stance phase and reduced angular velocity and joint power during push-off. In Study 2, the kinematics and kinetics of the two foot models were used to drive simulations of two Hill-type muscle models representing the gastrocnemius and soleus. The

reduced ankle joint motion of the multisegment foot model led to decreases in the active state of the two muscles. Combined, Study 1 and Study 2 illustrate that foot model topology plays an important role in the study of ankle joint function during running, affecting both rigid body analyses and muscle simulations. Study 3 sought to understand the effect of the MTP joint position on the moment-generating capacities of the ankle plantarflexor muscles. Eight subjects generated maximum isometric ankle plantarflexions with the MTP joint held in two positions: neutral and maximally dorsiflexed. These two positions potentially changed the length of the extrinsic toe flexor muscles and the length of the plantar aponeurosis, which may alter the length of the triceps surae MTU. No statistically or functionally significant effect of the MTP joint position on the maximum isometric ankle moment was found. This suggests that the connections between the MTP joint and the Achilles tendon do not influence the moment-generating capacities of the ankle plantarflexors and instead may serve other functions during locomotion. Together, the three studies of the dissertation illustrate the importance of capturing the motion of the foot in kinematic and kinetic analyses of the lower limb and its musculature, but suggest that ankle plantarflexor strength is not influenced by the connections between the foot and the ankle. Future work should focus on further understanding the interactions between the foot and ankle by utilizing multisegment foot models to investigate tasks with various mechanical demands.

TABLE OF CONTENTS

LIST OF FIGURES

LIST OF TABLES

ACKNOWLEDGEMENTS

Thank you to the many people who provided me with guidance, support, and advice during the completion of this dissertation. To the committee members, I am grateful for your efforts in advising and challenging me. To John, thank you for the invaluable feedback and mentorship you've provided since my first day on campus. To the faculty of the Department of Kinesiology and the Department of Mechanical and Nuclear Engineering, thank you for the instructive coursework and advice. Particularly, to the faculty and postdocs of the Biomechanics Lab, thank you for serving as daily role models and showing me how to be a good scientist. To my fellow Biomechanics Lab graduate students, both past and current, thank you for enriching my time in the lab with both productive and unproductive conversation. Finally, thank you to my family: to my parents for always supporting my education, and to my wife, Ashley, for her many years of support and patience as I worked to put this dissertation together.

Chapter 1

Introduction

1.1 Background & Motivation

As the foot lands and supports the weight of the body during locomotion, energy is absorbed, returned, dissipated, and transferred through movement of the foot bones and deformation of the foot's soft tissues (Ker, 1996; Ker et al., 1987; McDonald et al., 2016; Pain and Challis, 2001; Wager and Challis, 2016). Additionally, the muscles of the arch of the foot become active when the foot is loaded and have the capacity to generate energy by shortening the arch (Kelly et al., 2014). However, in biomechanical analyses, researchers typically treat the foot as a single rigid segment which omits these energy sources and sinks. This leads to three potential inaccuracies in the analysis of locomotion mechanics: 1) rotations of the foot joints are captured as rotations of the ankle joint, 2) energy contributions of some structures within the foot are neglected, and 3) the function of multi-joint muscles and connective tissues that span the ankle and foot joints may be ignored or incorrectly analyzed.

The first of these inaccuracies has been illustrated during walking, as analyses of the ankle and midfoot (tarsal and tarsometatarsal) joints have suggested that the motion (and the associated joint power) at the midfoot joints is incorrectly attributed to the ankle joint (Bruening et al., 2012; Dixon et al., 2012; MacWilliams et al., 2003; Pothrat et al., 2015). In addition, incorrect estimations of ankle joint motion could lead to incorrect estimations of ankle muscle-tendon unit (MTU) lengths and velocities. As models of human muscle rely on these quantities, inaccurate estimates could influence muscle model outputs, potentially altering the results of

muscle-driven simulations and our interpretation of the role of the ankle musculature during gait. The existence and magnitude of these effects have yet to be explored.

The second inaccuracy arising from single segment foot models, that the energy contributions from foot structures are largely ignored, has been investigated intermittently for decades. Analysis of the mechanical energy of a rigid single segment foot has illustrated that the foot (as a whole) absorbs energy during the stance phase of walking (Robertson and Winter, 1980; Siegel et al., 1996; Takahashi et al., 2012; Takahashi and Stanhope, 2013). However, studies on walking using a multisegment foot model have demonstrated that, during push-off, the midfoot joints generate mechanical energy while the metatarsophalangeal (MTP) joints absorb mechanical energy (Bruening et al., 2012; Dixon et al., 2012; MacWilliams et al., 2003). While these foot joint analyses have been performed on walking, fewer studies have explored the energy contributions of the foot joints during running. Some studies have investigated the energy contributions of the soft tissues of the foot, illustrating that the heel pad and arch ligaments absorb energy during landing and midstance, and that the arch ligaments store some of this energy before releasing it during the push-off phase. (Ker, 1996; Ker et al., 1987; McDonald et al., 2016; Pain and Challis, 2001; Wager and Challis, 2016). These studies of running and walking have provided evidence that foot energetics play a non-negligible role during human locomotion. Omitting this from analyses of the ankle may lead to inaccurate conclusions about joint energetics during locomotion. This dissertation seeks to provide additional explorations of these inaccuracies.

The third inaccuracy arising from treating the foot as a single segment relates to omitting relationships between the ankle and foot. These relationships are due to: 1) multi-joint muscles that cross the ankle, midfoot, and toe joints (such as the extrinsic toe flexor muscles: flexor hallucis longus and flexor digitorum longus), and 2) the interactions between the arch of the foot and the ankle plantarflexor muscles. Due to their anatomy, the kinematics of the ankle

plantarflexor muscles are dependent on multiple joint positions and velocities. For example, the moment-generating capacity of the extrinsic toe flexor muscles (flexor hallucis longus and flexor digitorum longus) at the MTP joints is altered by the ankle joint angle (Goldmann and Brüggemann, 2012). Similarly, due to connective tissues that span the joints of the foot, the MTP joints may exert an influence on the length of the gastrocnemius and soleus MTU. Forces in the plantar aponeurosis, which connects the toes to the calcaneus, rise with MTP joint dorsiflexion and Achilles tendon force (Carlson et al., 2000; Hicks, 1954) and provide a possible basis for interactions between the MTP joints and the ankle joint during locomotion. During cadaver simulations of walking, tensile forces within the plantar aponeurosis were directly related to Achilles tendon forces, which suggested that the plantar aponeurosis transferred forces to the forefoot during push-off (Erdemir et al., 2004). While we lack a full understanding of the interactions between the ankle plantarflexors, the arch of the foot, and the MTP joints during locomotion, relationships between them have been reported. Additional work is required to explore these interactions *in vivo* and investigate the functional implications on locomotion.

1.2 Purposes

The overall purpose of this dissertation was to further understand the function of the foot and ankle during running by exploring modeling choices and the interactions between the foot and ankle during the stance phase of running. The first study investigated how the topology of biomechanical foot models affected the calculations of ankle joint kinematics and kinetics (joint moments and powers) during running. The purpose of this study was to determine how a multisegment foot model (as opposed to the traditional single segment foot model) alters the interpretation of ankle joint function during locomotion. The second study compared the simulated function of the ankle plantarflexor muscles (active state & fiber kinematics) during locomotion

using a multisegment foot model and a single segment foot model. The purpose of this study was to determine the importance of using multisegment foot models to study the ankle musculature during running. The third study focused on the relationship between the MTP joints and the ankle plantarflexor muscles by exploring how the MTP joint angle influences the maximum moment generated by the ankle plantarflexors. The purpose was to further understand the interactions between the toes and the ankle plantarflexor muscles to assess the functional implications of this potential relationship.

1.3 Specific Aims & Hypotheses

Study one: Joint mechanics of the foot and ankle during running using a multisegment foot model

Aim 1a: Compare ankle joint angles, angular velocities, moments, joint powers and joint work during running using a multisegment foot model and a single (rigid) segment foot model.

Hypothesis 1a: Throughout stance, ankle joint kinematics (angles and angular velocities) and kinetics (moments, powers, work) computed with the multisegment foot model will differ from those computed using the single segment foot model.

Aim 1b: Determine the mechanical energy of the midtarsal joint (representing approximately the medial longitudinal arch) during the stance phase of running.

Hypothesis 1b: The midtarsal joint will absorb energy during early stance and generate energy during late stance.

Study two: Influences of foot model topology on simulations of the ankle plantarflexor muscles during running

Aim 2: Compare the active state of two ankle plantarflexor simulated using the kinematics from a multisegment foot model and a single segment foot model.

Hypothesis 2: The active states of the ankle plantarflexor muscles during running will be reduced when using the multisegment foot model compared with the single segment foot model.

Study three: The potential for the metatarsophalangeal joint position to modulate maximum isometric ankle plantarflexion moments

Aim 3: Determine how changes to the MTP joint angle influence the maximum voluntary ankle moment during isometric plantarflexions.

Hypothesis 3: Peak ankle plantarflexion moments will be greater with the MTP joints positioned at maximum extension than at their neutral resting angle.

1.4 Overview & Dissertation Structure

This dissertation focused on the modeling of the foot and the function of the ankle plantarflexors during human locomotion. In study one (Chapter 3), two linked rigid body models of the lower leg and foot were developed to calculate ankle joint kinematics and kinetics during running. These rigid body models differed in their treatment of the foot: the first model used a traditional, single segment foot, which comprised all structures between the ankle and metatarsophalangeal joints. The second model employed a foot with three segments representing the rearfoot, forefoot, and toes. Comparisons were made between the ankle joint kinematics and kinetics calculated with these two models. In study two (Chapter 4), two Hill-type ankle plantarflexor muscle models were simulated using the two foot models (single and multisegment)

to investigate the influence of foot model topology on muscle active states during running. In study three (Chapter 5), the role of the MTP joints in modulating maximal ankle plantarflexion strength was explored. Human subjects performed maximum voluntary ankle plantarflexions (isometric and isokinetic) against a dynamometer with their knee, ankle, and MTP joints positioned at different angles. Comparisons were made between the maximum voluntary ankle plantarflexion moments produced in each knee-ankle-MTP joint configuration. Chapter 2 comprises a survey of the relevant literature while Chapter 6 contains a summary of the three studies, the conclusions of the dissertation, and potential future studies.

Chapter 2

Review of Literature

The purpose of this chapter is to summarize the existing literature on the anatomy of the foot and ankle and the function of the ankle plantarflexor muscles during locomotion. Section 2.1 covers the anatomy of the foot, including a broad review of its anatomy and the use of biomechanical models to explore its function during human movements. Section 2.2 summarizes the kinematics and kinetics of the foot during human locomotion, specifically focusing on bone pin studies and explorations of foot and ankle energetics. Section 2.3 will cover the function and behavior of the ankle plantarflexor muscles during human locomotion, with a focus on the complexity of their relation to foot structures and their function during locomotion.

2.1 The Human Foot

2.1.1 Anatomy

The human foot comprises 26 bones connected by 33 joints. The tibia and talus articulate to form the talocrural (ankle) joint, which permits one degree of freedom about an axis oriented mediolaterally, inferiorly, and posteriorly. Distally, the talus articulates with the navicular bone (anteriorly, forming the talonavicular joint) and the calcaneus (inferiorly, forming the talocalcaneal or subtalar joint). In each of these joints, considerable motion can occur in all three planes. The calcaneus articulates with the cuboid at the lateral edge of the foot, forming the calcaneocuboid joint. The talonavicular joint and the calcaneocuboid joint together are known as the midtarsal joint (also known as the transverse tarsal joint or Chopart's joint). The navicular

and the cuboid move little relative to one another during locomotion and therefore can be modeled as a rigid unit (Wolf et al., 2008). The cuneiform bones form articulations with the five metatarsal bones (collectively, the metatarsus) at the first through fifth tarsometatarsal joints, which all exhibit different amounts of motion during locomotion (Arndt et al., 2007; Lundgren et al., 2008; Nester et al., 2007b). Beyond the metatarsus, the hallux comprises a distal phalanx and a proximal phalanx, the latter of which articulates with the first metatarsal by a hinge joint to form the first metatarsophalangeal joint. This joint permits sagittal plane motion and allows slight movement in the transverse plane. The other four toes each consist of three phalanges and articulate with the respective metatarsal bones with a collective axis of rotation (for the lumped segment of four toes, as is often used in biomechanical models of the foot) that runs mediolaterally and slightly posteriorly. On the plantar surface of the foot, fat pads lie inferior to the calcaneus (subcalcaneal fat pad) and the metatarsal heads.

2.1.2 Biomechanical models

The simplest model of the human foot is a single segment that represents all the structures between the ankle and metatarsophalangeal (MTP) joints. This model has been common in locomotion studies historically and continues to be the choice of many researchers. While the single segment model has been sufficient for many studies, more comprehensive models of the foot have provided an understanding of foot motion during locomotion. Carson et al. (2001) formed a three-segment foot model (hindfoot, forefoot, hallux; this model is known as the “Oxford Foot Model”) with six degrees of freedom permitted for each segment. Kinematics during walking were determined from skin markers, with joint angles defined according to the convention of Grood and Suntay (1983). The joint angles demonstrated low variation between trials, with eight of the nine joint angles (three angles each at the tibia-hindfoot, hindfoot-forefoot, forefoot-hallux joints) demonstrating a standard deviation (SD) of less than 1.1°, the

only exception being the forefoot-hallux angle in the sagittal plane. These low variations suggest that the model is repeatable, providing consistent results from trial to trial. Therefore, in experimental studies, larger differences in the joint angles could be due to changes between the experimental conditions. Between-day variation was higher, particularly at the first MTP joint which displayed a 95% confidence interval (CI) of ± 6.0 degrees for plantarflexion. Other between-day 95% CI were ± 1.4°, ± 3.2°, ± 3.0° for the ankle joint (plantarflexion, external rotation, inversion) and ± 2.9°, ± 4.3°, and ± 3.3 degrees for the midfoot (plantarflexion, abduction, supination). Between-tester variation was similar to the between-day variations.

MacWilliams et al. (2003) developed a detailed model comprising eight segments. Compared with the three segments of Carson et al. (2001), the additional segments were created by defining the calcaneus and cuboid as individual segments, splitting the forefoot into medial and lateral segments, and splitting the toes into medial and lateral segments. Joint angles were computed for the MTP, midtarsal, subtalar, calcaneocuboid, and ankle joints during walking. Intrasubject standard deviations were between 0.8 and 1.5 degrees for all joints except the MTP joints, which displayed much higher variability (SD: first MTP: 4.0°, medial MTP: 2.6°, lateral MTP: 2.9°). Joint moments were computed for all joints, with the rear- and midfoot joints displaying plantarflexion moments throughout stance and the MTP joints displaying plantarflexion moments during the second half of stance only. However, these kinetic analyses neglected contact forces between the medial and lateral segments, which may “corrupt” the kinetics at the proximal joints (Buczek et al., 2006).

2.2 The Foot and Ankle during Locomotion

2.2.1 Kinematics

Given the foot's complex bony anatomy, understanding of foot kinematics during locomotion has been best accomplished by a number of bone pin studies (Arndt et al., 2007; Lundgren et al., 2008; Nester et al., 2007a, 2007b; Okita et al., 2013, 2009). These studies have highlighted that the foot joints exhibit substantial rotations during the stance phase of both walking and running. Nester et al. (2007a) explored motion between pairs of bones during walking and found that the greatest sagittal plane range of motion (ROM) occurred between the navicular and medial cuneiform (11.6 ± 3.5°), and the cuboid and fifth metatarsal (10.0 ± 3.6°). However, motion of at least 4 degrees was found between all bone pairs studied. In the frontal plane, motion was observed between all bone pairs, with the greatest motion observed between the navicular and medial cuneiform (11.0 ± 2.4°), followed by motion between the calcaneus and navicular (9.5 ± 2.7°). Of additional interest was the considerable frontal plane ROM between the first and fifth metatarsals (8.7 ± 2.7° across the entire stance phase), which demonstrated that there is deformation of the transverse arch during walking, particularly in midstance (21-80% of stance; 6.5 ± 2.7° total excursion). The calcaneus-navicular articulation displayed the greatest transverse plane ROM, but this was also highly variable between subjects (11.3 ± 5.6°). While all other bone pairs exhibited at least four degrees of transverse plane motion, none exceeded seven degrees.

The results of Nester et al. (2007a) were partially echoed by Lundgren et al. (2008), who reported that sagittal plane ROM was greatest between the fifth metatarsal-cuboid (13.3 ± 1.4°), medial cuneiform-navicular (11.5 ± 1.8°), and cuboid-calcaneus (9.7 ± 5.2°) during walking. Frontal plane motion was substantial in all bone comparisons, exceeding 9.8 degrees for five of the seven joints. Similar to Nester et al. (2007a), these ranges of motion were highly variable

between subjects. In the transverse plane, the talonavicular joint displayed 16.9 ± 6.5° of total motion, nearly double that of any other bone comparison, but characterized by significant intersubject variation. Talus to first metatarsal motions, which impacts kinematic modeling choices, were large and exceeded the ROM at the ankle joint in all three cardinal planes (sagittal: 17.6 ± 2.7°, frontal: 9.6 ± 4.2°, transverse: 14.7 ± 5.3°). This illustrates that the midfoot bones between the talus and first metatarsal rotate considerably during the stance phase of walking and are not well represented by a single rigid body.

Similar to walking, movement of the foot bones during running is complex. Using bone pins, Arndt et al. (2007) observed sagittal plane motion (relative to the proximal bone) in all midfoot joints, with the lateral joints (calcaneocuboid and cuboid-fifth metatarsal) exhibiting the largest ranges. In the transverse plane, the cuboid-fifth metatarsal (9.6 ± 2.4°) and talonavicular (8.7 ± 1.4°) joints displayed the largest ROM. In the frontal plane, ranges of motion were dominated by the talonavicular joint (13.5 ± 4.1°), followed by the subtalar (8.9 ± 3.2°) and navicular-medial cuneiform (8.1 ± 2.6 °) joints. Together, these bone pin studies during both walking and running illustrate the complexity of foot kinematics during locomotion and highlight that modeling the foot as a single rigid body may not be valid.

Though the ranges of motion between the foot bones are large, some groups of bones move together and form functional kinematic units (Wolf et al., 2008). These units are comprised of bones whose joints rotate together during stance (either in the same direction or opposite directions) or bones with joints that do not rotate relative to the unit's other bones. These functional units gave rise to a suggested multisegment foot model with the following segments: calcaneus, navicular-cuboid, medial cuneiform-first metatarsal, and fifth metatarsal (Wolf et al., 2008). The validity of this model was supported by Okita et al. (2009), who illustrated that a two-segment foot model consisting of a hindfoot (calcaneus only) and forefoot (all other foot bones proximal to the MTP joint) captures the average kinematics of the underlying bones during

cadaveric gait simulations. However, the forefoot segment violated the rigid body assumption and average forefoot motion differed from first and fifth metatarsal bone motions. This was particularly evident in the frontal and transverse planes (Okita et al., 2009). Additional work from robotic gait simulations illustrated that rear- and midfoot joints rotate in joint pairs (talonavicular-calcaneocuboid and cubonavicular-talocalcaneal) throughout stance. During foot flat (20-70% of stance), the orientations between the joint axes are fixed, characterized by constant included angles between the joint helical axes (Okita et al., 2013). While these orientations remain constant, the bones of the joint pairs rotate throughout stance with particularly large rotations during push-off (Figure 2-1). This is in contrast to the midtarsal joint locking theory, which postulates that midtarsal joints do not rotate during mid and late stance, which transforms the foot into a rigid lever for propulsion (Mann and Inman, 1964). This occurs when the axes of the talonavicular and calcaneocuboid joints diverge with calcaneal inversion (Elftman, 1960). In cadaveric specimens, passive inversion of the calcaneus decreased sagittal plane metatarsal ROM, but increased (with a statistical trend towards significance, $p = 0.06$) frontal plane navicular ROM (Blackwood et al., 2005). However, little quantitative data from locomotion studies support this relationship causing midtarsal joint locking. Bone pin studies performed both *in vivo* and *in vitro* eschew the "locking" of the joints by quantifying the considerable rotations of these foot bones throughout stance and push-off. Instead, these studies suggest that the bones function in units, with consistent orientations between the axes of joint pairs during midstance and the bones rotating in concert.

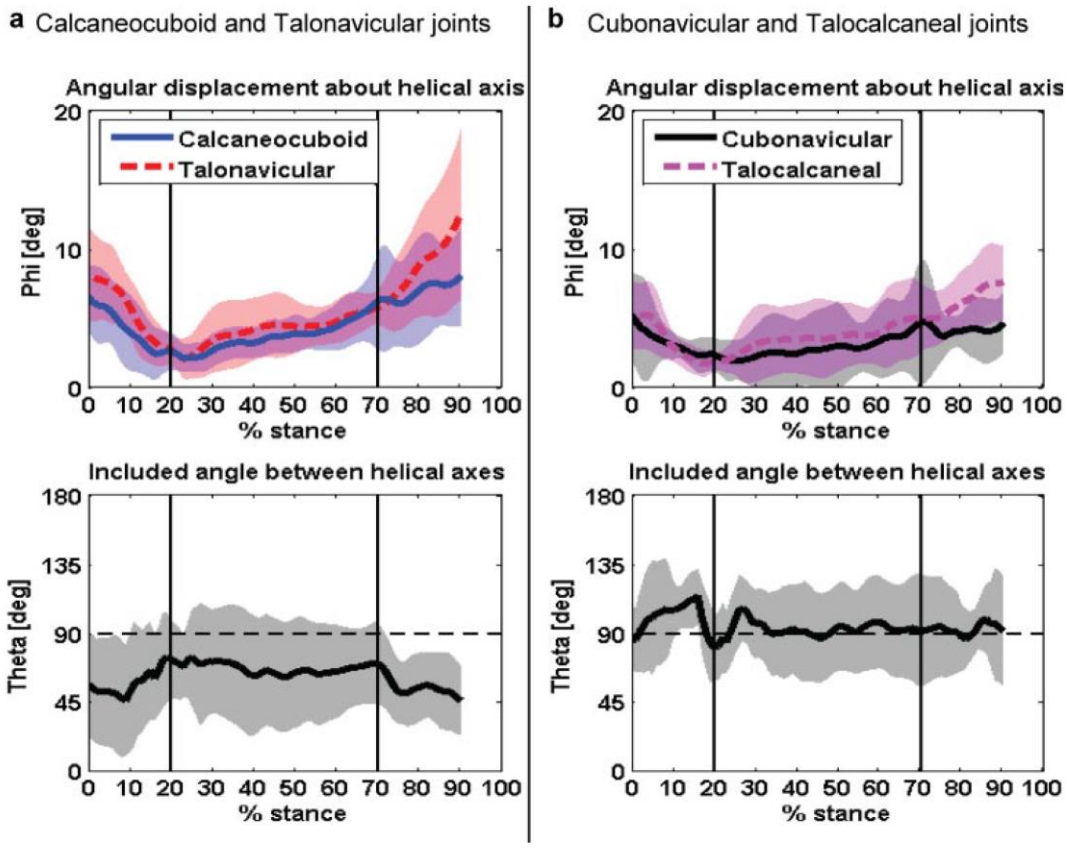

Figure 2-1 Angular displacement (top) about the helical axes of joints within the midfoot and included angles between the helical axes of joint pairs (bottom). The included angle plot for the midtarsal joints (bottom left) illustrate a constant orientation of these joints relative to each other throughout stance. The angular displacement plots (top) show rotations about the joint helical axes throughout stance and push-off. From Okita et al. (2013).

2.2.2 Kinetics

During locomotion, the hip, knee, and ankle coordinate to accelerate the limbs and the whole body center of mass (Zelik and Adamczyk, 2016). Of these joints, the ankle joint is a primary contributor to the mean mechanical power across the stance phase of walking and running (DeVita et al., 2007; Farris and Sawicki, 2012a; Winter, 1983). During the push-off phase of walking, the ankle's contribution may be over 70% of the total positive work (Zelik et al., 2015). In running, the positive work done by the ankle is approximately 70% of the total lower limb positive work (Stearne et al., 2014). However, these studies were performed using a

single segment foot model, which may overestimate the power output at the ankle joint. During walking, modeling the foot as multisegment kinematic chain produces peak ankle joint powers that are approximately half of those computed with a single segment foot. The power differences between the two foot models (single and multisegment) are due to differences in the ankle joint angular velocity, as the motion of the midfoot joints are accounted for at the ankle (Bruening et al., 2012; Dixon et al., 2012; MacWilliams et al., 2003; Pothrat et al., 2015). This discrepancy between the models calls into question the proportion of total power attributed to the ankle joint during walking and suggests that it may be lower than previously estimated.

In addition to overestimating peak ankle joint powers, modeling the foot as a single rigid link may improperly estimate the energy contributions of the foot. Robertson & Winter (1980) explored lower limb segment energies during walking with a two-dimensional lower body model consisting of the thigh, shank, and single segment foot. Segmental energy rates of change (from segment inertial properties, COM height, and COM linear and angular velocities) were compared to the total energy supplied to each segment from the inverse dynamics-based resultant joint moments and forces. Strong agreement between the two methods (inverse dynamics-based power and

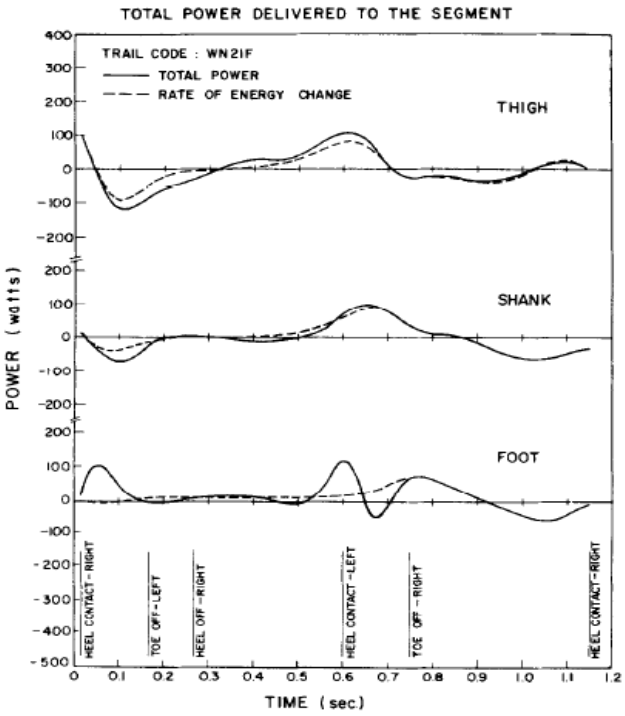

Figure 2-2 Comparison of thigh, shank, and foot energy profiles during walking using two calculation methods. Dotted lines indicate mechanical energy rate of change from kinematics and inertial properties. Solid lines indicate total energy supplied to each segment from resultant joint moments and forces computed through inverse dynamics. Considerable discrepancy was found for the foot segment during stance. From Robertson & Winter (1980).

segment COM-based power) was found for the thigh and shank segments (as is required by the work-energy theorem), but considerable discrepancies existed for the foot segment during the late single support and double support phases (Figure 2-2). Inverse dynamics-based powers for the foot oscillated between power generation and absorption, while segment COM-based calculations showed generation of power throughout stance. These differences illustrated experimental errors present in inverse dynamics analyses, which were in part due to representing the foot as a single segment. Siegel et al. (1996) reproduced the work of Robertson & Winter (1980) but used a three-dimensional model and represented the foot using a single deformable segment as opposed to the traditionally rigid model. The deformable nature of the segment is due to the inclusion of a term that accounts for the position of the foot COM relative to the center of pressure. A translational velocity for the foot segment, $\boldsymbol{v}_{ftd}$, was computed as:

$$\boldsymbol{v}_{ftd} = \boldsymbol{v}_{ft\_com} + (\boldsymbol{\omega}_{ft} \times \boldsymbol{r}_{cop-com})$$

Where,

$\boldsymbol{v}_{ft\_com}$ is the velocity of the foot COM

$\boldsymbol{\omega}_{ft}$ is the rotational velocity of the foot

$\boldsymbol{r}_{cop-com}$ is the vector from the foot COM to the COP

Power of the foot, P_{foot}, using this deformable model was the summation of the rotational and translational powers:

$$P_{foot} = \boldsymbol{M}_{free} \cdot \boldsymbol{\omega}_{ft} + \boldsymbol{F}_{grf} \cdot \boldsymbol{v}_{ftd}$$

Where,

$\boldsymbol{M}_{free}$ is the free moment

$\boldsymbol{F}_{grf}$ is the vector of ground reaction forces

Inclusion of foot deformation via the translational power term greatly improved the agreement between segmental energy changes (summation of mechanical energies) and computed segmental

power (Figure 2-3). The foot deformation portion of the power calculation ($\boldsymbol{F}_{grf} \cdot \boldsymbol{v}_{ftd}$) suggested that energy is absorbed early in the gait cycle and immediately before toe-off due to rotation of foot joints and compression of the plantar soft tissues. At various walking speeds (0.4-1.0 statures/s), analysis of the deformable foot power demonstrated that energy absorption within the foot is directly related to speed (Takahashi and Stanhope, 2013). However, although deformable, only one segment was used to represent the foot. Therefore, the individual energy contributions of segments or joints within the foot could not be estimated.

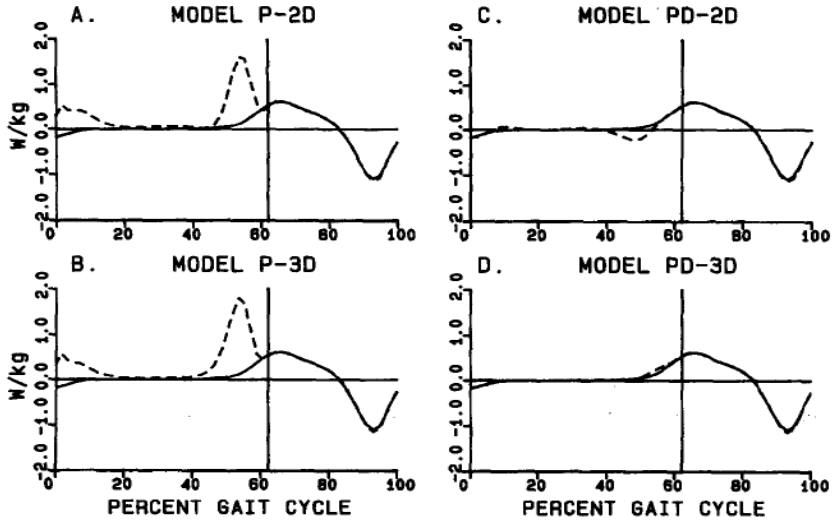

Figure 2-3 Comparison between foot segmental energy changes (solid line) and foot power computed using four different models during walking (dashed line). P-2D: rigid foot in two dimensions, P-3D: rigid foot in three dimensions, PD-2D: deformable foot in two dimensions, PD-3D: deformable foot in three dimensions. Including the deformation in the power calculation significantly improved agreement with segmental energy changes. From Siegel et al. (1996).

In addition to suggesting that ankle joint angular velocities and powers may be overestimated in many studies, multisegment foot models have characterized the kinetics of the joints within the foot during locomotion. These analyses highlight the potential importance of the foot joints as energy absorbers and generators. Scott & Winter (1993) estimated that the peak midtarsal joint moment during stance was two-thirds of the peak ankle joint moment and occurred just prior to 80% of stance. Combined with the observed plantarflexion of the midtarsal joint,

these data suggest that positive power is generated at the midtarsal joint during push-off (Figure 2-4). Dixon et al. (2012) and Bruening et al. (2012) both supported this, with the former reporting a peak midtarsal joint power of 1.1 $W \cdot kg^{-1}$ during walking.

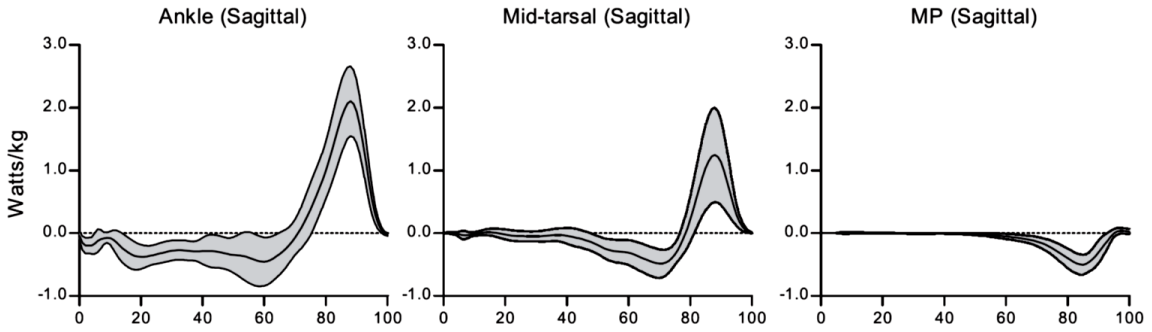

Figure 2-4 Sagittal plane joint powers for the ankle, midtarsal, and metatasophalangeal (MP) joints during the stance phase of walking. Midtarsal joint power was approximately half of the ankle joint power. From Bruening et al. (2012).

In both studies, midtarsal joint power equaled approximately half of the peak ankle joint power (which was computed using a multisegment foot model and was approximately half of the ankle joint power computed with a single segment foot model). Despite this power generation at the midtarsal joint, Takahashi & Stanhope (2013) illustrated that the entire foot (defined as all structures distal to the ankle) performed net negative work during the stance phase of walking (Figure 2-5). This suggested that significant energy absorption occurs elsewhere in the foot to offset the positive power generated at the midtarsal joint. This energy absorption likely occurs at the subcalcaneal fat pad during impact (Wearing et al., 2014) and at the MTP joints during push-off (Bruening et al., 2012). Though the net mechanical energy of the entire foot has not been quantified for running, the heel pad, midtarsal joint, and MTP joints seem to play a similar role as in walking (Ker, 1996; McDonald et al., 2016; Stefanyshyn and Nigg, 1997; Wager and Challis, 2016). During both walking and running, some of the energy absorbed by the MTP joint may be transferred to contribute to energy generated at the midtarsal joint (Bruening et al., 2012; McDonald et al., 2016; Wager and Challis, 2016).

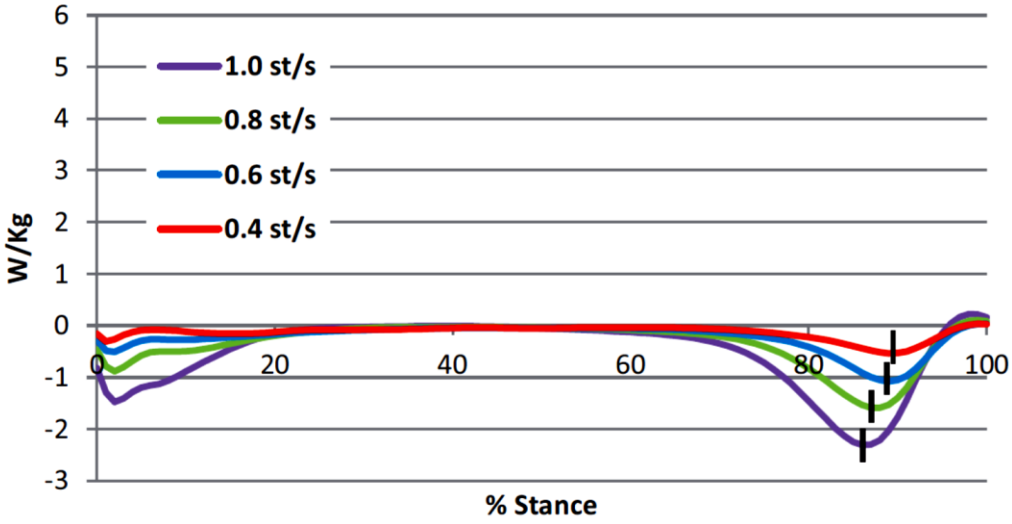

Figure 2-5 Power of the "distal foot" segment (all structures distal to the ankle joint) over the stance phase of walking at four speeds (st/s = statures per second). The foot absorbed energy during stance, with peak energy absorption during push-off. Increased speed resulted in greater energy absorption and an earlier peak absorption. From Takahashi & Stanhope (2013).

2.3 The Ankle Plantarflexor Muscles

There are eight muscles capable of producing ankle plantarflexion: the gastrocnemius, soleus, flexor hallucis longus (FHL), flexor digitorum longus (FDL), tibialis posterior, peroneus longus, peroneus brevis, and plantaris. This section covers the general anatomy of these muscles and discusses their function during locomotion. Emphasis will be placed on the triceps surae muscles (gastrocnemius and soleus) and the extrinsic toe flexor muscles (flexor hallucis longus and flexor digitorum longus) due to their importance in Chapters 3 and 5.

2.3.1 Anatomy and muscle architecture

The ankle plantarflexor muscles are diverse in their anatomy, collectively spanning the knee, the ankle, and many of the foot joints (including the metatarsophalangeal joints). Though some ankle plantarflexors are considered to be one joint muscles, all of them cross multiple joints (Table 2-1). Due to this multijoint anatomy, the ankle plantarflexor muscle lengths are a function of multiple joint rotations, which leads to complex relationships between the segment and muscle mechanics (Goldmann and Brüggemann, 2012; Hofmann et al., 2013; Prilutsky and Zatsiorsky, 1994). The triceps surae muscles cross the subtalar joint in the foot by way of the Achilles tendon inserting on the calcaneus and, therefore, can cause both inversion and eversion of the foot. The direction of subtalar joint rotation induced by the triceps surae is dependent on the subtalar joint position (Klein et al., 1996). In addition, relationships between the triceps surae and the toes may arise due to structures connecting the calcaneus and toes, such as the plantar aponeurosis. Cadaver dissections have shown that in neonates, the Achilles tendon and plantar aponeurosis are connected by a thick, fibrous band, but that this connection diminishes with age until the Achilles tendon and the plantar aponeurosis connect individually to the paratenon of the Achilles tendon or the periosteum of the calcaneus (Snow et al., 1995; Stecco et al., 2013). Additional evidence of this connection (Figure 2-6) has been shown using MRI in adult subjects up to 42 years of age (Shaw et al., 2008). Despite this diminished connection, the triceps surae muscles and plantar aponeurosis show some mechanical relationship even in aged specimens, as

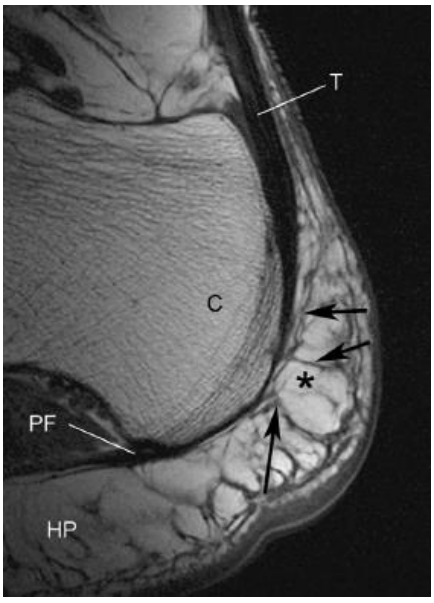

Figure 2-6 Sagittal plane non-fat suppressed MR image of the heel of a 42 year old female, showing the connection between the Achilles (T) and the plantar aponeurosis (PF). From Shaw et al. (2008).

Carlson et al. (2000) demonstrated that applying a tensile force to the Achilles tendon of cadaveric feet induced strain of the plantar aponeurosis. Furthermore, dorsiflexion of the toes tensions the plantar aponeurosis, increases the height of the medial longitudinal arch, and also alters the triceps surae MTU length (Hicks, 1954; Iwanuma et al., 2011a).

Table 2-1 Joints crossed by the ankle plantarflexor muscles.

Muscle	Joints crossed
Gastrocnemius	Knee, talocrural, subtalar
Soleus	Talocrural, subtalar
Flexor hallucis longus	Talocrural, subtalar, tarsals/tarsometatarsals, metatarsophalangeal
Flexor digitorum longus	Talocrural, subtalar, tarsals/tarsometatarsals, metatarsophalangeal
Tibialis posterior	Talocrural, subtalar, tarsals
Peroneus longus	Talocrural, subtalar, tarsals
Peroneus brevis	Talocrural, subtalar, tarsals
Plantaris	Knee, talocrural, subtalar

The gastrocnemius and soleus muscles (triceps surae) are the largest of the ankle plantarflexors and account for approximately 60% of their combined mass (Ward et al., 2009). In addition, their pennate fiber architecture results in large physiological cross-sectional areas (PCSA) compared to their anatomical cross-sectional areas (ACSA). In the soleus, the pennation angle is approximately 28.3 degrees (the largest pennation angle of the ankle plantarflexors; next largest: FHL, 16.9 degrees) which results in the soleus accounting for 59% of the total PCSA of the ankle plantarflexors, despite accounting for only 39% of the ACSA (Fukunaga et al., 1992). The two heads of the gastrocnemius combine to account for an additional 25% of the total

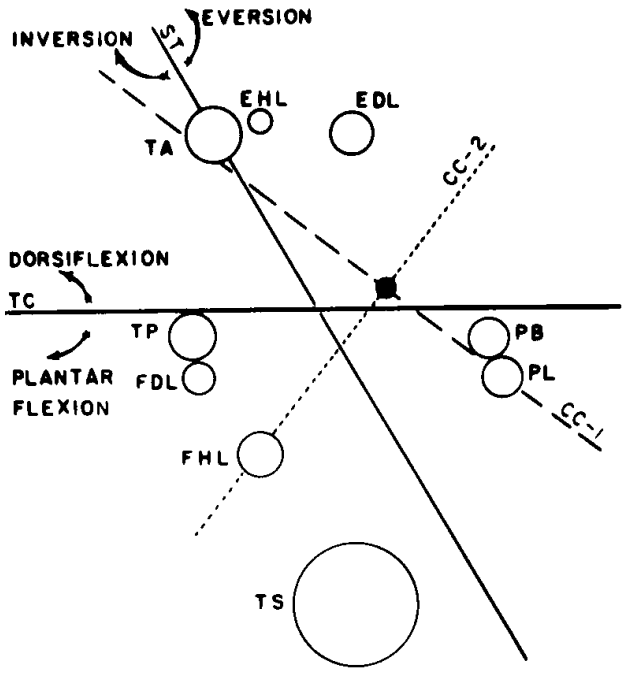

Figure 2-7 A representation of the size and moment arms of the ankle plantarflexor muscles with respect to various axes of the ankle and foot. Circle size indicates cross-sectional area and distance from each axis represents the muscle moment arm. TC = talocrural joint axis, CC-1, CC-2 = the axes of the calcaneocuboid joint, ST = subtalar joint axis. TS = triceps surae, FDL/FHL = flexor digitorum/hallicus longus, TP = tibialis posterior. From Elftman (1960).

plantarflexor PCSA, while the extrinsic toe flexors (FDL and FHL) contribute approximately 7 % of the PCSA (Fukunaga et al., 1992). Differences in the muscle moment arms within the ankle plantarflexors also highlight differences in their functional importance. The triceps surae muscles not only have the largest mass and PCSA, but also the largest moment arm with respect to the ankle joint (Figure 2-7). At the ankle joint, Klein et al. (1996) reported a mean (throughout the ankle joint range of motion) Achilles tendon moment arm of 52.8 mm, compared to a mean FHL moment arm of 26.6 mm (Figure 2-8). Hui et al. (2007) reported a mean ankle moment arm for the FDL of 19.6 ± 5.5 mm using the tendon excursion method in 8 cadaveric specimens.

Muscle architecture is similar among the ankle plantarflexors, with most having short pennated muscle fibers attached to long tendons. Fiber length to muscle length fractions are consistently reported around 0.20, with the exception of the gastrocnemius lateral head, which has longer fiber lengths and a shorter muscle length than the medial head (Friederich and Brand, 1990; Ward et al., 2009; Wickiewicz et al., 1983). The gastrocnemius and soleus insert at a common point on the calcaneus through the shared Achilles tendon. Despite this shared tendon,

the muscles likely function relatively independently due to differential sliding between the deep and superficial fibers of the Achilles tendon (Franz et al., 2015).

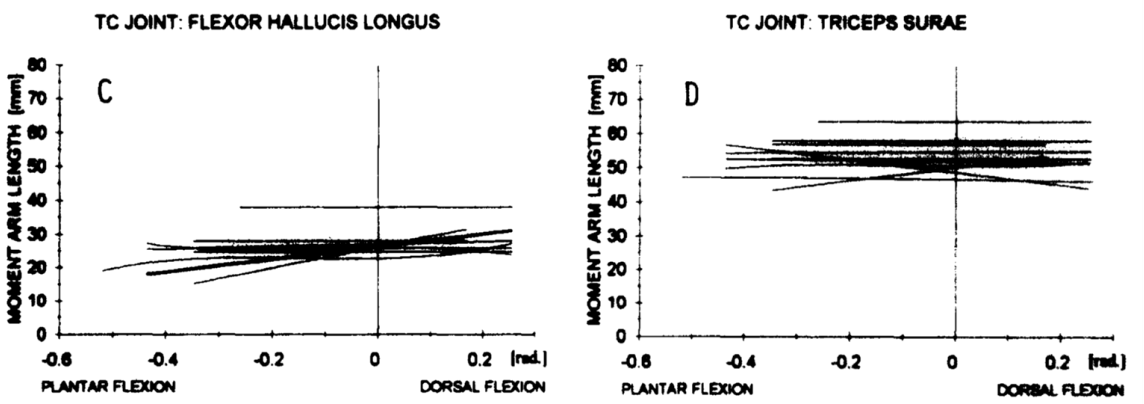

Figure 2-8 Moment arms of the flexor hallucis longus and triceps surae muscles with respect to the ankle joint. From Klein et al. (1996).

2.3.2 Force-length and force-velocity properties

The force-length (F-L) and force-velocity (F-V) properties of a muscle can have profound impacts on its function. While early studies of these properties used isolated non-human muscles, more recent work have estimated the properties *in vivo* using dynamometry to measure the resultant joint moment and joint angle simultaneously. Conclusions on the collective F-L and F-V properties of all the muscles performing a joint action can be drawn through angle-moment or angular velocity-moment relationships. Additionally, properties for a specific muscle have been estimated using imaging and/or mathematical muscle models. These modeling and imaging techniques have been used during static muscle actions and also during locomotion to provide insights on the expressed sections of the F-L and F-V properties of the ankle plantarflexor muscles during walking and running.

The F-L relationship describes a muscles ability to generate force at a given muscle length. In intact whole muscles, the F-L relationship has been characterized *in vivo* using isometric ankle plantarflexion contractions against a dynamometer footplate. Herzog et al. (1991) captured dynamometer measurements of ankle plantarflexor moments at a range of ankle and knee angles (ankle range: 90 – 120 degrees knee range: 70 – 170 degrees) and obtained the plantarflexor muscle-tendon unit length using the regression equations of Grieve et al. (1978). The F-L curve for the gastrocnemius was reconstructed from these measurements. With increasing gastrocnemius length, muscle force also increased, suggesting that the gastrocnemius operates on the ascending limb of its F-L curve *in vivo* (Figure 2-9). Winter and Challis (2008) found similar results (24 out of 28 subjects operating on the ascending limb) through reconstruction of the gastrocnemius F-L curve using isometric dynamometer measurements, regression equations, and tendon excursion. However, the gastrocnemius of three subjects operated on the descending limb and one operated on the plateau. Rubenson et al. (2012) reported F-L operating ranges for the human soleus and suggested soleus operating ranges are larger than those reported for the gastrocnemius (Figure 2-9). Subjects expressed mostly the ascending limb, but also the plateau (in eight of eight subjects) and the descending limb (in four of eight subjects).

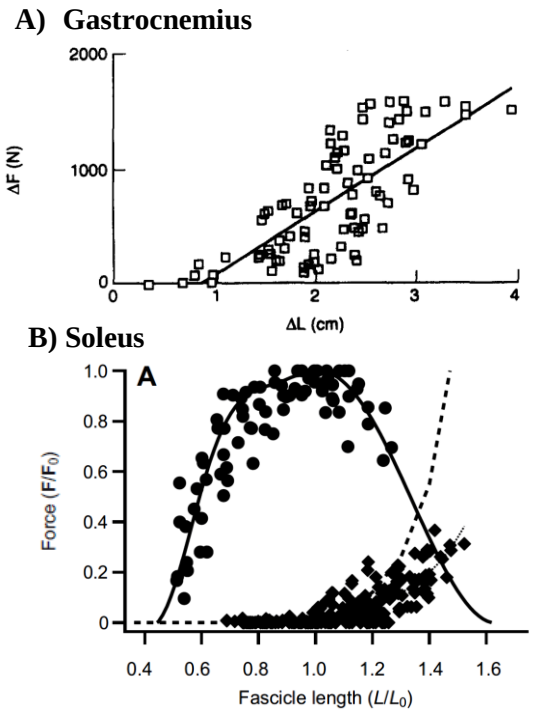

Figure 2-9 A) The gastrocnemius force-length curve reconstructed from *in vivo* measurements. Markers show subject measurements and the solid line is the line of best fit (Herzog et al., 1991).

B) The soleus force-length curve reconstructed from *in vivo* measurements. Markers indicate subject measurements (circles: active force-length, diamonds, passive force-length) and the lines indicate theoretical force-length curves (solid: active, dashed: passive; Rubenson et al., 2012).

The force-velocity (F-V) property describes a muscle's ability to generate force as a function of the muscle's velocity (Fenn and Marsh, 1935; Hill, 1938; Katz, 1939). As muscle shortening velocity increases, the force developed within the muscle is reduced until it reaches zero at the maximum shortening velocity (Figure 2-10). Conversely, as muscle lengthening velocity increases, the force developed within the muscle increases towards a plateau. The F-V curve for the human ankle plantarflexors *in vivo* has been estimated by measuring both the resultant joint moment and the ankle angle during contractions at a range of fixed angular velocities. Using a particular experimental protocol, force-velocity profiles similar to those of isolated muscle preparations have been found. Wickiewicz et al. (1984) obtained force-velocity curves for the ankle plantarflexors, but the relationship was not entirely similar to isolated muscle, as the force obtained isometrically was lower than the force obtained at low angular velocities. Bobbert and van Ingen Schneau (1990) indicated that these discrepancies between expected and experimental F-V curves could be explained by the muscle's contraction history, suggesting that during experimental measurements the muscle active state should be allowed rise prior to the start of joint rotation. Reconstructing the F-V relationship in this way produces a hyperbolic relationship similar to isolated muscle F-V relationships (Figure 2-11).

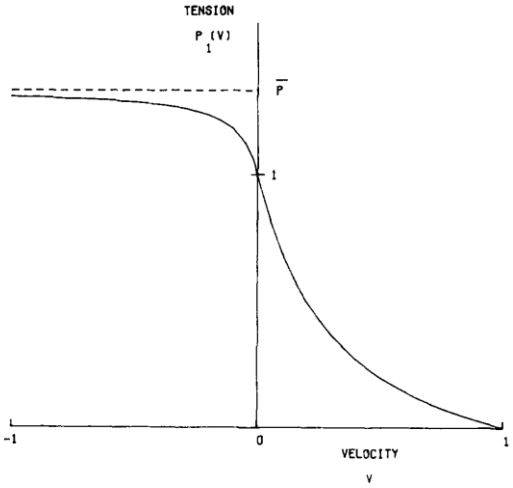

Figure 2-10 The force-velocity property of skeletal muscle, from Fitzhugh (1977).

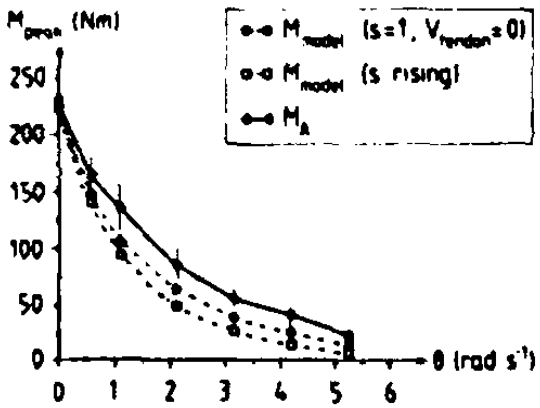

Figure 2-11 A reconstructed force-velocity relationship for the ankle plantarflexors, obtained through isokinetic dynamometry measurements and a model of muscle contraction. Solid black curve is the experimentally obtained relationship. The two dashed lines are simulated relationships using a muscle model and two different active state conditions. From Bobbert and van Ingen Schenau (1990).

2.3.3 Function during locomotion

During the stance phase of walking and running, approximately 40% of the positive lower limb mechanical work is performed by the ankle during push-off (Farris and Sawicki, 2012a). However, the ankle plantarflexor muscles consume proportionately less (30%) of the total metabolic energy during walking. This demonstrates that the plantarflexor muscles function at a relatively high efficiency during locomotion (Rubenson et al., 2006; Umberger, 2010). One explanation for this high efficiency centers on the ankle plantarflexors' relatively long and compliant tendons, which have been postulated to improve efficiency during locomotion in three ways: 1) long compliant tendons decouple muscle fiber lengthening from that of the MTU (Biewener et al., 1998; Herbert et al., 2002; Hof et al., 2002; Ishikawa et al., 2005; Lichtwark and Wilson, 2006; Roberts et al., 1997), 2) long compliant tendons generate MTU work and power during push-off by storing elastic energy during early stance and releasing it during late stance, and 3) long compliant tendons allow for short muscle fibers, which concentrates the muscle mass proximally and lowers the mass moment of inertia of the distal limbs, such as the shank.

Decoupling fiber length changes from MTU length changes can allow the muscle fibers to operate closer to their optimal fiber length, improving force generating capacity. Furthermore,

this decoupling minimizes the shortening required of the muscle fibers, which reduces metabolic energy expenditure (Fenn, 1923). However, this concept has been challenged for shortening that occurs in a stretch-shortening cycle (Holt et al., 2014). In some cases, long tendons allow the muscle fibers to operate isometrically (providing minimal energy expenditure) while the tendon performs the required lengthening and shortening. Evidence of this during human locomotion has been given by *in situ* and *in vivo* investigations. Hofmann et al. (2013) performed cadaveric gait simulations by mechanically pulling on the tendons of the lower leg and foot. When the extrinsic toe flexors (flexor hallucis longus and flexor digitorum longus) were forced to operate isometrically, the resulting muscle forces were similar to *in vivo* EMG-derived muscle forces. They also found the inverse; operating these muscles using EMG-derived muscle forces resulted in near isometric function of the muscles. Though these simulations were performed at only a fraction of *in vivo* walking speeds, this provided evidence that the extrinsic toe flexors function isometrically during walking, potentially transferring energy between the shank and foot and/or allowing the tendons to store and return elastic energy. In the triceps surae, muscle kinematics during walking and running have been estimated through simulation and ultrasound to provide insights into the operating lengths of the ankle plantarflexors during locomotion. Arnold and Delp (2011) created a musculoskeletal simulation of walking and demonstrated that the triceps surae muscles are active primarily on the descending limb of the F-L curve but shortened substantially during terminal stance and operated briefly on the plateau and ascending limb. However, these results were sensitive to tendon stiffness and the rigid body model utilized a single segment foot, which might have exaggerated the sagittal plane ankle joint angle (MacWilliams et al., 2003; Pothrat et al., 2015) and subsequently exaggerated the simulated muscle fiber lengths. Rubenson et al. (2012) collected combined ultrasound images of the soleus muscle fascicles during walking and running with subject-specific F-L properties to determine the length change of the fibers and the section of the F-L curve on which the fibers operate. During

both walking and running, the soleus operated primarily on the ascending limb. Length changes of the soleus fibers demonstrated lengthening then shortening during walking and shortening only during running (Figure 2-12).

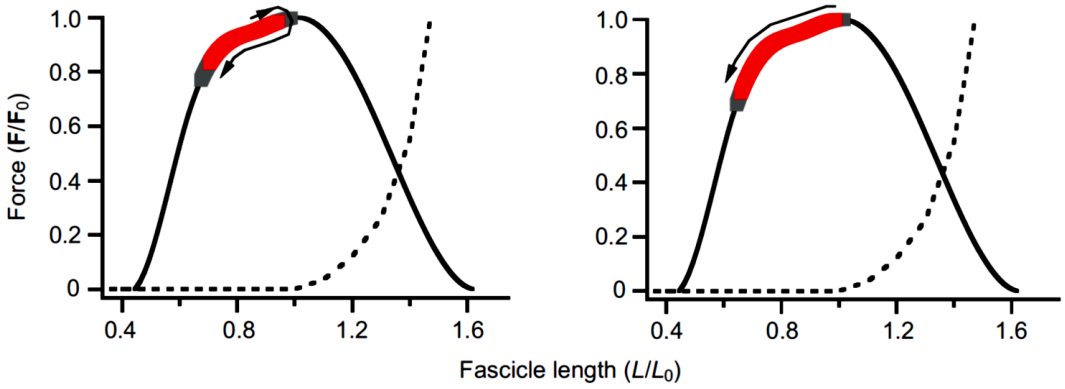

Figure 2-12 The operating range of the human soleus during walking (left) and running (right). The red bars show the area over which the soleus operates while active. The black arrow along the curve indicates the muscle length change during stance. From Rubenson et al. (2012).

Separating the muscle fiber length changes from the MTU fiber length changes also allows the plantarflexor muscles to operate at lower muscle fiber velocities to improve their force generating capacity. Lichtwark & Wilson (2006) presented *in vivo* ultrasound data for the medial gastrocnemius, which illustrated that length changes and velocity of the muscle fascicles and the MTU differed throughout stance. Fascicle shortening velocity was substantially slower than MTU velocity. Further, using a model of the medial gastrocnemius, Lichtwark and Wilson (2007) suggested that the Achilles tendon stiffness is optimized to maximize muscle efficiency (the ratio of muscle fascicle work to the sum of muscle fascicle work and heat) during locomotion (Lichtwark and Wilson, 2007). They performed muscle simulations with a tendon stiffness similar to *in vivo* measurements, then altered this stiffness by a factor of 0.5, 2, and 4. The *in vivo* stiffness value produced the highest muscle efficiency value, leading to the conclusion that the human Achilles tendon has the optimal properties for efficiency during locomotion. However, the muscle model length changes were determined from ankle angles determined using a single

segment foot model. While the results may not be sensitive to the ankle angle, it remains unclear how the differences in ankle angle produced by a multisegment foot model (Dixon et al., 2012; Pothrat et al., 2015) would impact these results. Lichtwark and Wilson (2008) performed additional optimizations to determine values for tendon stiffness and optimal fascicle length that maximized efficiency during walking, slow running, and fast running. Optimal tendon stiffness for walking was lower than that found *in vivo*, while optimal tendon stiffness for running was greater than found *in vivo*. Optimal fascicle length in both running and walking was shorter than that found *in vivo*. While it seems that a primary role of the Achilles tendon is to decouple muscle fascicle length and velocity from that of the MTU during locomotion, continued investigation is warranted to understand if the muscle architecture and behavior are optimized.

In addition to decoupling muscle fiber and MTU length changes, the elastic tendons of the ankle plantarflexor muscles store and return energy during locomotion, which is thought to improve muscle efficiency (Alexander and Bennet-Clark, 1977; Hof et al., 2002; Ishikawa et al., 2007, 2005; Ker et al., 1987; Lai et al., 2014; Rubenson et al., 2011). Cavagna et al. (1964) was among the first to propose this, based on unexpectedly large estimates of muscle efficiency during running (0.4 - 0.5, ratio of positive mechanical work to metabolic energy expenditure). This led to the suggestion that the kinetic energy lost during early stance was stored as elastic energy in contracted muscles and released during late stance. As this resulted in positive mechanical work with little metabolic energy expenditure, it could explain the unexpectedly high efficiency. Recent work has supported this mechanism in human muscle but suggests that tendons are the main site of energy storage and return during locomotion, not muscle fibers. As tendons are not subject to the same velocity constraints as muscle, this can increase the shortening speed of the triceps surae MTU beyond the maximum shortening velocity of the muscle fibers. This effect has been termed the ‘catapult action’ and has been shown to enhance the power generated by the MTU during the push-off phase of walking (Hof et al., 2002; Ishikawa et al.,

2005). During running, *in vivo* and *in situ* testing have suggested that the Achilles tendon recoil accounts for a majority of the triceps surae MTU power and 25% of the total mechanical power generated by the lower limb joints during the stance phase (Alexander and Bennet-Clark, 1977; Ker et al., 1987; Lai et al., 2014; Rubenson et al., 2011). This contribution to the MTU work is increased with increased running speed (Lai et al., 2014).

2.4 Summary

The previous sections have summarized studies on the anatomy of the foot and ankle and their function during locomotion. This includes an overview of the anatomy and models that have been used to study foot function (section 2.1), the foot's kinematics and kinetics during locomotion (section 2.2), and the structure and function of the ankle plantarflexor muscles (section 2.3). Biomechanical models of the foot have ranged from extremely simple (a single segment) to extremely complex (nine segments) and have shown to influence the calculated ankle joint kinematics and kinetics during walking. The effect of foot model topology on ankle joint kinematics and kinetics during running is unclear. The kinematics of the foot bones during locomotion are complex, with bone pin studies during *in situ* and *in vivo* locomotion indicating that the bones of the foot rotate considerably in all three planes throughout stance. This suggests that single segment foot models may not properly capture foot kinematics during running and may omit important energetic contributions, but this has yet to be shown experimentally. Further, these potentially neglected foot joint kinematics may influence the behavior of the ankle plantarflexor muscles, due to the multijoint anatomy of the muscles and adjacent tissues such as the plantar aponeurosis. The ankle plantarflexors function efficiently during locomotion, in part due to the elasticity of the Achilles tendon. This elasticity allows for the near isometric operation of the triceps surae muscle fibers and may store and return elastic energy during stance.

However, the effect of foot motions and model topology on the analysis of these functions requires additional investigation.

Chapter 3
Joint mechanics of the foot and ankle during running using a multisegment foot model

3.1 Abstract

In human locomotion, a majority of the lower limb power is generated at the ankle joint, which underscores the importance of studying ankle joint mechanics to understand human gait. Traditionally, ankle joint mechanics have been studied using models that treat the foot as a single rigid segment which comprises all bones between the ankle and metatarsophalangeal joints. However, this contrasts with the more complex structure and mobility of the human foot, which could alter the results of rigid body analyses. This study sought to compare ankle joint kinematics and kinetics during running using a single segment foot model (SINGLE) and a multisegment foot model (MULTI; three segments). Seven participants ran at 3.1 $m \cdot s^{-1}$ while the positions of markers on the shank and foot were tracked and ground reaction forces were measured. Ankle joint kinematics, resultant joint moments, joint work, and instantaneous joint power were determined using both the SINGLE and MULTI models. Differences between the two models across the entire stance phase were tested using statistical parametric mapping. During the stance phase, MULTI produced ankle joint angles that were typically closer to neutral and angular velocities that were reduced compared with SINGLE. Instantaneous joint power and joint work during late stance were both reduced in MULTI, suggesting that SINGLE overestimated ankle joint power and work during the push-off phase of running. These results are similar to those obtained during walking and demonstrate the importance of foot model topology in analyses of the ankle joint during running.

3.2 Introduction

Insights into ankle joint function during running have been largely shaped by joint power analyses, which have suggested that the ankle is the largest contributor to lower limb positive work and a primary generator of power during stance (Farris and Sawicki, 2012a; Stearne et al., 2014; Winter, 1983; Zelik et al., 2015). However, the lower limb models that are typically used to compute ankle power use rigid bodies to represent the thigh, shank, and foot. While rigid bodies may be sufficient to capture the general behavior of the thigh and shank, the foot has a more complex structure and is not well modeled by a single rigid segment (Robertson and Winter, 1980; Siegel et al., 1996). This is visible in studies of the ankle during walking, which have suggested that ankle joint angular velocity and power are overestimated with single segment foot models compared to multisegment foot models (Bruening et al., 2012; Dixon et al., 2012; MacWilliams et al., 2003; Pothrat et al., 2015).

Models that better capture the behavior of the human foot and ankle have become more prevalent in walking research but have yet to be used to study running. Siegel et al. (1996) analyzed foot segment energy during walking using a deformable model that included energy changes due to movement of the foot's center of mass (e.g., from plantar soft tissue and arch deformation). This model demonstrated improved agreement with the work-energy theorem and has been used to characterize the energy profile of the combined foot-ankle system in walking (Siegel et al., 1996; Takahashi et al., 2017, 2012; Takahashi and Stanhope, 2013). Multisegment foot models that use three or more segments to capture foot kinematics (typically at least the hindfoot, forefoot, and hallux) have also become more prevalent in walking investigations, particularly for clinical use (Carson et al., 2001; Leardini et al., 2007; MacWilliams et al., 2003). Along with highlighting discrepancies in ankle joint power during walking, these models have demonstrated changes in foot kinematics across speeds and slopes, explored plantar aponeurosis

loading during stance, and illustrated foot segment coordination during weight acceptance and push-off (Arnold et al., 2017; Caravaggi et al., 2010, 2009; Chang et al., 2008; Tulchin et al., 2010, 2009). Multisegment foot models have also revealed that the midfoot joints generate power during the push-off phase of walking (Bruening et al., 2012; Dixon et al., 2012; MacWilliams et al., 2003; Pothrat et al., 2015). While multisegment foot models have improved understanding of foot and ankle function during walking, most studies of running continue to use a single segment foot model. Therefore, ankle joint power values and the distribution of power among the lower limb joints during running warrants reinvestigation. Furthermore, use of a multisegment foot model to analyze running gait can quantify foot segment and joint kinematics to permit investigation of the arch of the foot, which may play an important energetic role (Kelly et al., 2016; Ker et al., 1987; McDonald et al., 2016; Stearne et al., 2016; Wager and Challis, 2016).

The primary purpose of this study was to compare the ankle joint mechanics of the stance phase of running using two foot models: a multisegment foot model (MULTI; three segments) and a single segment foot model (SINGLE). It was hypothesized that MULTI and SINGLE would result in different ankle joint kinematics (angles and angular velocities) and ankle joint kinetics (joint moments, powers, and work). Therefore, the null hypothesis was that SINGLE and MULTI would produce statistically equivalent joint kinematics and kinetics throughout stance. The secondary purpose of this study was to assess the energy profile of the midfoot joint (defined as a collective representation of the midtarsal and tarsometatarsal joints) during the stance phase of running.

3.3 Methods

All subjects (n = 7) were runners who regularly completed at least 10 miles weekly and did not report any musculoskeletal injury in the past six months. Informed consent was obtained

prior to participation and all protocols were approved by the Institutional Review Board at The Pennsylvania State University (Appendix A).

Each subject ran barefoot down a 15m runway at a self-selected speed (instructed to choose a comfortable, “regular run” pace) using a rearfoot strike pattern. Passive retroreflective skin markers were placed on 27 bony landmarks of the pelvis, thigh, shank, and foot (sectioned into three segments) using double-sided tape (Table 3-1). Markers were attached directly to the skin and were flattened slightly on one side to improve adherence. Marker positions during each trial were tracked by a six-camera motion capture system (Motion Analysis Corporation, Mountain View, CA) sampling at 150 Hz. Ground reaction forces and moments (GRF) were collected at 1500 Hz from a 90 x 60 cm force plate (Model 9287A, Kistler Instrument Corporation, Amherst, NY). All data were lowpass filtered in the forward and reverse directions using a second-order recursive Butterworth filter. Marker positions were filtered with a cutoff frequency of 10 Hz and the GRF data were filtered with a cutoff frequency of 45 Hz.

Table 3-1 The 27 markers used to track the segments and bony landmarks of the pelvis, leg, and foot.

Abbreviation	Description of marker location
RASIS, LASIS	Anterior superior iliac spines
RPSIS, LPSIS	Posterior superior iliac spines
TH1, TH2, TH3, TH4	A cluster of four markers on the anterolateral thigh
LK	Lateral knee defined by the lateral femoral condyle
SH1, SH2, SH3, SH4	A cluster of four markers on the anterolateral shank
LM	Lateral malleolus
MM	Medial malleolus
CA	Insertion of the Achilles tendon on the calcaneus (calcaneoachilles)
PT	Peroneal trochlea of the calcaneus
ST	Sustentaculum tali
NAV	Navicular tuberosity
M1B	Base of the first metatarsal
M1H	Head of the first metatarsal
M5B	Base of the fifth metatarsal
M5H	Head of the fifth metatarsal
HAL	Distal edge of the proximal phalanx of the hallux
T2	Distal edge of middle phalanx of the second toe
T5	Distal edge of middle phalanx of the fifth toe

Ankle angles were determined using two kinematic models: a multisegment foot model and a single segment foot model (Figure 3-1). MULTI comprised three segments, similar to Okita et al. (2009): 1) rearfoot (RF): calcaneus; 2) forefoot (FF): all bones between the navicular and metatarsals, inclusive; and 3) toes (TOE): all five toes lumped into one segment. The ankle joint in MULTI was defined as the articulation between the shank and RF segment. SINGLE used one rigid segment to represent all the bones between the ankle and MTP joints. The toes were neglected except as a point at which the ground reaction forces could act. The ankle was defined as the joint between this single foot segment and the shank. Reference frame definitions

for the single segment of SINGLE and the RF segment of MULTI were identical to allow direct comparison of the ankle kinematics between the two models (Table 3-2).

Static trials were used to create local segment reference frames and define the neutral positions for each joint, similar to Caravaggi et al. (2009). Inertial properties and center of mass (COM) locations for the shank were calculated from the subject mass and limb dimensions as in Winter (2009). Moment of inertia tensors and masses for the foot segments were the same for all subjects and were as in Anderson and Pandy (1999), with their single segment foot values split into equal halves for the RF and FF segments. Foot segment center of mass (COM) locations were calculated as the average of each segment's marker locations. The origin of each segment reference frame was located at the segment's COM. Marker and force plate data were extracted from C3D files using The Biomechanical ToolKit (Barre and Armand, 2014) and calculations were performed in MATLAB 2015a.

Table 3-2 Definitions of unit vectors used to define segment reference frames for the segments of the multisegment foot model. The single segment foot model shares the same reference frame definition as the rearfoot to standardize the ankle joint convention. See Table 3-1 for full marker names.

Segment	x-axis (inv/eversion)	y-axis (ab/adduction)	z-axis (plantar/dorsiflexion)
Rearfoot	CA to M1H	Cross product: *x*-axis and vector from CA to midpoint of M1H and M5H	Cross product: *x* and *y* axes
Forefoot	Cross product: *y* and *z* axes	Cross product of *z*-axis and vector from M5H to M1H	M1H to M5H
Toes	M1H to HAL	Cross product: *x*-axis and vector from T5 to HAL	Cross product: *x* and *y* axes

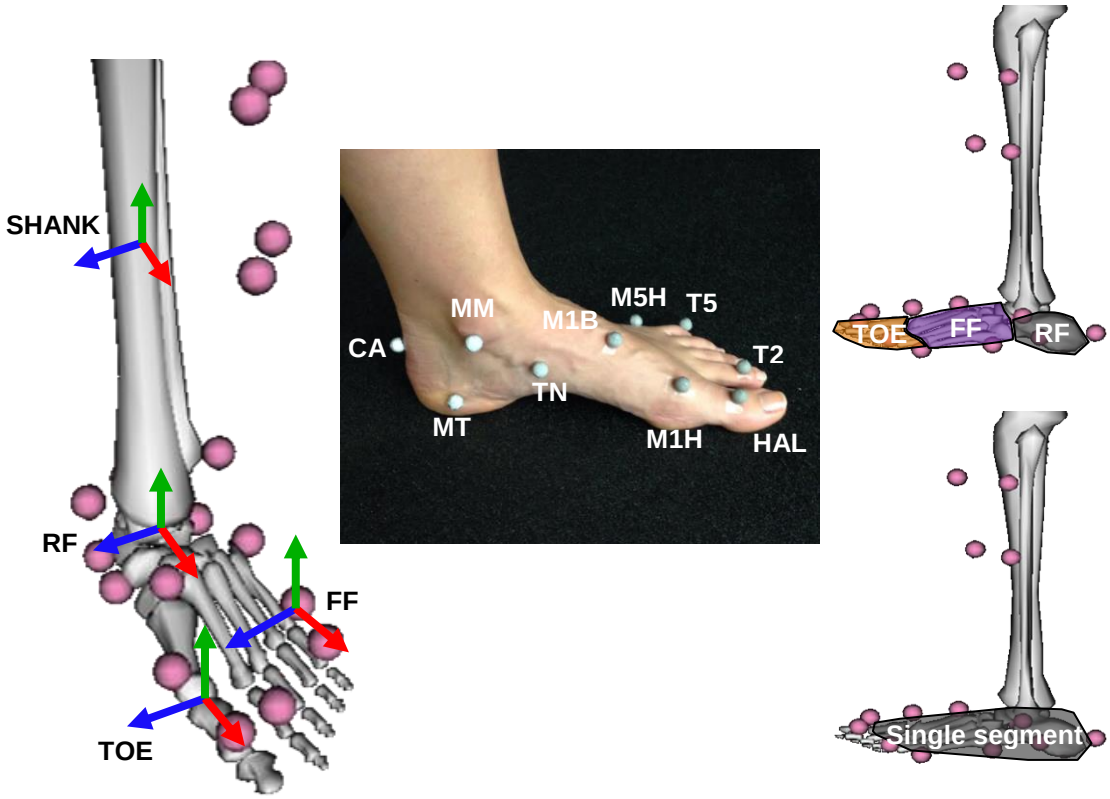

Figure 3-1 The segment reference frames for the multisegment foot model (left), marker set (center), and the two foot models (right). The SHANK reference frame was the same for both models and the single segment foot reference frame in SINGLE was the same as the RF reference frame in MULTI. The multisegment foot model included three segments (RF = rearfoot, FF = forefoot, and TOE). Images generated by OpenSim 3.1 (Delp et al., 2007). In each reference frame, the red arroe indicates the x-axis, the green arrow indicates the y-axis, and the blue arrow indicates the z-axis.

Segment rotation matrices for each trial were computed from the marker locations (Challis, 1995) and used to compute joint rotation matrices for the ankle joint (RF relative to shank), the midtarsal joint (FF relative to RF), and the MTP joint (TOE relative to FF). Joint rotation matrices were expressed relative to the neutral standing position and decomposed into Cardan angles using a ZXY sequence. Rotations about the x-axis corresponded to frontal plane motion (inversion/eversion), the y-axis corresponded to transverse plane motion (ab/adduction), and the z-axis corresponded to sagittal plane motion (flexion/extension).

Performing inverse dynamics with MULTI required knowledge of the forces and moments acting on each foot segment (RF, FF, TOES). During foot flat, multiple segments could

be in contact with the ground, with the GRF distributed among these segments. Two approaches to deal with this were tested in a single subject: 1) the subject was asked to perform targeted landings on two adjacent force plates with the midfoot joint landing on the junction, and 2) the entire GRF was assigned to only one foot segment at a time, with the segment assignment determined as a function of the center of pressure (COP). The two approaches resulted in nearly equivalent resultant joint moments, therefore, the second approach was chosen to limit the effect of force plate targeting, reduce the number of trials, and avoid potential inconsistencies from combining multiple trials (see Appendix B). At each point during the stance phase, the GRF was assigned to the segment whose boundary (defined by the proximal and distal joint centers) contained the COP location.

Resultant joint forces and moments during stance were determined through recursive Newton-Euler inverse dynamics. Joint centers were the same in both models and were chosen as the midpoint between markers LM and MM (ankle), the midpoint between markers NV and M5B (midtarsal), and at the location of the M1H marker (MTP). At each joint and for each timepoint during the stance phase, the instantaneous mechanical power, P_j, was calculated as the scalar product of the resultant joint moment and joint angular velocity:

$$P_j = \boldsymbol{M}_j \cdot \boldsymbol{\omega}_j$$

Where,

$\boldsymbol{M}_j$ is the resultant joint moment vector

$\boldsymbol{\omega}_j$ is the joint angular velocity vector

Periods of positive and negative instantaneous power during stance were integrated and summed to obtain the total positive and negative work at each joint.

Resultant joint moments, powers, and work were normalized to body mass. Statistical analyses for time series data were performed using statistical parametric mapping (SPM), which

tests for differences in vector fields instead of scalar values and are more appropriate for time series data that do not vary randomly (Pataky, 2010; Pataky et al., 2013). SPM is analogous to traditional scalar statistics but accounts for covariance along the field and field smoothness and size. Random field behavior determines if the test statistic (in this study, *t or* T^2) exceeds the critical threshold for a chosen Type I error rate ($\alpha = 0.05$). In this study, 3-dimensional data (e.g., joint angles), were tested with SPM paired Hotelling's T^2 tests. If significance was reached, SPM paired t-tests were performed on the three vector components and a Sidak corrected threshold of $\alpha = 0.0170$ was used to maintain a familywise error rate of $\alpha = 0.05$. However, it should be noted that testing each vector component separately does not account for inter-component covariance, which may have resulted in Type II errors for individual component *post-hoc* tests. For 1-dimensional data (e.g., instantaneous joint power), SPM paired t-tests were performed. For non-time-based scalar data (e.g., joint work), traditional paired Student's t-tests were performed. Statistical tests were performed in Python 3.6.1 (Anaconda Distribution, Continuum Analytics, Austin, TX) with the spm1d package (Pataky, 2012; version M.0.4.5, www.spm1d.org) or MATLAB R2016a (version 9.0.0.361340) with the Statistics and Machine Learning Toolbox (The Mathworks Inc., Natick, MA).

3.4 Results

3.4.1 Ankle kinematics comparison

Significant differences in ankle angle between SINGLE and MULTI were found during the stance phase, as the T^2 test statistic exceeded the critical threshold of 99.729 (Figure 3-2). Therefore, the null hypothesis that ankle angles were equal between the two models was rejected. *Post-hoc* paired t-tests on the ankle angle components (frontal, transverse, sagittal planes) revealed significant differences between MULTI and SINGLE in all three planes (Figure 3-3). During early stance (16 – 27%), MULTI displayed slightly less ankle adduction than SINGLE. During midstance, MULTI displayed reduced dorsiflexion from 40 – 61% of stance. During late stance, MULTI exhibited both reduced plantarflexion (86 – 100% stance) and reduced adduction (90 -100% stance) angles compared with SINGLE.

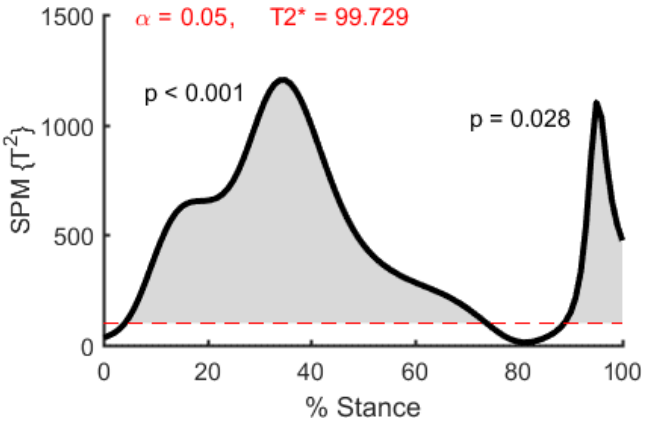

Figure 3-2 A paired Hotelling's T^2 test revealed a significant difference in ankle angle. The red dotted line indicates the threshold for statistical significance and gray shaded regions signifiy points where the test statistic exceeded the threshold.

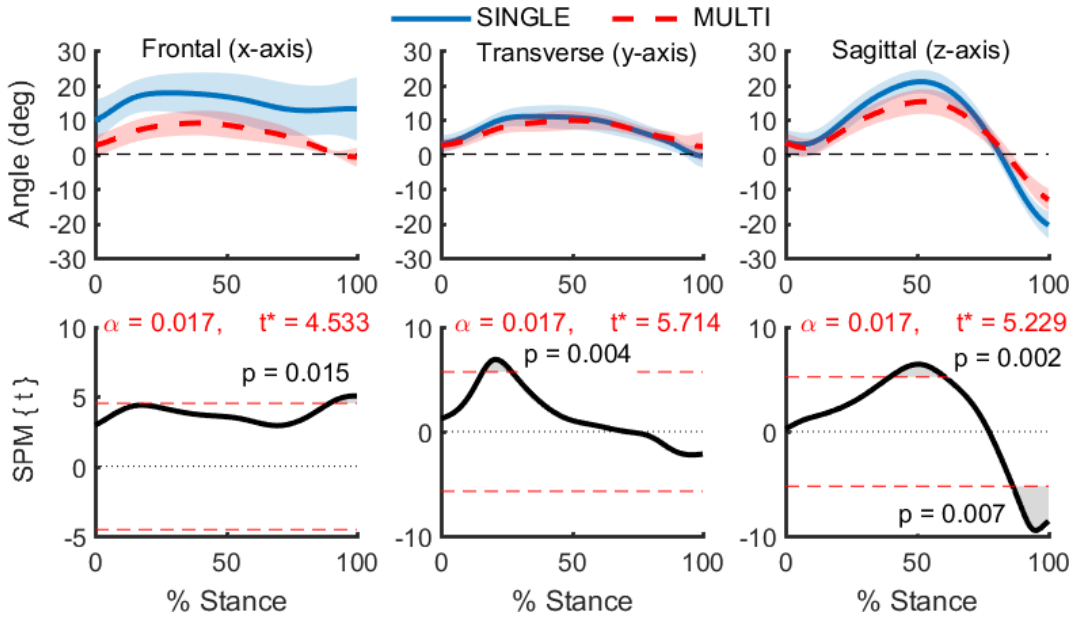

Figure 3-3 Comparison of ankle angles during stance computed using two different foot models: SINGLE - single segment foot (solid blue), MULTI - multisegment foot (dotted red). Data computed from barefoot running at 3.1 m/s. Shaded regions show ± 1 S.D. The top row shows ankle angles throughout the stance phase. Angle conventions are inversion(+)/eversion(-), abduction(+)/adduction(-), and dorsiflexion(+)/plantarflexion(-). The bottom row shows results from paired t-tests btween SINGLE and MULTI, with the red dotted lines representing the t-statistic threshold for statistical significance. Gray shaded areas outside of the red dotted lines show regions with significant differences between SINGLE and MULTI.

Ankle angular velocity was also significantly different between SINGLE and MULTI, as the T^2 test statistic exceeded the critical threshold of 250.722 (Figure 3-4). Therefore, the null hypothesis that the ankle angular velocities were similar between the models was rejected. *Post-hoc* paired t-tests on the angular velocity components between SINGLE and MULTI revealed differences in the transverse plane and sagittal planes (Figure 3-5). In the sagittal plane, MULTI exhibited reduced dorsiflexion velocity during early stance and reduced

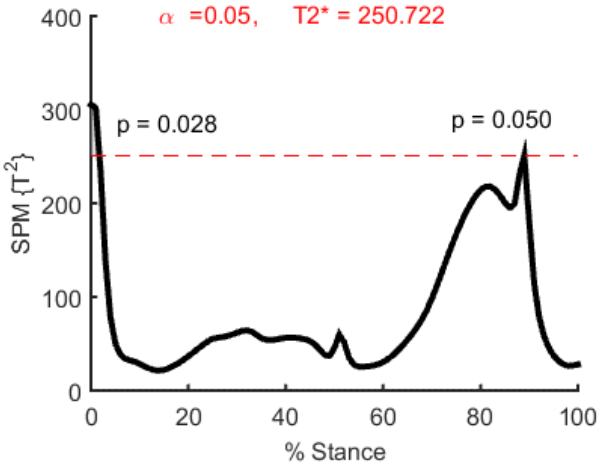

Figure 3-4 A paired Hotelling's T^2 test revealed a significant difference in ankle angular velocities during stance. The red dotted line indicates the threshold for statistical significance and gray shaded regions signifiy points where the test statistic exceeded the threshold..

plantarflexion velocity during late stance. In the transverse plane, the angular velocities of the two models occasionally differed in sign (Figure 3-5, top center plot). Near 30% of stance, MULTI displayed little to no ankle rotation in the direction of abduction (positive rotations about the y-axis), while SINGLE displayed a small rotation velocity towards adduction. The opposite pattern was found during late stance with MULTI reporting rotations in the adduction direction (negative angular velocity) and SINGLE reporting close to zero angular velocity.

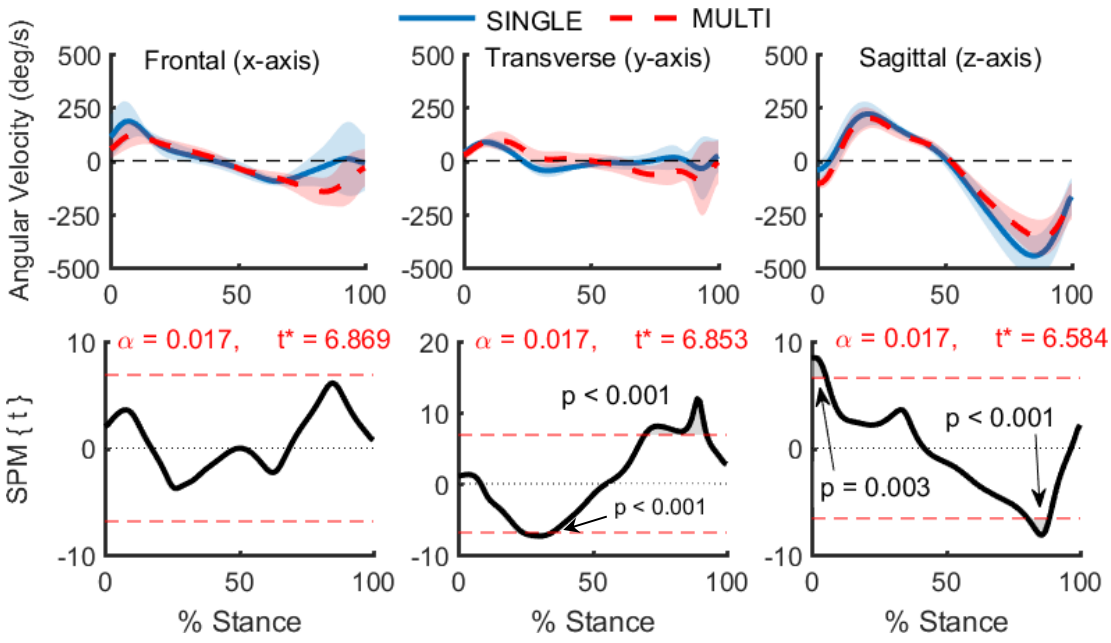

Figure 3-5 Comparison of ankle angular velocities during stance computed using two different foot models: SINGLE - single segment foot (solid blue), MULTI - multisegment foot (dotted red). Data computed from barefoot running at 3.1 m/s. Shaded regions show ± 1 S.D. The top row shows ankle angular velocities throughout the stance phase. Angle conventions are inversion(+)/eversion(-), abduction(+)/adduction(-), and dorsiflexion(+)/plantarflexion(-). The bottom row shows results from paired t-tests btween SINGLE and MULTI with the red dotted lines representing the t-statistic threshold for statistical significance. Gray shaded areas outside of the red dotted lines show regions with significant differences between SINGLE and MULTI.

3.4.2 Ankle kinetics comparison

Ankle joint moments computed using the two models were significantly different during the stance phase, as the T^2 test statistic exceeded the critical threshold of 261.959 (Figure 3-6). *Post-hoc* paired t-tests on the joint moment components between SINGLE and MULTI displayed significant differences in the frontal and sagittal plane during early and midstance and differences in all three planes during late stance (Figure 3-7). Though these differences were

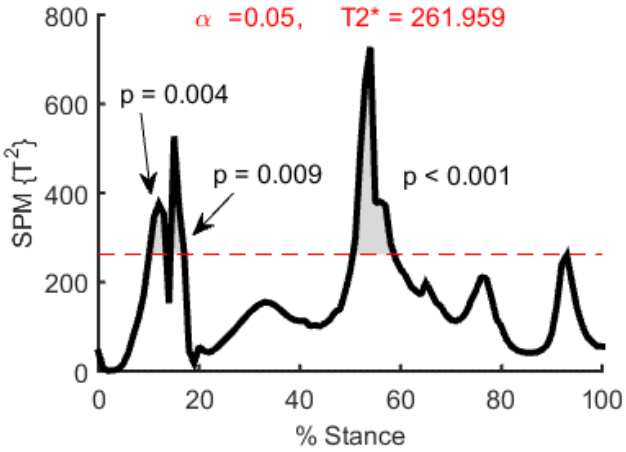

Figure 3-6 A paired Hotelling's T^2 test revealed a significant difference in the ankle joint moments during stance. The red dotted line indicates the threshold for statistical significance and gray shaded regions signifiy points where the test statistic exceeded the threshold.

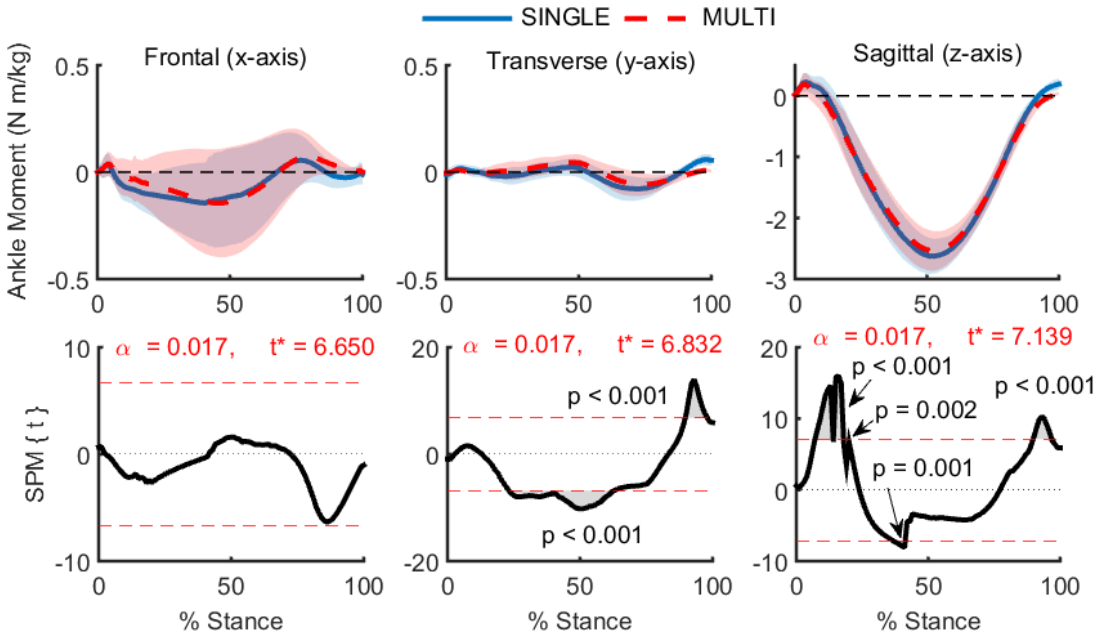

Figure 3-7 Comparison of ankle joint moments during stance computed using two different foot models: SINGLE - single segment foot (solid blue), MULTI - multisegment foot (dotted red). Data computed from barefoot running at 3.1 m/s. Shaded regions show ± 1 S.D. The top row shows ankle angles throughout the stance phase. Angle conventions are inversion(+)/eversion(-), abduction(+)/adduction(-), and dorsiflexion(+)/plantarflexion(-). The bottom row shows results from paired t-tests btween SINGLE and MULTI with the red dotted lines representing the t-statistic threshold for statistical significance. Gray shaded areas outside of the red dotted lines show regions with significant differences between SINGLE and MULTI.

statistically significant, they were relatively small in magnitude and likely have little functional significance. For example, the significantly different cluster at 31 – 42% of stance (Figure 3-7, far right plots), represents a difference between the models of 0.02 ± 0.008 N·m·kg^{-1}.

Instantaneous ankle joint power was also significantly different between SINGLE and MULTI as the T^2 critical threshold of 5.785 was exceeded during 76 – 83% of stance ($p < 0.001$; Figure 3-8). Therefore, the null hypothesis that the models produced equal ankle joint power was rejected. During this period, ankle power computed with MULTI was lower than the ankle power computed with SINGLE with a mean difference between the models (across all subjects) ranging from 0.9 to 3.1 W·kg^{-1}. This represents a difference of 18 – 22% of the ankle power computed by SINGLE and suggests that traditional single segment foot models overestimate ankle joint power during a portion of push-off.

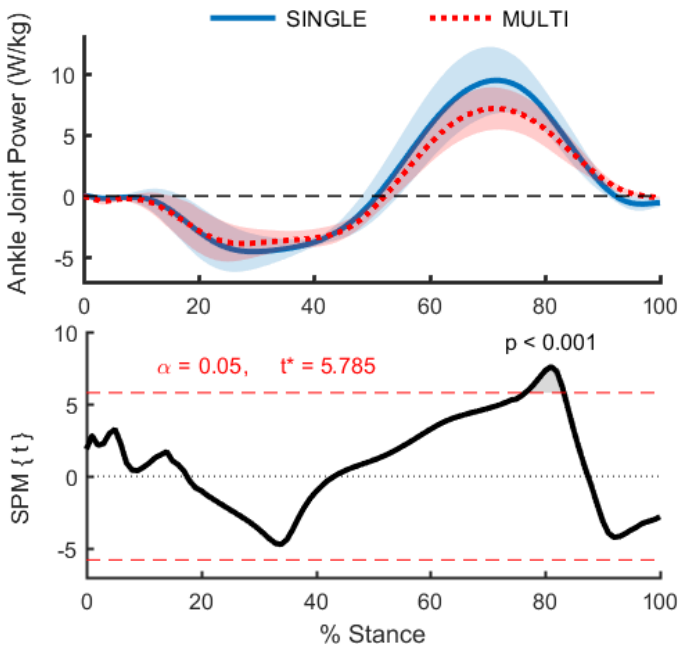

Figure 3-8 Comparison of instantaneous ankle joint power during stance computed using two different foot models: SINGLE - single segment foot (solid blue), MULTI - multisegment foot (dotted red). Data computed from barefoot running at 3.1 m/s. Shaded regions show ± 1 S.D. Bottom plot shows results from a paired t-test, with the red dotted lines representing the t-statistic threshold for statistical significance. Gray shaded areas outside of the red dotted lines show regions with significant differences between SINGLE and MULTI.

The difference between the two models occurred around 80% of stance, just after the peak ankle power production (which occurred at 72% of stance for both models). These joint power differences were primarily due to the differences in joint angular velocity between the models, as these velocity differences were much larger than the joint moment differences.

Positive ankle joint work was significantly different between SINGLE and MULTI, with MULTI generating 41% less positive work than SINGLE during push-off (Figure 3-9; mean difference = 0.33 ± 0.03 J·kg^{-1}; $p < 0.001$). A significant difference in negative ankle joint work was also detected between MULTI and SINGLE, with MULTI absorbing 28% less energy during early stance (mean difference = 0.12 ± 0.06 J·kg^{-1}; $p = 0.001$).

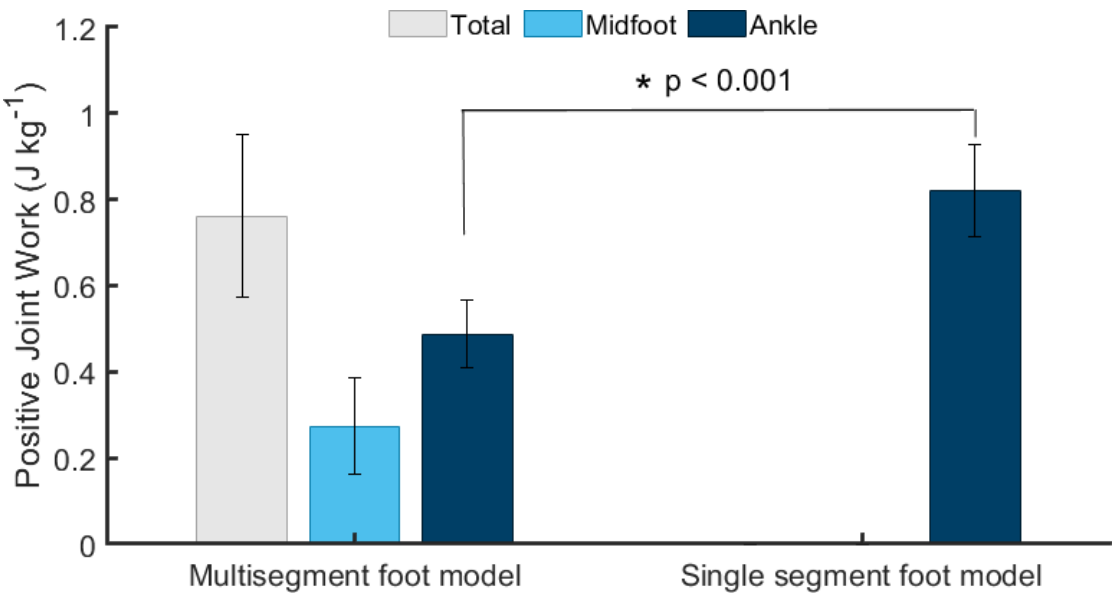

Figure 3-9 Comparison of positive joint work performed at each joint in the two models: MULTI = multisegment foot model (left bar group), SINGLE = single segment foot model (right bar). Ankle positive work (dark blue) was significantly different between the foot models, but the summed ankle and midfoot from MULTI (gray bar) was similar to ankle joint work from SINGLE (dark blue), suggesting that SINGLE captured midfoot joint power in the ankle joint power.

3.4.3 Midfoot joint mechanics

In MULTI, the midfoot joint was defined as the orientation of the FF segment relative to the RF segment and represented the collective behavior of all the joints between the talus and metatarsals. All results presented in this subsection are from MULTI only, as SINGLE did not include a midfoot joint. During stance, the midfoot joint absorbed energy during early stance and generated energy during late stance, similar to the temporal pattern found at the ankle (Figure 3-10). A SPM paired t-test between the ankle and midfoot joint powers (both computed using MULTI) revealed that the ankle absorbed more power than the midfoot during portions of early stance (at foot contact, $p < 0.046$, and at 23 – 33% of stance, $p < 0.001$). However, the ankle and midfoot joint generated statistically similar amounts of power throughout late stance. During push-off, the midfoot joint generated a peak of 5.6 ± 1.2 W·kg^{-1} of joint power. Despite similar power generation, positive joint work during stance was greater in the ankle than the midfoot joint ($p = 0.01$; difference = 0.25 ± 0.17 J·kg^{-1}; Figure 3-9). The sum of the positive work performed at the midfoot joint and ankle joint in MULTI was similar to the positive work performed at the ankle joint in SINGLE. This suggests that positive ankle joint

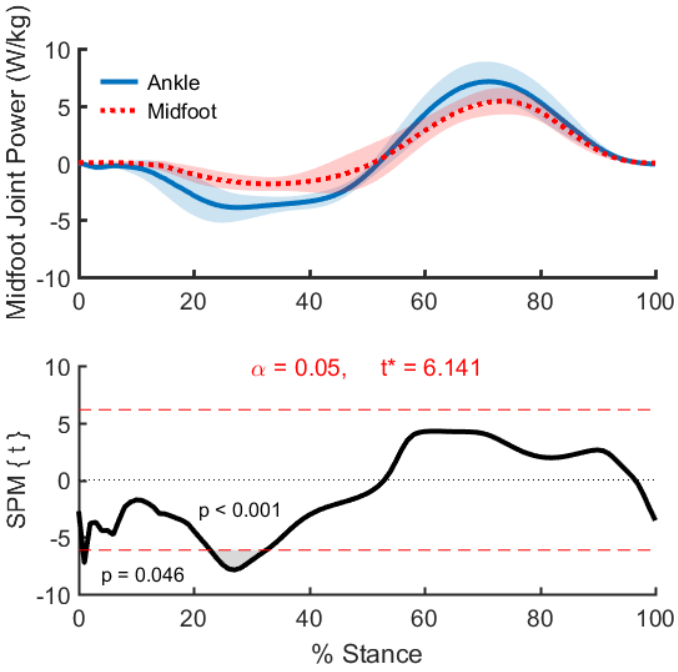

Figure 3-10 Joint powers at the ankle joint (solid blue) and midfoot joint (dashed red) during the stance phase of running. The "midfoot joint" is defined as the orientation of the FF segment relative to the RF segment and represents the collective function of all the joints between the talus and metarasals (midtarsal and tarsometatarsal joints).

work in SINGLE was a combination of work done by the joints of the midfoot and the ankle joint combined, thereby overestimating the ankle's contribution to positive work during stance.

3.5 Discussion

This study has demonstrated that foot model topology can influence the analysis of ankle joint mechanics during running. It was hypothesized that a multisegment foot model (MULTI) would alter ankle joint kinematics and kinetics compared with a single segment foot model (SINGLE). This hypothesis was supported as stance phase ankle joint angles, angular velocities, joint moments, joint power, and positive joint work were different between MULTI and SINGLE. As joint kinematics and kinetics play a central role in our interpretation of joint and muscle function during locomotion, these results provide evidence that oversimplification of the foot in biomechanical modeling can produce potentially incorrect outcomes for ankle joint mechanics. This study also suggests that single segment foot models omit potentially important information about energy contributions from the arch of the foot during running. In MULTI, the midfoot joint generated substantial energy during stance (statistically similar to that generated by the ankle joint). These results indicate that the arch of the foot plays a potentially important energetic role during running, as it both absorbs energy during early stance and generates energy during late stance. Ignoring midfoot joint work by using models that are too simple may incorrectly attribute work done by the muscles, tendons, and ligaments of the foot to the muscles and tendons of the ankle joint.

The work and power differences between the two models were caused mainly by kinematic differences. Ankle joint angles between SINGLE and MULTI were different across all three planes of movement, with the largest differences occurring in the frontal and sagittal planes. Overall, temporal profiles were similar, but ankle angles from MULTI tended to remain closer to

neutral than those from SINGLE. In the frontal plane, MULTI was less everted than SINGLE (by approximately 0.15 radians) throughout most of stance (except the period between 57% and 78%). In the sagittal plane, MULTI exhibited 28.5 degrees of total excursion while SINGLE exhibited 41.7 degrees of total excursion. The lower total excursion of MULTI was due to both a reduction in dorsiflexion during midstance and a reduction in plantarflexion during late stance (Figure 3-3). The excursion from MULTI was closer to that reported by the bone pin investigations (30.4 ± 4.3 degrees; calcaneus, talus, and tibia motions similar to the ankle joint definition in this study) of Arndt et al. (2007). The reduced sagittal plane rotations in MULTI occurred over the same period of time, therefore, sagittal plane angular velocity was reduced in MULTI compared to SINGLE. However, MULTI computed faster transverse plane rotations than SINGLE and produced slight adduction of the ankle (negative rotation about the y-axis) during push-off that was not using SINGLE.

The differences in angular velocity were the main cause of the differences in ankle joint power, as the differences in ankle joint moments were small and occurred only during early and terminal stance (88 – 100% of stance). During the periods where the foot models produced different moments, ankle joint power was not significantly different. In SINGLE, the foot as a whole (ankle to MTP joints) was tracked by three markers distributed along the length of the foot (posterior calcaneus, 1st and 5th metatarsal heads). This model captured midfoot joint motion as ankle joint motion, which increased total ankle joint range of motion and angular velocity during stance, particularly during push-off. Experimental ankle kinematics are widely used to validate musculoskeletal models and tune model parameters (Hicks et al., 2015). Considering the differences between the two models studied here, researchers should use caution when tuning musculoskeletal model parameters to create simulations that match experimental kinematics obtained using single segment foot models. When these experimental results must be used,

sensitivity analyses should assess the effect of altered ankle joint kinematics on the resulting model parameters and outputs.

Midfoot joint kinematics during stance were similar to ankle joint kinematics, with dorsiflexion (arch angle and length increasing) during early stance and plantarflexion (arch angle and length decreasing) during late stance. Throughout stance, the midfoot joint generated a plantarflexion moment, with a peak of 1.95 ± 0.25 $N \cdot m \cdot kg^{-1}$. This resulted in substantial energy generation at the midfoot joint during push-off as the arch shortened, which was not statistically different from ankle joint power (Figure 3-10). The biological source of this mechanical power was likely the numerous muscles and passive tissues that cross the midtarsal and tarsometatarsal joints. However, due to their size, it is unclear whether these tissues are capable of producing the requisite power (peak mean ± SD: 5.4 ± 1.2 $W \cdot kg^{-1}$), which suggests that energy may be transferred to the midfoot joint from the ankle and/or MTP joints due to their multi-joint anatomy (Prilutsky and Zatsiorsky, 1994). Energy transfer between the MTP joints and the arch during running is thought to occur via the plantar aponeurosis (McDonald et al., 2016; Wager and Challis, 2016) and could also occur via the extrinsic toe flexors (FDL and FHL), which cross the ankle joint and function isometrically during walking (Hofmann et al., 2013). Energy transfer from the ankle to the midfoot joint could occur via the plantar aponeurosis, as it's force has been correlated to the Achilles tendon force (Carlson et al., 2000; Erdemir et al., 2004). This correlation is present despite little to no anatomical connection to the Achilles tendon in adults (Snow et al., 1995). The similarity in the energy profiles of the ankle and midfoot joints presented here suggest that the plantar aponeurosis and Achilles tendon may act similar to a multi-joint MTU between the shank and forefoot.

Limitations to this study were related to both the modeling and experimental methodology. Modeling the foot as a three-segment system required assumptions about the mobility of the foot during locomotion. In MUTLI, ankle rotations were defined as rotation of

the calcaneus relative to the tibia. During the stance phase of running, rotations of the calcaneus relative to the talus are 5-6 degrees in the sagittal and transverse planes, and 8 degrees in the frontal plane (Arndt et al., 2007). By defining the ankle as the articulation between the tibia and calcaneus, MULTI captured subtalar joint rotation as ankle joint rotation. Though this may have influenced the estimated ankle joint power, SINGLE also captured the same subtalar joint rotations within ankle joint rotation. Therefore, this should not affect the comparisons between the two models. Furthermore, the muscles that control the ankle joint also partially control the subtalar joint, so it may be reasonable to combine subtalar and ankle joint motions. In MULTI, the forefoot segment comprised all bones between the talus and phalanges and therefore represented the collective motion of all joints within that range. This definition of the forefoot segment has been shown to violate the rigid body assumption as the first and fifth metatarsal move relative to each other (Okita et al., 2009) and the foot's mediolateral arch deforms during stance. While this produced error mostly outside the sagittal plane, segment deformation could nonetheless influence the midfoot joint power during late stance. Furthermore, this study did not (mathematically) include energy changes that arose from the deformation of the plantar tissues in the foot, which may be meaningful (Takahashi and Stanhope, 2013). The experimental data collection required participants to land on the force plate. While explicit directions about where to land were not given to the participants, force plate targeting presents a potential source of error. Changes to multisegment foot kinematics during targeted running have not been published, but targeted running has minimal effects on ground reaction forces and thigh, shank, and foot (a single segment model) angles during running (Challis, 2001; Grabiner et al., 1995; Wearing et al., 2000). As the same data were used for kinematic calculations in both models, the difference between MULTI and SINGLE would likely be unchanged by force plate targeting. In the statistical testing of 3-dimensional vector data, *post-hoc* tests were conducted using paired t-tests

between SINGLE and MULTI on each vector component. It should be noted that this does not account for the covariance between the three vector components.

In conclusion, this study has provided evidence that ankle joint kinematics and kinetics during running differ as a function of foot model topology. The use of a multisegment foot model, as opposed to the traditional single segment foot model, resulted in altered kinematics characterized by a more neutral position of the ankle, reduced sagittal plane angular velocity throughout stance, and increased transverse plane velocity during push-off. Ankle joint power and positive work during late stance were reduced by approximately 25% when using a multisegment foot model compared to a single segment foot model. The multisegment foot model also revealed that the arch of the foot may play an important energetic role during stance, as midfoot joint power generation during late stance was not significantly different from ankle joint power generation. These results show the importance of tracking the calcaneus separately from the rest of the foot and including a midfoot joint in studies of the human ankle during running.

References

Anderson, F.C., Pandy, M.G., 1999. A Dynamic Optimization Solution for Vertical Jumping in Three Dimensions. Comput. Methods Biomech. Biomed. Engin. 2, 201–231.

Arndt, A., Wolf, P., Liu, A., Nester, C., Stacoff, A., Jones, R., Lundgren, P., Lundberg, A., 2007. Intrinsic foot kinematics measured in vivo during the stance phase of slow running. J. Biomech. 40, 2672–2678.

Arnold, J.B., Caravaggi, P., Fraysse, F., Thewlis, D., Leardini, A., 2017. Movement coordination patterns between the foot joints during walking. J. Foot Ankle Res. 10, 47.

Barre, A., Armand, S., 2014. Biomechanical ToolKit: Open-source framework to visualize and process biomechanical data. Comput. Methods Programs Biomed. 114, 80–87.

Bruening, D.A., Cooney, K.M., Buczek, F.L., 2012. Analysis of a kinetic multi-segment foot model part II: Kinetics and clinical implications. Gait Posture 35, 535–540.

Caravaggi, P., Pataky, T., Goulermas, J.Y., Savage, R., Crompton, R., 2009. A dynamic model of the windlass mechanism of the foot: evidence for early stance phase preloading of the plantar aponeurosis. J. Exp. Biol. 212, 2491–2499.

Caravaggi, P., Pataky, T., Günther, M., Savage, R., Crompton, R., 2010. Dynamics of longitudinal arch support in relation to walking speed: contribution of the plantar aponeurosis. J. Anat. 217, 254–261.

Carlson, R.E., Fleming, L.L., Hutton, W.C., 2000. The biomechanical relationship between the tendoachilles, plantar fascia and metatarsophalangeal joint dorsiflexion angle. Foot Ankle Int. 21, 18–25.

Carson, M.C., Harrington, M.E., Thompson, N., O'Connor, J.J., Theologis, T.N., 2001. Kinematic analysis of a multi-segment foot model for research and clinical applications: a repeatability analysis. J. Biomech. 34, 1299–1307.

Challis, J.H., 2001. The Variability in Running Gait Caused by Force Plate Targeting. J. Appl. Biomech. 17, 77–83.

Challis, J.H., 1995. A procedure for determining rigid body transformation parameters. J. Biomech. 28, 733–737.

Chang, R., Van Emmerik, R., Hamill, J., 2008. Quantifying rearfoot–forefoot coordination in human walking. J. Biomech. 41, 3101–3105.

Delp, S.L., Anderson, F.C., Arnold, A.S., Loan, P., Habib, A., John, C.T., Guendelman, E., Thelen, D.G., 2007. OpenSim: Open-Source Software to Create and Analyze Dynamic Simulations of Movement. IEEE Trans. Biomed. Eng. 54, 1940–1950.

Dixon, P.C., Böhm, H., Döderlein, L., 2012. Ankle and midfoot kinetics during normal gait: A multi-segment approach. J. Biomech. 45, 1011–1016.

Erdemir, A., Hamel, A.J., Fauth, A.R., Piazza, S.J., Sharkey, N.A., 2004. Dynamic loading of the plantar aponeurosis in walking. J. Bone Jt. Surg. 86, 546–552.

Farris, D.J., Sawicki, G.S., 2012. The mechanics and energetics of human walking and running: a joint level perspective. J. R. Soc. Interface 9, 110–118.

Grabiner, M.D., Feuerbach, J.W., Lundin, T.M., Davis, B.L., 1995. Visual guidance to force plates does not influence ground reaction force variability. J. Biomech. 28, 1115–1117.

Hicks, J.L., Uchida, T.K., Seth, A., Rajagopal, A., Delp, S.L., 2015. Is my model good enough? Best practices for verification and validation of musculoskeletal models and simulations of movement. J. Biomech. Eng. 137, 020905.

Hofmann, C.L., Okita, N., Sharkey, N.A., 2013. Experimental evidence supporting isometric functioning of the extrinsic toe flexors during gait. Clin. Biomech. 28, 686–691.

Kelly, L.A., Lichtwark, G.A., Farris, D.J., Cresswell, A., 2016. Shoes alter the spring-like function of the human foot during running. J. R. Soc. Interface 13, 20160174.

Ker, R.F., Bennett, M.B., Bibby, S.R., Kester, R.C., Alexander, R.M., 1987. The spring in the arch of the human foot. Nature 325, 147–149.

Leardini, A., Benedetti, M.G., Berti, L., Bettinelli, D., Nativo, R., Giannini, S., 2007. Rear-foot, mid-foot and fore-foot motion during the stance phase of gait. Gait Posture 25, 453–462.

MacWilliams, B.A., Cowley, M., Nicholson, D.E., 2003. Foot kinematics and kinetics during adolescent gait. Gait Posture 17, 214–224.

McDonald, K.A., Stearne, S.M., Alderson, J.A., North, I., Pires, N.J., Rubenson, J., 2016. The Role of Arch Compression and Metatarsophalangeal Joint Dynamics in Modulating Plantar Fascia Strain in Running. PLOS ONE 11, e0152602.

Okita, N., Meyers, S.A., Challis, J.H., Sharkey, N.A., 2009. An objective evaluation of a segmented foot model. Gait Posture 30, 27–34.

Pataky, T.C., 2012. One-dimensional statistical parametric mapping in Python. Comput. Methods Biomech. Biomed. Engin. 15, 295–301.

Pataky, T.C., 2010. Generalized n-dimensional biomechanical field analysis using statistical parametric mapping. J. Biomech. 43, 1976–1982.

Pataky, T.C., Robinson, M.A., Vanrenterghem, J., 2013. Vector field statistical analysis of kinematic and force trajectories. J. Biomech. 46, 2394–2401.

Pothrat, C., Authier, G., Viehweger, E., Berton, E., Rao, G., 2015. One- and multi-segment foot models lead to opposite results on ankle joint kinematics during gait: Implications for clinical assessment. Clin. Biomech. 30, 493–499.

Prilutsky, B.I., Zatsiorsky, V.M., 1994. Tendon action of two-joint muscles: Transfer of mechanical energy between joints during jumping, landing, and running. J. Biomech. 27, 25–34.

Robertson, D.G.E., Winter, D.A., 1980. Mechanical energy generation, absorption and transfer amongst segments during walking. J. Biomech. 13, 845–854.

Siegel, K.L., Kepple, T.M., Caldwell, G.E., 1996. Improved agreement of foot segmental power and rate of energy change during gait: Inclusion of distal power terms and use of three-dimensional models. J. Biomech. 29, 823–827.

Snow, S.W., Bohne, W.H., DiCarlo, E., Chang, V.K., 1995. Anatomy of the Achilles tendon and plantar fascia in relation to the calcaneus in various age groups. Foot Ankle Int. Am. Orthop. Foot Ankle Soc. Swiss Foot Ankle Soc. 16, 418–421.

Stearne, S.M., Alderson, J.A., Green, B.A., Donnelly, C.J., Rubenson, J., 2014. Joint kinetics in rearfoot versus forefoot running: implications of switching technique. Med. Sci. Sports Exerc. 46, 1578–1587.

Stearne, S.M., McDonald, K.A., Alderson, J.A., North, I., Oxnard, C.E., Rubenson, J., 2016. The Foot's Arch and the Energetics of Human Locomotion. Sci. Rep. 6, 19403.

Takahashi, K.Z., Kepple, T.M., Stanhope, S.J., 2012. A unified deformable (UD) segment model for quantifying total power of anatomical and prosthetic below-knee structures during stance in gait. J. Biomech. 45, 2662–2667.

Takahashi, K.Z., Stanhope, S.J., 2013. Mechanical energy profiles of the combined ankle–foot system in normal gait: Insights for prosthetic designs. Gait Posture 38, 818–823.

Takahashi, K.Z., Worster, K., Bruening, D.A., 2017. Energy neutral: the human foot and ankle subsections combine to produce near zero net mechanical work during walking. Sci. Rep. 7, 15404.

Tulchin, K., Orendurff, M., Adolfsen, S., Karol, L., 2009. The Effects of Walking Speed on Multisegment Foot Kinematics in Adults. J. Appl. Biomech. 25, 377–386.

Tulchin, K., Orendurff, M., Karol, L., 2010. The effects of surface slope on multi-segment foot kinematics in healthy adults. Gait Posture 32, 446–450.

Wager, J.C., Challis, J.H., 2016. Elastic energy within the human plantar aponeurosis contributes to arch shortening during the push-off phase of running. J. Biomech. 49, 704–709.

Wearing, S.C., Urry, S.R., Smeathers, J.E., 2000. The effect of visual targeting on ground reaction force and temporospatial parameters of gait. Clin. Biomech. 15, 583–591.

Winter, D.A., 2009. Biomechanics and Motor Control of Human Movement, 4th ed. John Wiley & Sons, Inc., Hoboken, NJ.

Winter, D.A., 1983. Moments of force and mechanical power in jogging. J. Biomech. 16, 91–97.

Zelik, K.E., Takahashi, K.Z., Sawicki, G.S., 2015. Six degree-of-freedom analysis of hip, knee, ankle and foot provides updated understanding of biomechanical work during human walking. J. Exp. Biol. 218, 876–886.

Chapter 4

Influences of foot model topology on simulations of the ankle plantarflexor muscles during running

4.1 Abstract

Ankle plantarflexor muscle simulations are commonly used to provide insights into gastrocnemius and soleus function during human locomotion. However, these simulations have typically modeled the foot using a single rigid segment, which contrasts with the structure and mobility of the human foot. Here, a traditional single segment foot model was compared with a multisegment foot model (rearfoot, forefoot, and toes) for simulating the gastrocnemius and soleus muscles during the stance phase of running. Hill-type muscle models were used to represent the gastrocnemius and soleus. Experimental kinematics from seven healthy volunteers running at 3.1 m/s were used to drive both the single and multisegment foot models. The resulting ankle joint kinematics were used to estimate the muscle-tendon unit lengths and forces, which served as inputs into the gastrocnemius and soleus muscle models. For muscles, the multisegment foot model produced a lower simulated active state than the single segment foot model during mid- and late stance. These differences were due to muscle lengths that were closer to the optimal length and slower muscle velocities, which resulted from reductions to ankle joint excursion and ankle joint angular velocities when using the multisegment foot model. A sensitivity analysis demonstrated that the muscle model parameters and muscle architecture did not influence the active state difference, as 99.6% (soleus) and 97.6% (gastrocnemius) of all simulations resulted in a lower active state for the multisegment foot model. This suggests that kinematically-driven simulations of the ankle plantarflexors are influenced by the underlying foot model and that generating accurate ankle plantarflexor simulations partially relies on capturing rearfoot (calcaneus) motion separate from forefoot motion.

4.2 Introduction

Simulations of human movement provide a non-invasive, inexpensive and versatile method to understand muscle function. However, while simulations can provide valuable insights, they can also be highly sensitive to the underlying muscle and kinematic models. As no model is a perfect representation of the human form, important choices about model complexity must be made and these choices can influence simulations outcomes. Historically, the complexity of models utilized to simulate human running have ranged from simple models that describe a feature of running gait (e.g., spring-mass models; Blickhan, 1989), to detailed musculoskeletal models that simulate the 3-dimensional kinematics and kinetics of running (e.g., Hamner et al., 2010). While simple models typically provide results that are easier to interpret, they risk excluding important mechanical and physiological relationships. Conversely, more comprehensive models capture additional details but can require substantial computational time, rely on many unknown or difficult-to-measure parameters, and produce more complex results which can be harder to interpret. Therefore, in determining the proper complexity for a model, it is important to explore which components of the model influence the conclusions drawn from simulations and which components can be omitted without much impact on the results.

In simulations of the ankle plantarflexor muscles, the kinematic model of the foot may be a critical component, as the motion of the calcaneus partially determines the kinematics of the muscle-tendon units. While many simulations have modeled the foot using a single rigid segment (e.g., Robertson and Winter, 1980), some have modeled the foot using multiple rigid segments, with the foot sectioned into (at least) the rearfoot and forefoot (e.g., Dixon et al., 2012; MacWilliams et al., 2003). As the many joints of the human foot can move substantially during locomotion (Arndt et al., 2007; Nester et al., 2007a; Okita et al., 2013; Wolf et al., 2008), these multisegment models are likely more representative of the human form than single segment foot

models. Kinematic studies of the ankle have suggested that multisegment foot models produce different ankle joint kinematics during walking than single segment foot models (Dixon et al., 2012; Pothrat et al., 2015). In Chapter 3, the comparison between ankle mechanics for single and multisegment foot models was extended to running, and it was reported that ankle joint kinematics and power are significantly greater using the single segment foot model. Subsequently, this chapter aims to explore whether using a multisegment foot model alters ankle plantarflexor muscle simulations compared with a single segment foot model. As the multisegment foot model produced lower ankle joint velocities, there should be a corresponding reduction in muscle-tendon complex velocities. A reduction in muscle-tendon velocity should mean a lower muscle fiber velocity, which, due to muscle force-velocity properties, should correspond to an increase in muscle force. This increase in muscle force would require a reduced active state, thus the multisegment foot model should produce lower active states than the single segment foot model. Different muscle-tendon kinematics may also reduce the fiber lengths at which the gastrocnemius and soleus operate during force production which may also influence muscle active state because of muscle force-length properties. These factors (changes in muscle fiber velocities and lengths) are important because Hill-type muscle simulations are sensitive to length-dependent parameters (e.g., tendon slack length and optimal fiber length; Scovil and Ronsky, 2006).

The purpose of this study was to compare the active state of two simulated ankle plantarflexor muscles during running using two kinematic foot models: 1) a multisegment foot model (MULTI), and 2) a single segment foot model (SINGLE). A Hill-type model was used to model each muscle-tendon unit: 1) a uniarticular ankle plantarflexor muscle that represented the soleus, and 2) a biarticular ankle plantarflexor muscle (crossing the ankle and knee joints) that represented the gastrocnemius. It was hypothesized that the active state of both ankle plantarflexor muscles would be reduced when simulated using MULTI compared with SINGLE. It was expected

that the reduced sagittal plane ankle angular velocity in the multisegment model would slow the fiber shortening velocities and therefore reduce the active state in the simulations performed.

4.3 Methods

To explore the influence of foot model topology on simulations of the ankle plantarflexor muscles, two kinematic foot models (single segment, SINGLE; multisegment, MULTI) were used to estimate the MTU lengths of the gastrocnemius and soleus (Figure 4-1). The simulations were driven using the mean kinematics and kinetics of the stance phase of seven healthy runners who ran barefoot at 3.1 m/s across an in-ground force plate. Kinematics of the shank, rearfoot, forefoot, and toes were collected using 27 passive retroreflective markers placed on bony landmarks of the lower limb, including 11 markers placed directly on the foot. Marker positions during each trial were tracked by a six-camera motion capture system (Motion Analysis Corporation, Mountain View, CA) sampling at 150 Hz. Marker positions were filtered using a second-order recursive Butterworth filter with a cutoff frequency of 10 Hz. Ground reaction forces and moments (GRF) were collected at 1500 Hz from a 90 x 60 cm force plate (Model 9287A, Kistler Instrument Corporation, Amherst, NY). The GRF data were lowpass filtered using a second-order recursive Butterworth filter with a cutoff frequency of 45 Hz. Details regarding the definition of each foot model, markers used to track each segment, and the calculation of the ankle joint kinematics is described in detail in Chapter 3.

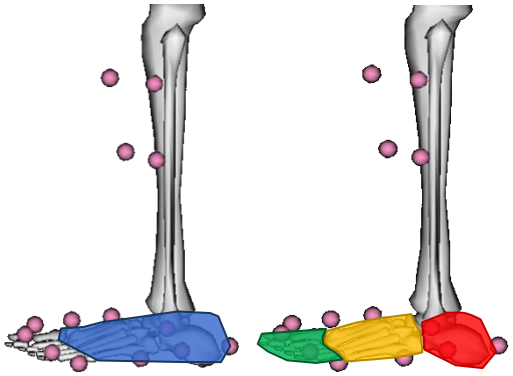

Figure 4-1 Diagram of the two kinematic foot models used to determine ankle angle.
SINGLE: one segment was used to represent the bones between the ankle and metatarsophalangeal joints.
MULTI: three segments defined separate rearfoot (blue), forefoot (yellow), and toes (green) segments.

In short, SINGLE used one segment to represent all bones between the ankle and metatarsophalangeal joints, which was consistent with traditional biomechanical analyses (e.g., Winter, 2009). MULTI used three segments to represent the foot bones: the rearfoot, forefoot, and toes. Both models used the same ankle joint definition, with the only difference being the markers associated with the distal segment of the joint. In SINGLE, the distal segment was defined as the entire foot and was tracked using markers on the heel, first metatarsal head, and fifth metatarsal head. In MULTI, the distal segment was the calcaneus and was tracked by three markers on the heel. For additional details, see Chapter 3 (page 33).

The soleus and gastrocnemius muscles were each modeled using a Hill-type muscle model. Though these muscles both insert on the calcaneus via the Achilles tendon, cadaveric studies and ultrasound imaging have demonstrated that the tendons arising from the two muscles may function independently, as evidenced by intratendinous sliding and non-uniform strain within the Achilles tendon (Arndt et al., 2012; Franz et al., 2015; Slane and Thelen, 2014). Therefore, the two muscles were modeled using separate Hill-type models, each with their own muscle force, MTU kinematics, and model parameters. For each foot model, sagittal plane ankle and knee kinematics were averaged across subjects and input into the equations of Grieve et al. (1978) to determine MTU length change as a function of the ankle and knee joint angles. The equations of Grieve et al. (1978) estimated the MTU length changes as a percent of shank length, therefore, the computed length changes were multiplied by the subjects' mean shank length to convert them to an absolute value,

$$\Delta l_{MTU,SOL} = (A_2\theta_A^2 + A_1\theta_A + A_0) \cdot l_{shank} \quad (4.1)$$

$$\Delta l_{MTU,GAS} = (A_5\theta_K^2 + A_2\theta_A^2 + A_4\theta_K + A_1\theta_A + A_3 + A_0) \cdot l_{shank} \quad (4.2)$$

Where,

$\Delta l_{MTU,SOL}$ and $\Delta l_{MTU,GAS}$ are the change in length of the soleus and gastrocnemius muscle-tendon units, respectively

Constants A_0, A_1, and A_2 are equal to -22.18468, 0.30141, and -0.00061

Constants A_3, A_4, and A_5 are equal to 6.46251, -0.07987, and 0.00011

θ_A and θ_K is the ankle and knee joint angles, respectively

Muscle-tendon lengths were then determined using the muscle's reference length, which was the assumed to be the sum of the muscle's optimal fiber length and resting tendon length,

$$l_{MTU} = \left(l_{f,opt} + l_{t0}\right) + \Delta l_{MTU} \tag{4.3}$$

Where,

l_{MTU} is the muscle-tendon unit length

$l_{f,opt}$ is the optimal muscle fiber length

l_{t0} is the resting tendon length

To compute the Achilles tendon moment arm, the equation of Grieve et al. (1978) was differentiated with respect to the ankle joint angle and then multiplied by the subjects' mean shank length to convert the relative value of Grieve et al. (1978) to an absolute value,

$$r_{AT} = (2\,A_2\theta_A + A_1) \cdot l_{shank} \tag{4.4}$$

Where,

r_{AT} is the Achilles tendon moment arm

θ_A is the ankle joint angle

Both the gastrocnemius and soleus models used the same Achilles tendon moment arm due to a common insertion on the calcaneus. Muscle forces were computed from the resultant ankle joint moment; it was assumed that two-thirds of the moment was provided by the soleus and one-third provided by the gastrocnemius (Out et al., 1996), though this was subsequently varied by changing the muscle force ratio parameter, α, in a sensitivity analysis. Therefore,

$$F_{PF} = \frac{M_j}{r_{AT}} \tag{4.5}$$

$$F_{PF} = F_{SOL} + F_{GAS} \tag{4.6}$$

$$F_{SOL} = \alpha \cdot F_{GAS} \tag{4.7}$$

Where,

F_{PF} is the total plantarflexor muscle force required (sum of the two muscle models)

M_j is the resultant ankle joint moment

r_{AT} is the moment arm of the Achilles tendon

F_{SOL} is the force of the soleus muscle model

F_{GAS} is the force of the gastrocnemius muscle model

α is the ratio of soleus to gastrocnemius muscle force, initially assumed to be 2

The force output of each muscle model was described by,

$$F_m = q \cdot fl(l_f) \cdot fv(v_f) \cdot F_{m,max} \tag{4.8}$$

Where,

F_m is the force output of the muscle model (F_{GAS} or F_{SOL})

q is the muscle model active state ($0 \leq q \leq 1$)

fl is the fraction of the maximum isometric force possible by the muscle due to its force-length properties, which are dictated by fiber length (l_f)

fv is the fraction of the maximum isometric force possible by the muscle due to its force-velocity properties, which are dictated by fiber velocity (v_f)

$F_{m,max}$ is the maximum possible isometric force output for the muscle model

The goal of the analysis was to solve for the model's active state, q, and compare the active state between the two kinematic foot models. Once F_m was determined for each muscle, tendon strain was computed using the model's force relative to the maximum isometric force,

$$\varepsilon_t = c \cdot \frac{F_m}{F_{m,max}} \tag{4.9}$$

Where,

ε_t is the tendon strain

F_m is the muscle force at the current time point

$F_{m,max}$ is the maximum possible isometric force output for the muscle model

c is a constant defining the tendon strain at $F_{m,max}$

Tendon length, l_t, was calculated from tendon strain using the resting tendon length, l_{t0},

$$l_t = l_{t0} + \varepsilon_t \cdot l_{t0} \tag{4.10}$$

and subtracted from MTU length to obtain muscle fiber length, l_f,

$$l_f = l_{MTU} - l_t \tag{4.11}$$

Subsequently, the force-length fraction at a given fiber length was computed,

$$fl = 1 - \left[\frac{l_f - l_{f,opt}}{w \cdot l_{f,opt}}\right]^2 \tag{4.12}$$

Where,

w is the width of the force-length curve

The force-velocity fraction during muscle shortening was determined by the equation of Hill (1938),

$$fv = \frac{v_{fmax} - v_f}{v_{fmax} + k \cdot v_f} \tag{4.13}$$

Where,

v_{fmax} is the maximum shortening velocity of the muscle

v_f is the muscle fiber velocity

k is a parameter specifying the shape of the force-velocity curve

During muscle lengthening, the force-velocity fraction was determined by the equation of Fitzhugh (1977),

$$fv = 1.5 - 0.5\left[\frac{v_{fmax} + v_f}{v_f \cdot (v_{fmax} - 2 \cdot k)}\right] \tag{4.14}$$

With the muscle kinematics and forces determined, each muscle's active state, q, was obtained by solving equation (4.8),

$$q = \frac{F_m}{fl(l_f) \cdot fv(v_f) \cdot F_{m,max}} \tag{4.15}$$

Simulations were performed using the kinematics from each foot model and a set of nominal muscle model parameters (Table 4-1). However, as muscle models are sensitive to the parameters that describe the muscle model's architecture and functional relationships, sensitivity analyses were performed by varying seven of the model parameters (See Appendix C, Table C-1 and Table C-2). Simulations were performed for each possible combination of the seven parameters, yielding 15,360 simulations. Sensitivity of the model to each parameter was also assessed by varying each parameter in isolation. The parameters are interdependent and therefore interact with each other, however this analysis shows that some parameters were more sensitive to the choice of foot model than others. All analyses were performed in MATLAB R2016a (9.0.0.341360).

Table 4-1 Nominal muscle model parameter values used during the simulations.

	$\boldsymbol{l_{f,opt}}$ (m)	$\boldsymbol{l_{t0}}$ (m)	$\boldsymbol{w}$ $(-)$	$\boldsymbol{c}$ $(-)$	$\boldsymbol{v_{f,max}}$ $(\boldsymbol{l_{f,opt}/s})$	$\boldsymbol{k}$ $(-)$	$\boldsymbol{F_{m,max}}$ (N)
Soleus	0.076	0.226	0.56	0.05	8	2.44	4000
Gastrocnemius	0.055	0.365	0.56	0.05	8	2.44	2000

$l_{f,opt}$ = optimal fiber length, l_{t0} = tendon slack length, w = width of force-length relationship curve, c = tendon strain at maximum isometric muscle force, $v_{f,max}$ = maximum unloaded fiber shortening velocity, k = force-velocity curvature parameter, $F_{m,max}$ = maximum isometric muscle force.

4.4 Results

This section presents the results of the muscle model simulations using the kinematics from the two foot models, SINGLE and MULTI. Due to their relevance to this chapter, the experimental data that were used to drive the muscle models (from Chapter 3) are presented in Section 4.4.1. Section 4.4.2 and 4.4.3 give the results from the soleus and gastrocnemius simulations using the nominal set of muscle model parameters (Table 4-1). The results of the sensitivity analyses for the gastrocnemius and soleus are presented in Sections 4.4.4 and 4.4.5, respectively.

4.4.1 Experimental data

The kinematics and kinetics of SINGLE and MULTI are presented in detail in Chapter 3. However, as the differences in sagittal plane ankle kinematics and joint moments between SINGLE and MULTI are pertinent to this chapter, these are re-presented in brief here.

The model was driven using the mean ankle angle in the sagittal plane during the stance phase of running, which demonstrated greater range of motion for SINGLE than MULTI (SINGLE: 45.7 deg, MULTI: 30.5 deg). This greater range of motion was produced by both a larger peak dorsiflexion angle during midstance and a larger peak plantarflexion angle during late stance. Furthermore, SINGLE exhibited greater ankle joint angular velocity compared with MULTI (peak plantarflexion velocity, SINGLE: 547 deg/s, MULTI: 388 deg/s).

The sagittal plane ankle joint moments were used to estimate the muscle forces for the gastrocnemius and soleus. While the ankle moments were slightly different between SINGLE (peak moment: 2.61 BW) and MULTI (peak moment: 2.51 BW), this had a negligible effect on both the gastrocnemius and soleus simulations. The 0.1 BW difference in the ankle moment led

to less than a 0.01 change in the active state difference between SINGLE and MULTI for both muscles.

4.4.2 Soleus nominal simulation

For the soleus simulation with the nominal muscle model parameters, the active state was lower in MULTI than SINGLE during mid- and late stance (Figure 4-2; peak difference = 0.3). During early stance, SINGLE and MULTI produced identical active states. Midstance differences were primarily due to fiber velocity differences, as the soleus fibers shortened in SINGLE but remained nearly isometric in MULTI. During late stance, the fibers in SINGLE shortened more rapidly than those in MULTI (peak fiber velocity difference = 1.6 $l_{f,opt} \cdot s^{-1}$), which reduced the muscle's force generating capacity and increased SINGLE's required active state. This was compounded by MULTI operating closer to the optimal fiber length than SINGLE (peak difference = 0.05 $l_{f,opt}$), which further increased the active state required by SINGLE. The more favorable operating conditions (decreased shortening velocity and fiber lengths closer to optimal fiber length) in MULTI continued until the end of stance, except for a brief period when the fiber lengths were equal. The maximum difference in active state between SINGLE and MULTI occurred at 80% of stance, despite the similarity in fiber lengths at that time. This suggested that the active state difference was primarily due to the differences in fiber shortening velocity.

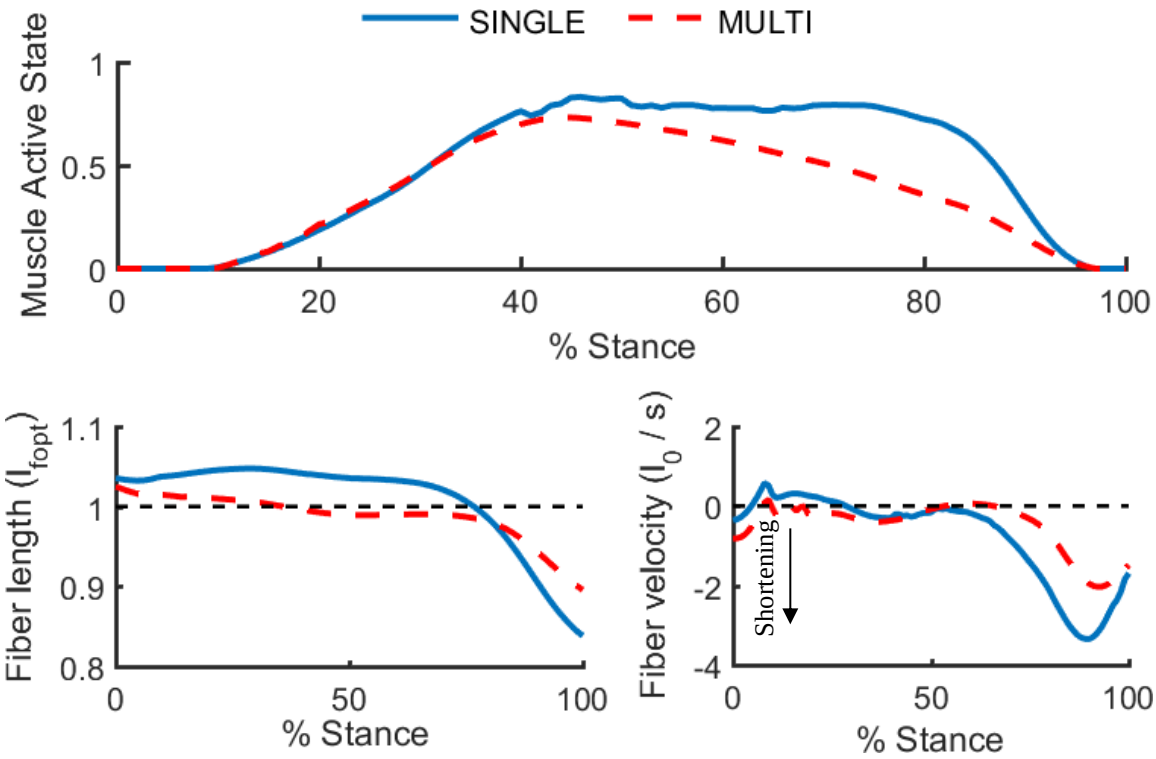

Figure 4-2 Soleus muscle active state (top) and fiber kinematics (bottom) computed using ankle joint kinematics from the two foot models. The active state using MULTI was lower than that obtained using SINGLE due to more optimal fiber lengths (bottom left) and reduced shortening velocity (bottom right). SINGLE = single segment foot model, dashed red line; MULTI = multisegment foot model, solid blue line.

4.4.3 Gastrocnemius nominal simulation

Using the nominal muscle model parameters for the gastrocnemius, SINGLE and MULTI produced similar active states from foot contact until approximately 45% of stance (Figure 4-3). However, after 45% of stance, MULTI required less gastrocnemius active state than SINGLE (peak reduction using MULTI = 0.58). This difference in late stance had two distinct periods. From 45% to 65% of stance, the difference between SINGLE and MULTI was small (mean difference = 0.1). However, after 65% of stance, the difference increased as the active state of SINGLE rose sharply and the active state of MULTI continued to decline (mean difference = 0.35). The decrease in active state for MULTI was attributed primarily to fiber velocity. While the fibers of SINGLE shortened after 65% of stance, the fibers of MULTI lengthened briefly and

then shortened, but at a lower velocity than in SINGLE. Fiber length was also different between SINGLE and MULTI during late stance, but the effect of fiber length on the active state difference was smaller than the effect of fiber velocity. The difference in the force-velocity coefficient (fv in Eq. 4.6) between SINGLE and MULTI peaked at 0.54, while the difference in the force-length coefficient (fl in Eq 4.6) peaked at 0.13. The peak differences in fiber length and fiber velocity were 0.09 $l_{f,opt}$ and 3.1 $l_{f,opt} \cdot s^{-1}$, respectively.

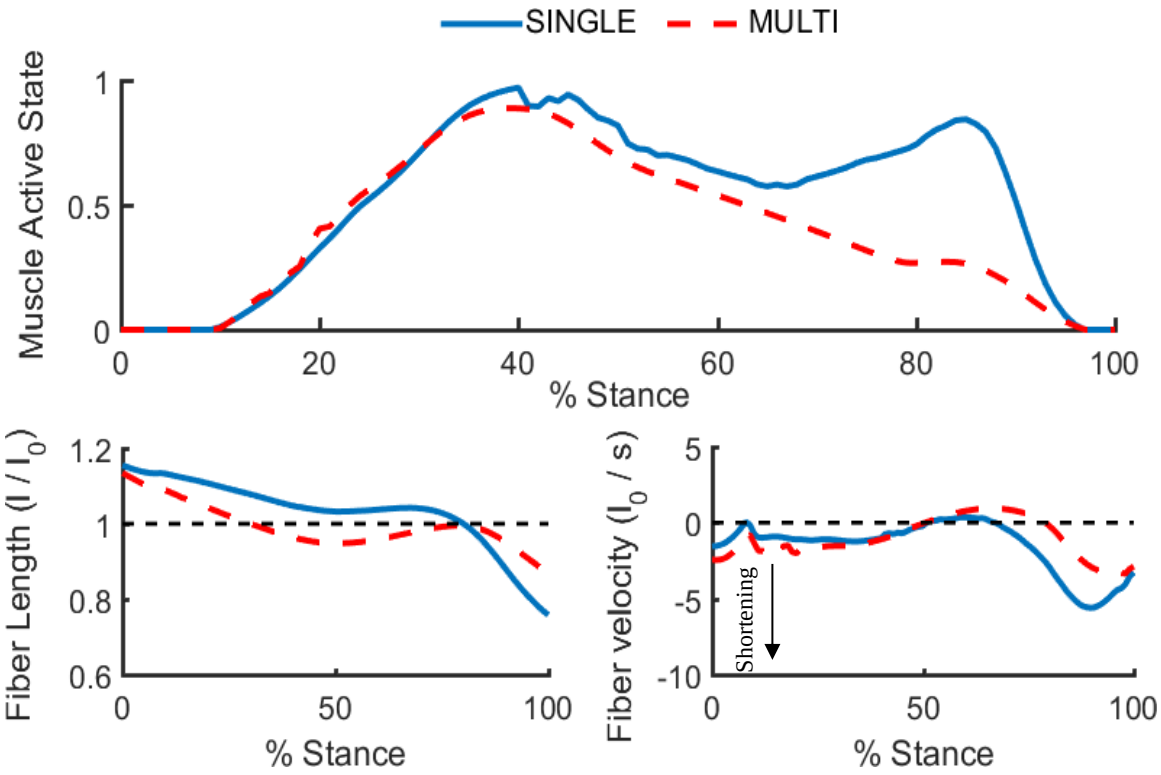

Figure 4-3 Gastrocnemius muscle active state (top) and fiber kinematics (bottom) computed using ankle joint kinematics from the two foot models. The active state using MULTI was lower than that obtained using SINGLE due to more optimal fiber lengths (bottom left) and reduced shortening velocity (bottom right). SINGLE = single segment foot model, dashed red line; MULTI = multisegment foot model, solid blue line.

4.4.4 Soleus muscle model sensitivity

For the soleus, sensitivity to muscle model parameters was typically greater for SINGLE than MULTI (Figure 4-4). Simulations were performed using all combinations of soleus muscle parameter values. To easily compare the results of each simulation, the difference in the active state between SINGLE and MULTI was integrated over the stance phase. Of the 15,360 parameter combinations, 99.6% resulted in a lower integrated active state for MULTI than SINGLE. Nearly half (48%) produced greater than a 30% reduction in the integrated active state for MULTI. Changing the parameters individually from their nominal values (while keeping the other parameters at their nominal value) illustrated how each parameter affected the temporal profile of the active state (Figure 4-5). Sensitivity of the soleus model was highest to the

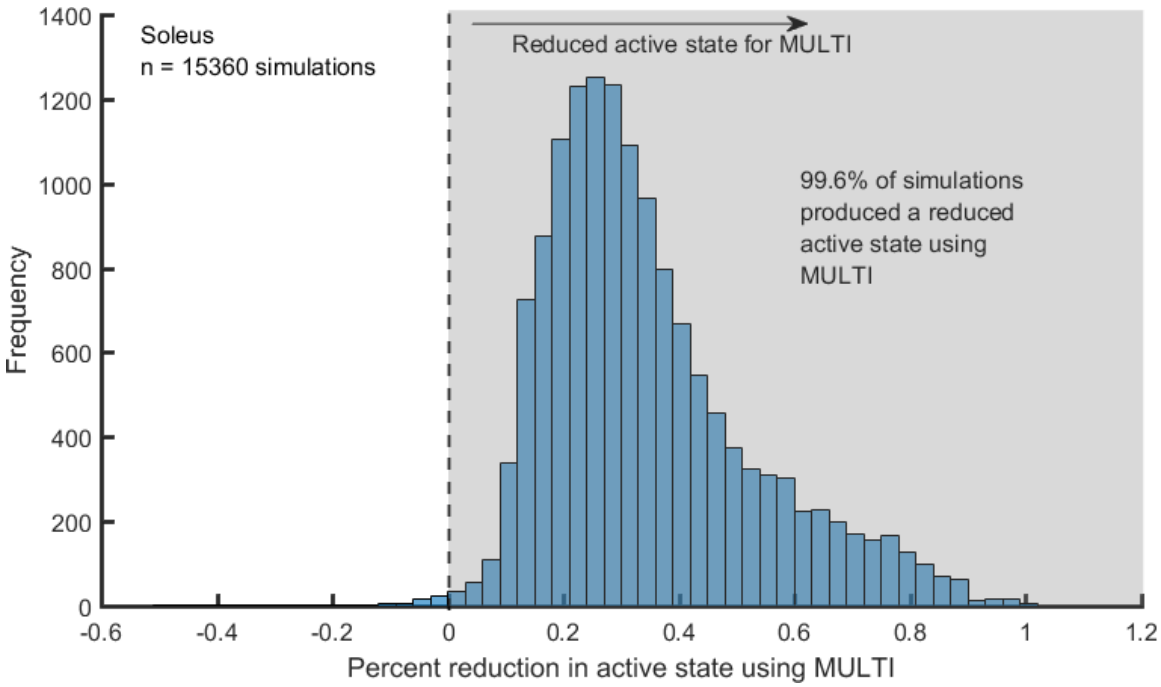

Figure 4-4 The distribution of the difference in soleus active state between multisegment foot model (MULTI) compared to a single segment foot model (SINGLE). The active state difference was integrated over the stance phase for 15360 simulations with varying muscle model parameters to assess the sensitivity of the results. Positive values along the x-axis (gray shaded region) indicate the simulations for which MULTI produced a lower integrated active state.

optimum fiber length ($l_{f,opt}$), tendon slack length (l_{t0}), and tendon compliance (c). This was primarily due to the increased ankle plantarflexion excursions and velocities of SINGLE, which exaggerated the sensitivity to parameters that are most strongly linked to the fiber kinematics.

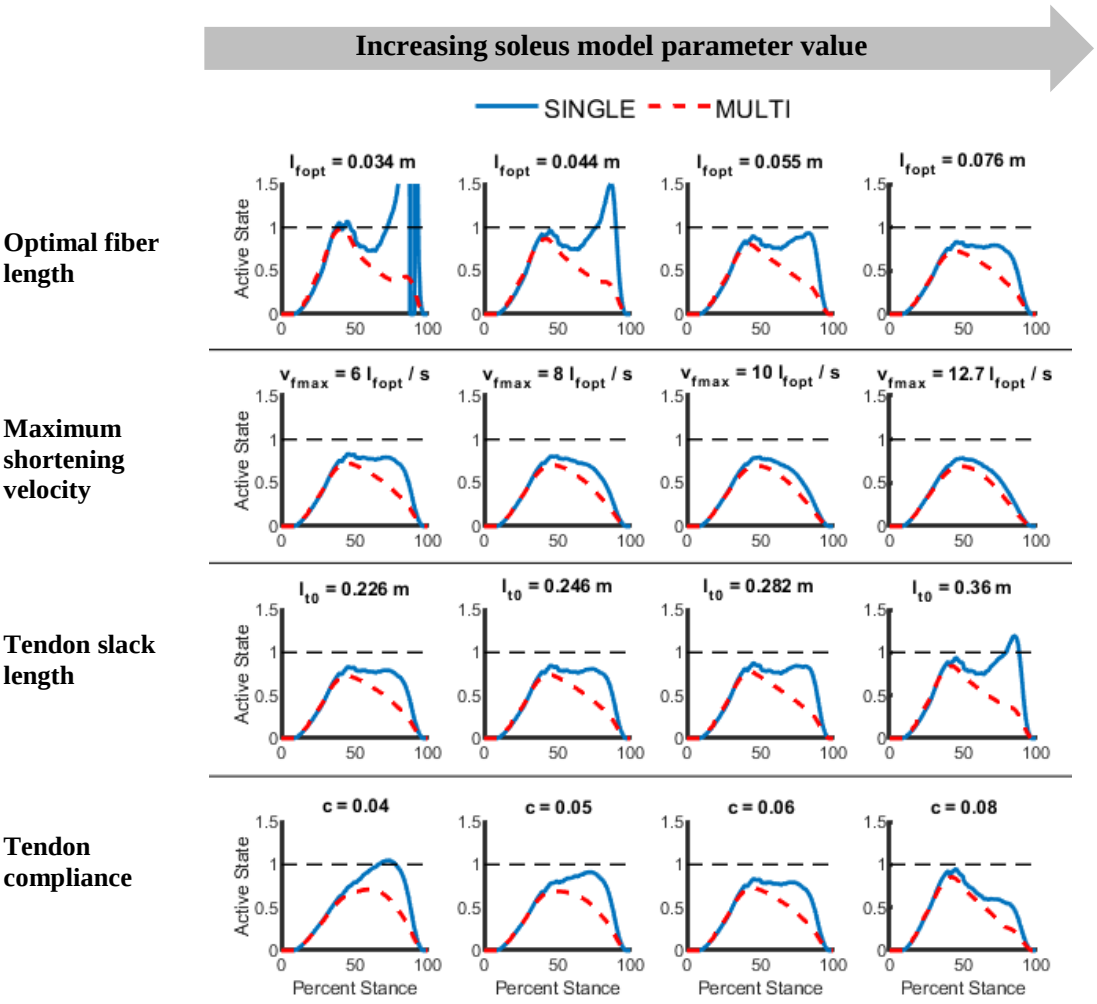

Figure 4-5 Sensitivity of the soleus active state to the muscle model parameters. Results for each foot model are shown, demonstrating that the ankle joint kinematics from MULTI lead to less sensitivity for the muscle model during running. Each row is dedicated to one parameter, with increasing parameter values from left to right. SINGLE = single segment foot model, solid blue line; MULTI = multisegment foot model, dashed red line. $l_{f,opt}$ = optimal fiber length, $v_{f,max}$ = maximum unloaded fiber shortening velocity, l_{t0} = tendon slack length, c = tendon strain at maximum isometric muscle force.

4.4.5 Gastrocnemius muscle model sensitivity

Similar to the soleus, the sensitivity of the gastrocnemius model was typically greater for SINGLE than MULTI (Figure 4-6). Across simulations performed using all parameter combinations, the active state (integrated over the stance phase) of MULTI was lower than SINGLE for 97.6% of parameter combinations. Of the 15,360 simulations, 56% produced greater than a 30% reduction in the integrated active state for MULTI. This was primarily due to the high shortening velocities induced by the ankle kinematics of SINGLE compared with MULTI. The higher shortening velocities in SINGLE resulted in large increases in active state that arose from small changes to some parameter values, due to the nonlinear relationship between shortening velocity and the muscle's active state.

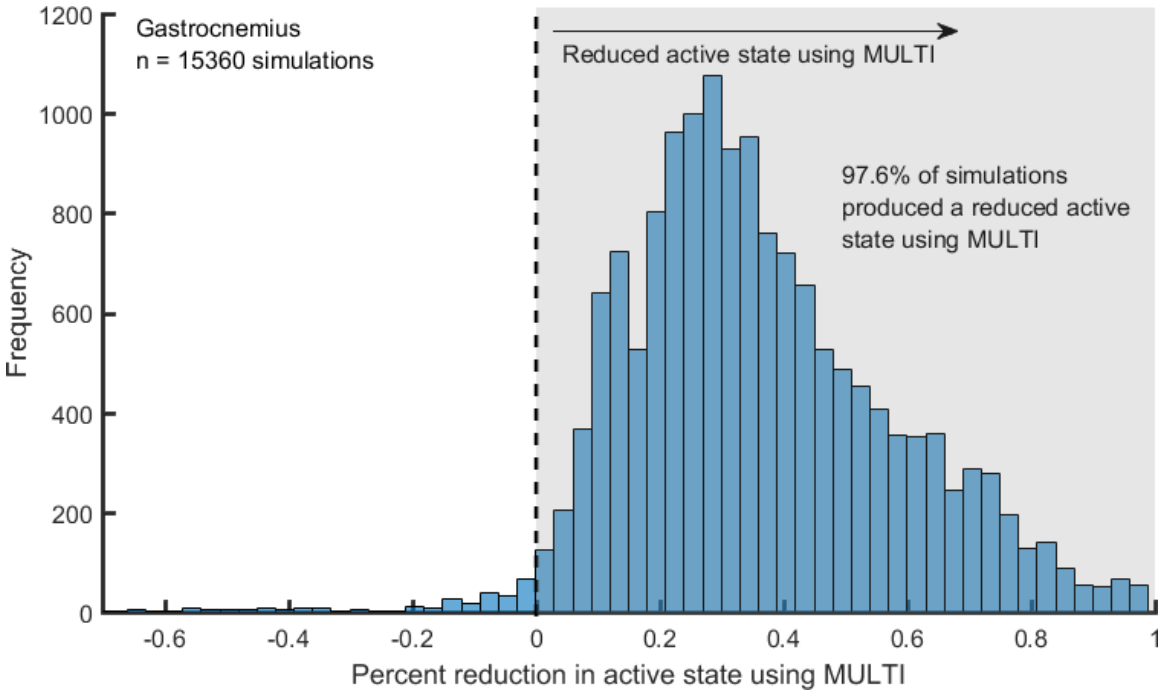

Figure 4-6 The distribution of the difference in gastrocnemius active state between multisegment foot model (MULTI) compared to a single segment foot model (SINGLE). The active state difference was integrated over the stance phase for 15360 simulations with varying muscle model parameters to assess the sensitivity of the results. Positive values along the x-axis (gray shaded region) indicate the simulations for which MULTI produced a lower integrated active state.

Assessing the sensitivity of the active state to individual parameters (varied in isolation) provided some insights into which parameters the model is most sensitive to at the nominal levels. The sensitivity of the gastrocnemius muscle model to its parameters was similar to that of the soleus, as MULTI displayed less sensitivity to all parameters than SINGLE (Figure 4-7).

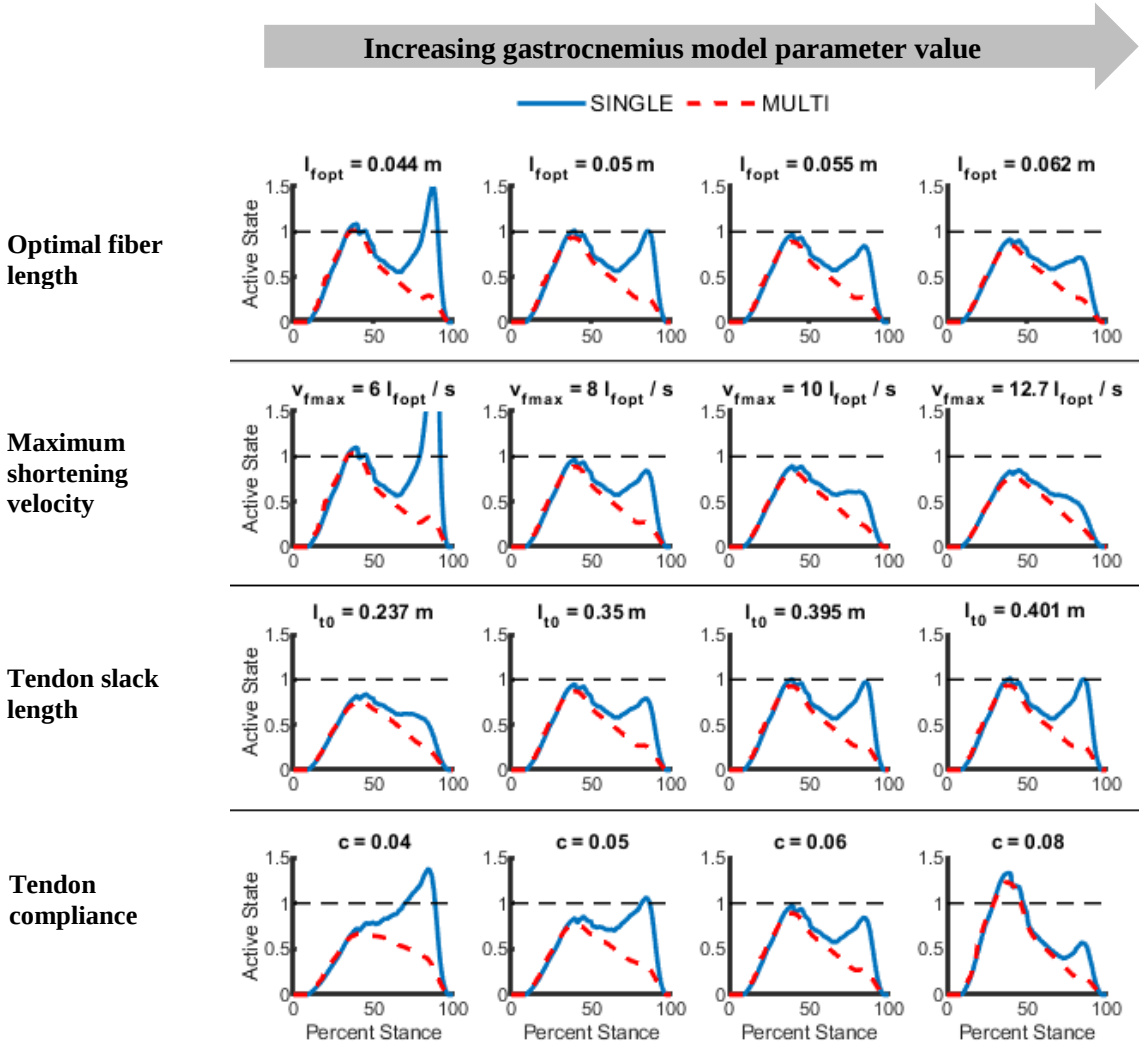

Figure 4-7 Sensitivity of the gastrocnemius active state to muscle model parameters. Results for each foot model are shown, demonstrating that the ankle joint kinematics from MULTI lead to less sensitivity for the muscle model during running. Each row is dedicated to one parameter, with increasing parameter values from left to right. SINGLE = single segment foot model, solid blue line; MULTI = multisegment foot model, dashed red line. $l_{f,opt}$ = optimal fiber length, $v_{f,max}$ = maximum unloaded fiber shortening velocity, l_{t0} = tendon slack length, c = tendon strain at maximum isometric muscle force.

4.5 Discussion

By simulating the ankle plantarflexor muscles using both a single segment foot model (SINGLE) and a multisegment foot model (MULTI), this study highlighted that foot model topology influences simulated active states of ankle plantarflexors during running. It was hypothesized that MULTI would reduce the active states of the gastrocnemius and soleus muscles compared with SINGLE. This hypothesis was supported as MULTI produced lower active states than SINGLE for both muscles. This reduction held across nearly all (97.6% gastrocnemius, 99.6% soleus) of the 15,360 simulations in which muscle architecture and properties were varied using different combinations of muscle model parameter values. The active state reductions in MULTI were primarily evident during push-off for both models. However, some muscle model parameter combinations also generated differences early in stance.

For the soleus, active state was similar between MULTI and SINGLE during early stance, but MULTI produced a lower soleus active state during late stance. In both foot models, the onset of soleus active state occurred around 10% of stance and peaked slightly before 50% of stance. However, in SINGLE, the active state plateaued from 50% to 80% of stance, while in MULTI the active state declined during this period. Electromyography (EMG) recordings of *in vivo* soleus muscle activity bore more resemblance to the temporal pattern of MULTI than SINGLE. This suggests that simulations using MULTI may produce a better representation of *in vivo* soleus behavior, at least when using the nominal muscle model parameters used in this study. Rubenson et al. (2012) reported that soleus EMG readings peaked slightly after 50% of stance then declined until toe-off. Cappellini et al. (2006) reported a sharp rise in surface EMG readings during early stance, a peak in activity just before 50% of stance, and a gradual decline from 50% of stance until toe-off. In both studies, the pattern of EMG recordings agreed more closely with MULTI, as both MULTI and these *in vivo* recordings declined quickly after the peak active state.

The peak magnitude of soleus muscle activity from Rubenson et al. (2012) was slightly below 0.8, which is between the maxima of SINGLE and MULTI in this study (SINGLE: 0.83, MULTI: 0.73).

Active state differences in the soleus between SINGLE and MULTI were primarily due to differences in fiber shortening velocity and, therefore to a lesser extent, fiber length. The ankle joint moments and Achilles tendon moment arm (and therefore, the muscle forces) were nearly identical between the two models and played a negligible role in the active state differences. During early stance, MULTI and SINGLE had similar soleus active states despite different fiber kinematics. When using SINGLE, the soleus fibers lengthened slightly during early stance, while in MULTI the soleus fibers shortened very slightly. This led to a more favorable early stance force-velocity fraction in SINGLE. However, SINGLE also operated farther from the optimal fiber length during early stance, which offset the more favorable force-velocity conditions. During the last 60% of stance, MULTI generated a lower active state than SINGLE, primarily due to MULTI's reduced fiber shortening velocity during this period (peak soleus shortening velocity; MULTI: 2.18 $l_{f,opt} \cdot s^{-1}$, SINGLE: 3.35 $l_{f,opt}/s$). The shortening velocities of MULTI agreed closely with *in vivo* values for running near 3.0 $m \cdot s^{-1}$ reported by Lai et al. (2015), whereas the faster shortening velocity of SINGLE was closer to *in vivo* values for faster running at 5.0 $m \cdot s^{-1}$ (Lai et al., 2015). Total fiber shortening during stance was smaller for MULTI (0.18 $l_{f,opt}$) than SINGLE (0.27 $l_{f,opt}$), but the outputs of both MULTI and SINGLE agreed well with *in vivo* measurements (Lai et al., 2015; Rubenson et al., 2012). However, the temporal profile of *in vivo* fiber length measurements was closer to MULTI, as neither Lai et al. (2015) nor Rubenson et al. (2012) reported fiber lengthening during early stance (as was found in SINGLE). The temporal profile of fiber lengths for MULTI was particularly similar to Rubenson et al. (2012), as they both displayed shortening during early stance, nearly isometric behavior during midstance, and

shortening again during late stance. However, total shortening and shortening velocities were greater in Rubenson et al. (2012).

The gastrocnemius displayed similar results to the soleus, as the active state during late stance was reduced for MULTI compared with SINGLE. Both SINGLE and MULTI exhibited a peak around 40% of stance. However, MULTI generated a decline in gastrocnemius active state between 40% and toe-off, while SINGLE generated an additional rise near 65% of stance leading to a second active state peak near 85% of stance. This bimodal active state is inconsistent with *in vivo* EMG readings from the medial and lateral heads of the gastrocnemius during slow running. Instead, *in vivo* EMG patterns display a peak at or before 50% of stance followed by a consistent decline until toe-off, and are therefore more similar to MULTI (Ishikawa et al., 2007; Kyrolainen et al., 1999; Lichtwark and Wilson, 2006).

Gastrocnemius fiber kinematics between SINGLE and MULTI displayed a similar trend to those of the soleus. Active state was similar for the two models during early stance, but MULTI operated closer to the optimal fiber length while SINGLE operated at lower shortening velocities. These conditions offset to produce the similar active state during early stance. During late stance, the gastrocnemius fibers of MULTI shortened less (total fiber excursion: MULTI = 0.27 $l_{f,opt}$, SINGLE = 0.40 $l_{f,opt}$) and shortened more slowly (gastrocnemius peak shortening velocity: MULTI = 3.35 $l_{f,opt} \cdot s^{-1}$, SINGLE = 5.60 $l_{f,opt}/s$) than those of SINGLE. Total fiber excursion in MULTI (14 mm) was similar to reported *in vivo* values (13 – 16 mm) obtained via ultrasound imaging while running at similar speeds (Farris and Sawicki, 2012b; Ishikawa et al., 2007; Ishikawa and Komi, 2007).

For both the soleus and gastrocnemius, this study strongly suggests that foot model topology plays an integral role in the conclusions that are drawn from simulations of human running. The use of MULTI decreased the active state during push-off, which was primarily the result of reduced fiber shortening velocities and more optimal fiber lengths compared with

SINGLE. As many simulation studies of the ankle choose to use a single segment foot model, these results imply that such studies are likely to overestimate the muscle active state, fiber shortening, and fiber shortening velocities of the ankle plantarflexors. These overestimates could have effects on the simulated metabolic cost of running (and the relative distribution of that cost across muscles of the lower leg) as estimation of muscle energy expenditure relies on mechanical work and shortening/lengthening heat (Bhargava et al., 2004; Umberger et al., 2003). Similarly, the differences in ankle joint angle between SINGLE and MULTI resulted in a smaller moment arm for MULTI, which increased the required muscle force and, therefore, tendon elongation. This reduced the energy stored in the Achilles tendon by 18.5% for MULTI compared with SINGLE. In forward simulations that optimize muscle activations to generate model kinematics, choice of foot model is also likely to have an effect, particularly in simulations which aim to match experimental ankle angles derived from a single segment foot model.

Limitations in this study were present in both the experimental kinematics and muscle simulations. In the muscle model, MTU length changes were derived from the equations of Grieve et al. (1978), which only consider the effect of sagittal plane angles. Frontal plane ankle angles may also influence MTU length changes, although this influence is small as the Achilles tendon moment arm about the subtalar joint axis is approximately 10% of its moment arm about the ankle joint axis (Klein et al., 1996). However, omission of frontal plane effects is unlikely to alter the results of the muscle simulations as the frontal plane ankle kinematics were similar between SINGLE and MULTI when the ankle plantarflexor muscles were active. The muscle models used were simplified phenomenological representations of the ankle plantarflexors and did not include effects due to pennation angle or fiber rotation (e.g., Azizi et al., 2008) and muscle history effects. Additionally, the models sought to represent the function of the whole muscle belly and not individual muscle fibers. The simulations were driven by the mean kinematics and kinetics of seven subjects, which neglected the variability between subjects,

which could be influential. The features of the experimental data used in the muscle simulations (sagittal plane ankle kinematics and kinetics) displayed low inter-subject variability (kinematics mean coefficient of variation = 0.17) and therefore were unlikely to alter the conclusion that SINGLE and MULTI generated different muscle active states.

This study has provided evidence that, when driven by experimental ankle kinematics, simulations of the ankle plantarflexor muscles are influenced by foot model topology. During simulations of running, deriving muscle-tendon unit kinematics using a multisegment foot model in place of the traditional single segment foot model reduced the muscle active states during the push-off phase. These reductions were primarily due to reduced fiber shortening velocities that resulted from lower sagittal plane ankle angular velocities. In a sensitivity analysis, muscle architecture and properties were varied across 15,360 simulations and nearly all (soleus: 99.6% and gastrocnemius: 97.6%) simulations produced a reduced active state using the multisegment foot model. In total, this work has highlighted that the definition of the ankle joint is important for ankle plantarflexor muscle simulations, as the different kinematics between foot models alters the muscle kinematics and active state.

References

Anderson, F.C., Pandy, M.G., 1999. A dynamic optimization solution for vertical jumping in three dimensions. Comput. Methods Biomech. Biomed. Engin. 2, 201–231.

Arampatzis, A., Stafilidis, S., DeMonte, G., Karamanidis, K., Morey-Klapsing, G., Brüggemann, G.P., 2005. Strain and elongation of the human gastrocnemius tendon and aponeurosis during maximal plantarflexion effort. J. Biomech. 38, 833–841.

Arndt, A., Bengtsson, A.-S., Peolsson, M., Thorstensson, A., Movin, T., 2012. Non-uniform displacement within the Achilles tendon during passive ankle joint motion. Knee Surg. Sports Traumatol. Arthrosc. 20, 1868–1874.

Arndt, A., Wolf, P., Liu, A., Nester, C., Stacoff, A., Jones, R., Lundgren, P., Lundberg, A., 2007. Intrinsic foot kinematics measured in vivo during the stance phase of slow running. J. Biomech. 40, 2672–2678.

Arnold, E.M., Ward, S.R., Lieber, R.L., Delp, S.L., 2010. A Model of the Lower Limb for Analysis of Human Movement. Ann. Biomed. Eng. 38, 269–279.

Bhargava, L.J., Pandy, M.G., Anderson, F.C., 2004. A phenomenological model for estimating metabolic energy consumption in muscle contraction. J. Biomech. 37, 81–88.

Blickhan, R., 1989. The spring-mass model for running and hopping. J. Biomech. 22, 1217–1227.

Cappellini, G., Ivanenko, Y.P., Poppele, R.E., Lacquaniti, F., 2006. Motor Patterns in Human Walking and Running. Journal of Neurophysiology 95, 3426–3437.

Challis, J.H., 2004. Examination of the scaling of human jumping. J. Strength Cond. Res. 18, 803–809.

Delp, S.L., 1990. Surgery simulation: A computer-graphics system to analyze and design musculoskeletal reconstructions of the lower limb. (Doctoral dissertation). Stanford University.

Dixon, P.C., Böhm, H., Döderlein, L., 2012. Ankle and midfoot kinetics during normal gait: A multi-segment approach. J. Biomech. 45, 1011–1016.

Domire, Z.J., Challis, J.H., 2007. The influence of squat depth on maximal vertical jump performance. J. Sports Sci. 25, 193–200.

Farris, D.J., Sawicki, G.S., 2012. Human medial gastrocnemius force–velocity behavior shifts with locomotion speed and gait. Proc. Natl. Acad. Sci. 109, 977–982.

Franz, J.R., Slane, L.C., Rasske, K., Thelen, D.G., 2015. Non-uniform in vivo deformations of the human Achilles tendon during walking. Gait Posture 41, 192–197.

Grieve, D.W., Pheasant, S., Cavanagh, P.R., 1978. Prediction of gastrocnemius length from knee and ankle posture, in: Jorgenson, K. (Ed.), Biomechanics VI-A. University Park Press, Baltimore, MD, pp. 405–412.

Ishikawa, M., Komi, P.V., 2007. The role of the stretch reflex in the gastrocnemius muscle during human locomotion at various speeds. J. Appl. Physiol. 103, 1030–1036.

Ishikawa, M., Pakaslahti, J., Komi, P.V., 2007. Medial gastrocnemius muscle behavior during human running and walking. Gait Posture 25, 380–384.

Kyrolainen, H., Komi, P.V., Belli, A., 1999. Changes in muscle activity patterns and kinetics with increasing running speed. J. Strength Cond. Res. 13, 400–406.

Lai, A., Lichtwark, G.A., Schache, A.G., Lin, Y.-C., Brown, N.A.T., Pandy, M.G., 2015. In vivo behavior of the human soleus muscle with increasing walking and running speeds. J. Appl. Physiol. 118, 1266–1275.

Lichtwark, G.A., Wilson, A.M., 2007. Is Achilles tendon compliance optimised for maximum muscle efficiency during locomotion? J. Biomech. 40, 1768–1775.

Lichtwark, G.A., Wilson, A.M., 2006. Interactions between the human gastrocnemius muscle and the Achilles tendon during incline, level and decline locomotion. J. Exp. Biol. 209, 4379–4388.

MacWilliams, B.A., Cowley, M., Nicholson, D.E., 2003. Foot kinematics and kinetics during adolescent gait. Gait & Posture 17, 214–224.

Nagano, A., Gerritsen, K.G., 2001. Effects of neuromuscular strength training on vertical jumping performance—a computer simulation study. J. Appl. Biomech. 17, 113–128.

Nester, C.J., Jones, R.K., Liu, A., Howard, D., Lundberg, A., Arndt, A., Lundgren, P., Stacoff, A., Wolf, P., 2007. Foot kinematics during walking measured using bone and surface mounted markers. J. Biomech. 40, 3412–3423.

Okita, N., Meyers, S.A., Challis, J.H., Sharkey, N.A., 2013. Midtarsal joint locking: New perspectives on an old paradigm. J. Orthop. Res. 110-115.

Out, L., Vrijkotte, T.G.M., van Soest, A.J., Bobbert, M.F., 1996. Influence of the parameters of a human triceps surae muscle model on the isometric torque-angle relationship. J. Biomech. Eng. 118, 17–25.

Pandy, M.G., Zajac, F.E., Sim, E., Levine, W.S., 1990. An optimal control model for maximum-height human jumping. J. Biomech. 23, 1185–1198.

Pothrat, C., Authier, G., Viehweger, E., Berton, E., Rao, G., 2015. One- and multi-segment foot models lead to opposite results on ankle joint kinematics during gait: Implications for clinical assessment. Clin. Biomech. 30, 493–499.

Robertson, D.G.E., Winter, D.A., 1980. Mechanical energy generation, absorption and transfer amongst segments during walking. J Biomech 13, 845–854.

Rubenson, J., Pires, N.J., Loi, H.O., Pinniger, G.J., Shannon, D.G., 2012. On the ascent: the soleus operating length is conserved to the ascending limb of the force–length curve across gait mechanics in humans. J. Exp. Biol. 215, 3539–3551.

Scovil, C.Y., Ronsky, J.L., 2006. Sensitivity of a Hill-based muscle model to perturbations in model parameters. J. Biomech. 39, 2055–2063.

Slane, L.C., Thelen, D.G., 2014. Non-uniform displacements within the Achilles tendon observed during passive and eccentric loading. J. Biomech. 47, 2831–2835.

Umberger, B.R., Gerritsen, K.G.M., Martin, P.E., 2003. A model of human muscle energy expenditure. Comput. Methods Biomech. Biomed. Engin. 6, 99–111.

van Soest, A.J., Schwab, A.L., Bobbert, M.F., van Ingen Schenau, G.J., 1993. The influence of the biarticularity of the gastrocnemius muscle on vertical-jumping achievement. J. Biomech. 26, 1–8.

Wakeling, J.M., Lee, S.S.M., Arnold, A.S., de Boef Miara, M., Biewener, A.A., 2012. A muscle's force depends on the recruitment patterns of its fibers. Ann. Biomed. Eng. 40, 1708–1720.

Winter, D.A., 2009. Biomechanics and Motor Control of Human Movement, 4th ed. John Wiley & Sons, Inc., Hoboken, NJ.

Wolf, P., Stacoff, A., Liu, A., Nester, C., Arndt, A., Lundberg, A., Stuessi, E., 2008. Functional units of the human foot. Gait Posture 28, 434–441.

Chapter 5

The potential for the metatarsophalangeal joint position to modulate maximum isometric ankle plantarflexion moments

5.1 Abstract

The ankle joint is a primary contributor of positive power during running, driven by the ankle plantarflexor muscles. The force generating capacity of these muscles are known to be influenced by the ankle angle and knee angle, but the metatarsophalangeal (MTP) joint may also affect these muscles. This effect may arise due to lengthening of the flexor hallucis longus and flexor digitorum longus with MTP joint extension and possible connections between the plantar aponeurosis and Achilles tendon, which could affect the force-generating capacities of the triceps surae. To determine the influence of the MTP joints on the force-generating capacities of the ankle plantarflexors muscles, eight healthy subjects exerted maximum isometric ankle plantarflexion contractions on a dynamometer. The MTP joints were held in either a neutral or fully extended position while the knee joint (90 degrees flexion or fully extended) and ankle joint (4 angles) were systematically varied, giving 16 different leg configurations. There was no significant effect of MTP joint position on the maximum ankle plantarflexion moment ($p = 0.41$). Ankle joint angle and knee joint both had a significant effect ($p < 0.001$). This suggests that: 1) the FHL and FDL contribute little to the ankle joint moment, 2) the force-generating capacities of the FHL and FDL are unchanged by MTP joint extension, and/or 3) MTP joint extension has a negligible influence on the force-generating capacities of the gastrocnemius and soleus muscles.

5.2 Introduction

During the push-off phase of running, positive power generated at the ankle constitutes the majority of the mechanical power generated by the lower limb during stance (Farris and Sawicki, 2012a; Winter, 1983; Zelik et al., 2015). This power is primarily generated by the triceps surae, which are influenced by the positions of the both the ankle joint and, due to the biarticular nature of the gastrocnemius, the knee joint. However, the angle of the metatarsophalangeal (MTP) joint may also influence ankle function during running, as the extrinsic toe flexor muscles (flexor hallucis longus, FHL; flexor digitorum longus, FDL) are multijointed and span the ankle and MTP joints. Furthermore, extension of the MTP joints (e.g., lifting the toes off the ground) shortens the arch of the foot, which tensions the plantar aponeurosis (PA) and enhances force transfer between the Achilles tendon and the PA (Carlson et al., 2000; Hicks, 1954). In running, the MTP joints extend during terminal stance and may influence how the neuromuscular system generates the required ankle joint moment and power.

MTP joint extension may affect the contributions of the FDL and FHL to the ankle joint moment by altering the muscles' force-generating capacities. Bojsen-Møller & Lamoreaux (1979) suggested that FHL lengthening occurs during walking and noted that dorsiflexion of the toes stretches the FHL such that it "reaches a higher tension" during late stance. Goldmann & Brüggemann (2012) demonstrated that MTP joint extension increased the maximum isometric flexor moment at the MTP joints and used cadaveric estimates of FDL and FHL MTU length changes to suggest that the increase was due to lengthening of the FDL and FHL muscle fibers. Given the multijoint nature of the FDL and FHL, it is plausible that changes to their force-generating capacities induced by MTP joint extension could also increase the maximum ankle joint moment.

In addition to extrinsic toe flexor muscle changes, MTP joint extension may also influence ankle joint moments through tensioning of the PA and shortening of the medial longitudinal arch (Carlson et al., 2000; Hicks, 1954). There is evidence that the PA is anatomically connected to the Achilles tendon (Shaw et al., 2008; Snow et al., 1995; Stecco et al., 2013) and such a connection could explain the observation of Carlson et al. (2000) that extension of the MTP joints enhanced transmission of Achilles tendon forces to the PA. Additionally, simulations of walking using cadaveric lower limbs (with tensile forces applied directly to the Achilles tendon) displayed a correlation between the Achilles tendon force and PA force (Erdemir et al., 2004). Therefore, in addition to an anatomical connection, these results suggest a functional relationship between the PA and Achilles tendon. In tandem, these two potential mechanisms suggest that PA strain may have the capacity to alter Achilles tendon strain and, therefore, influence the function of the gastrocnemius and soleus. If the Achilles tendon and PA are connected via continuous fibers, force in the PA could lengthen the Achilles tendon and the triceps surae muscle fibers, effectively allowing the PA, Achilles tendon, and triceps surae to act as a continuous muscle-tendon unit. The triceps surae likely operate on the ascending limb of their force-length curves (Herzog et al., 1991; Maganaris, 2003; Rubenson et al., 2012; Winter and Challis, 2008) and therefore any lengthening of the muscle fibers could produce improvements to their force-generating capacities.

The purpose of this study was to explore the potential of the MTP joints to alter the maximum voluntary ankle plantarflexion moment. It was hypothesized that the maximum ankle plantarflexor moment would be greater with MTP joints held in extension compared with the MTP joints in the neutral position. The accompanying null hypothesis was that the ankle joint moments would not change with MTP joint extension. Rejecting the null hypothesis would primarily support one of three explanations (or a combination thereof): 1) the FDL and FHL make a meaningful contribution to the ankle plantarflexor moment and their force generating

capacities are improved with MTP joint extension, 2) the MTP joint affects the force-generating capacities of the primary ankle plantarflexor muscles (gastrocnemius and soleus) due to lengthening of the Achilles tendon and potentially the muscle fibers. Importantly, these two explanations are not mutually exclusive, as they could occur simultaneously. To explore this hypothesis and its underlying explanations, the maximum voluntary ankle plantarflexion moment was elicited at 16 different combinations of MTP, ankle, and knee joint positions. These maximum moments were compared to determine if MTP joint position is a regulator of ankle plantarflexion moments or if the anatomical and mechanical connections between the toes and ankle play no role in modulating ankle joint moments.

5.3 Methods

Eight healthy subjects with no lower limb or foot injuries in the previous 6 months volunteered to participate. All procedures were approved by the Institutional Review Board at The Pennsylvania State University and informed consent was obtained from all subjects (Appendix A).

5.3.1 Foot anthropometry measurements

Prior to dynamometer testing, subjects were assessed for Foot Posture Index (Redmond et al., 2006), navicular height, and passive range of motion of the first MTP joint in seated and standing positions (Table 5-1). Foot Posture Index was determined using six visual observations which were combined to form a score ranging from -12 to +12, with -12 to -6 representing a supinated foot posture, -5 to +5 representing a neutral foot posture, and +6 to +12 representing a pronated foot posture. Navicular height was measured as the distance from the floor to the navicular tubercle, which was digitized from a sagittal plane photograph of the foot. Navicular

drop was calculated as the difference between seated and standing navicular heights. To measure first MTP joint passive range of motion, dots were drawn on the navicular tubercle, first metatarsal head, and distal tip of the proximal phalanx of the hallux. Photographs of the medial side of the foot with the subject seated and standing were taken with the first MTP joint in two positions: neutral and maximally extended (defined by the subject perceiving the range of motion endpoint). The first MTP joint angle was calculated as the planar angle formed between points on the navicular tubercle, the first metatarsal head, and the hallux. The passive range of motion was recorded as the difference between the neutral and extended MTP joint positions. Photographs were digitized using ImageJ (National Institutes of Health, USA; https://imagej.nih.gov/ij/).

Table 5-1 Subject foot characteristics. Foot Posture Index classifications and scores are as in Redmond et al. (2006). Navicular height was defined as the distance from the floor to the navicular tubercle. Navicular drop was calculated as the difference in navicular height between seated and standing positions. First MTP joint range of motion (ROM) was assessed by passively moving the hallux to the end of its range of motion, with the 1st MTP joint angle defined as the sagittal plane angle formed by the navicular tubercle, 1st metatarsal head, and the distal end of the proximal phalanx of the hallux.

Subject	**Foot Posture Index**	**Navicular Height (cm)**	**Navicular Drop (cm)**	**1st MTP Joint ROM (degrees)**	
				Seated	*Standing*
1	2 - Neutral	6.1	0.2	56.1	47.9
2	5 - Neutral	5.5	0.2	32.6	29.1
3	4 - Neutral	5.9	0.4	32.9	13
4	2- Neutral	4.9	0.6	59.3	59.3
5	3- Neutral	5.1	0.5	53	58.1
6	0- Neutral	5	0.5	43.7	35.5
7	5- Neutral	5.6	0.6	48	47.7
8	7 - Pronated	4.4	0.4	66	56.3

5.3.2 Dynamometry protocol

Subjects performed maximum voluntary isometric contractions (MVIC) on a dynamometer (Biodex Medical Systems, Shirley, NY) in 16 different combinations of knee angle, ankle angle, and MTP joint angle. In each knee-ankle-MTP joint position, subjects performed two ankle plantarflexion MVIC repetitions lasting 3 seconds each with 15 seconds of rest. The knee angle systematically varied between 0 degrees (full extension) and 90 degrees. The ankle angle was varied between 10 degrees dorsiflexion, 0 degrees (neutral), 10 degrees plantarflexion, and 20 degrees plantarflexion. The MTP joint angle was set to either full extension (end of the subject's voluntary range of motion) or neutral (the subject's resting MTP joint position with the foot unloaded). All 16 possible combinations of these joint angles were tested.

5.3.3 Dynamometry setup

The neutral ankle angle (0 degrees) was set equal to the subject's standing ankle angle, which was determined during quiet standing by drawing a line perpendicular to the floor on the subject's shank. The standing ankle angle was replicated on the dynamometer by rotating the ankle joint such that this line was aligned with a line perpendicular to the dynamometer foot plate, thus creating a common reference plane between the standing position (the ground) and the seated position (the footplate) in the dynamometer. The dynamometer axis was aligned with the subject's approximate anatomical ankle joint axis using a custom pointer device that extended the dynamometer axis onto the subject's foot using a metal rod. The subject's anatomical ankle joint axis was assumed to pass through a point 11 mm anterior and 12 mm inferior to the most lateral point on the lateral malleolus (Isman and Inman, 1969). The orientation of the ankle joint axis was assumed to be tilted 5 degrees in the frontal plane, such that the axis pointed medially and slightly superiorly (medial endpoint was proximal to the lateral endpoint). This 5-degree angle in

the frontal plane was within 1 standard deviation of the mean frontal plane orientation found in cadaveric specimens (Inman, 1976).

5.3.4 Custom dynamometer foot and toe plates

Measures were taken to ensure that moments generated by the MTP joints during maximal ankle plantarflexion did not corrupt the measurement of the ankle joint moment. With the MTP joints in the neutral position, the toes were in contact with the dynamometer foot plate and, therefore, could exert a force on the foot plate and artificially inflate the measured ankle moment. However, with the MTP joints extended, the toes did not rest on the dynamometer foot plate and therefore could not contribute to the measured moment. This inconsistency between the MTP joint positions could have created an effect of reduced ankle moments with MTP joint extension. Therefore, a partial foot plate (extending from the heel to the metatarsal heads) was bolted to the dynamometer foot plate (Figure 5-1) which ensured that the toes would not contribute to the measured moment in both MTP joint positions.

To alter the MTP joint angle, an aluminum toe plate was attached to the subject's toes using cloth athletic tape. A nylon strap ran through two slots in the toe plate (Figure 5-1), which allowed the toe plate angle to be adjusted to hold the subject's MTP joint in extension. As the straps ran approximately parallel to the dynamometer footplate, any forces transmitted through the straps (e.g., from the subject generating a moment at the MTP joint) produced negligible changes in the dynamometer measured ankle joint moments. This allowed subjects to freely exert maximum ankle joint moments without the need to avoid generating MTP joint moments.

Figure 5-1 Two views of the setup used to alter MTP joint angle and remove the potential effect of the toe forces. A partial foot plate was bolted on top of the dynamometer foot plate and an aluminum toe plate with a nylon strap was used to hold the MTP joint angle during testing.

5.3.5 Statistical analyses

A three-factor repeated measures ANOVA was used to test for significant differences in ankle plantarflexion moments between the two MTP joint positions. The three within-subject factors were knee angle (2 levels), ankle angle (4 levels), and MTP joint position (2 levels). The type I error rate was set at $\alpha = 0.05$. Normality and homogeneity of variances were confirmed using the Anderson-Darling test and Bartlett's test, respectively. Post-hoc pairwise comparisons were evaluated with Tukey's HSD test. Statistical tests were performed in Minitab 18.1 and MATLAB R2018b (9.5.0.944444).

5.4 Results

There was no significant effect of MTP joint position on the ankle plantarflexion moment (p = 0.41; Figure 5-2). Across the 8 subjects and 8 different knee-ankle angle combinations, the mean difference in the ankle plantarflexion moment between MTP joint neutral and MTP joint extended was 2.6 ± 12.8 N·m.

A significant effect of knee position on ankle plantarflexion moment was found, with larger moments occurring with the knee fully extended (p < 0.001). A significant effect of ankle position on ankle joint moment (p < 0.001) was also found, with larger moments occurring with greater dorsiflexion. Tukey pairwise comparisons demonstrated statistically significant differences for each angle pair except 10 degrees dorsiflexion and neutral (p = 0.063). From neutral to 20 degrees plantarflexion, the maximum moment declined with increasing plantarflexion (all p-values ≤ 0.001). No significant interaction effects between the ankle, knee, and MTP joint positions were found (all p-values ≥ 0.44).

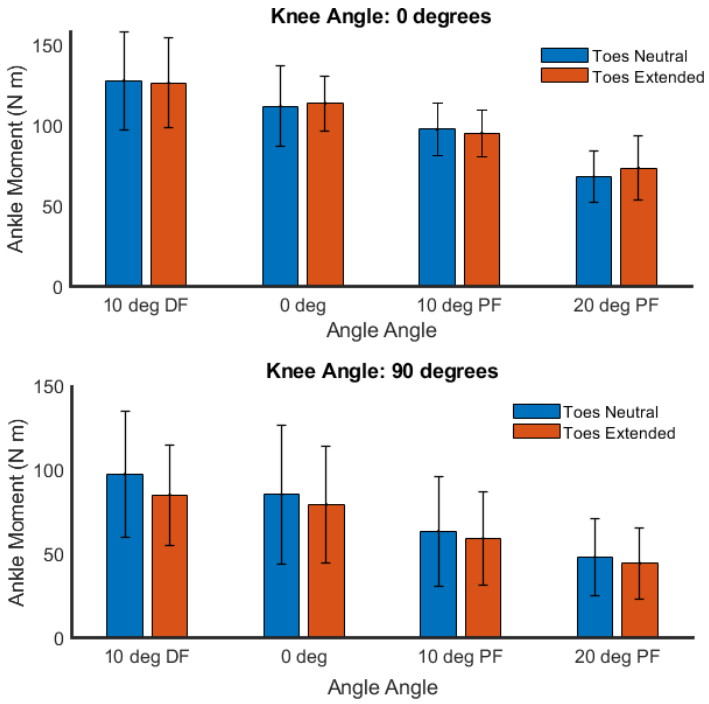

Figure 5-2 Mean maximum isometric ankle moment across 8 subjects across 4 ankle angles, two knee joint positions (top plot: 0 degrees, bottom plot: 90 degrees), and two MTP joint positions. Blue bars (left) show data for the MTP joints in a neutral position. Red bars (right) show data for the MTP joints extended to the end of the subject's voluntary range of motion. Error bars show ± 1 standard deviation of the mean. No significant differences were found between the MTP netural and MTP extended conditions.

Exploring the results of individual subjects bolsters the lack of a significant within-subjects effect. With the knee fully extended (Figure 5-3) and the ankle dorsiflexed to 10 degrees, five subjects displayed a reduced ankle moment with the MTP joint extended, while two subjects displayed an increase in the ankle moment, and one subject exhibited nearly equal ankle moments. Of the five subjects in which the ankle moment was reduced with MTP joint extension, only two displayed similar results at other ankle joint angles.

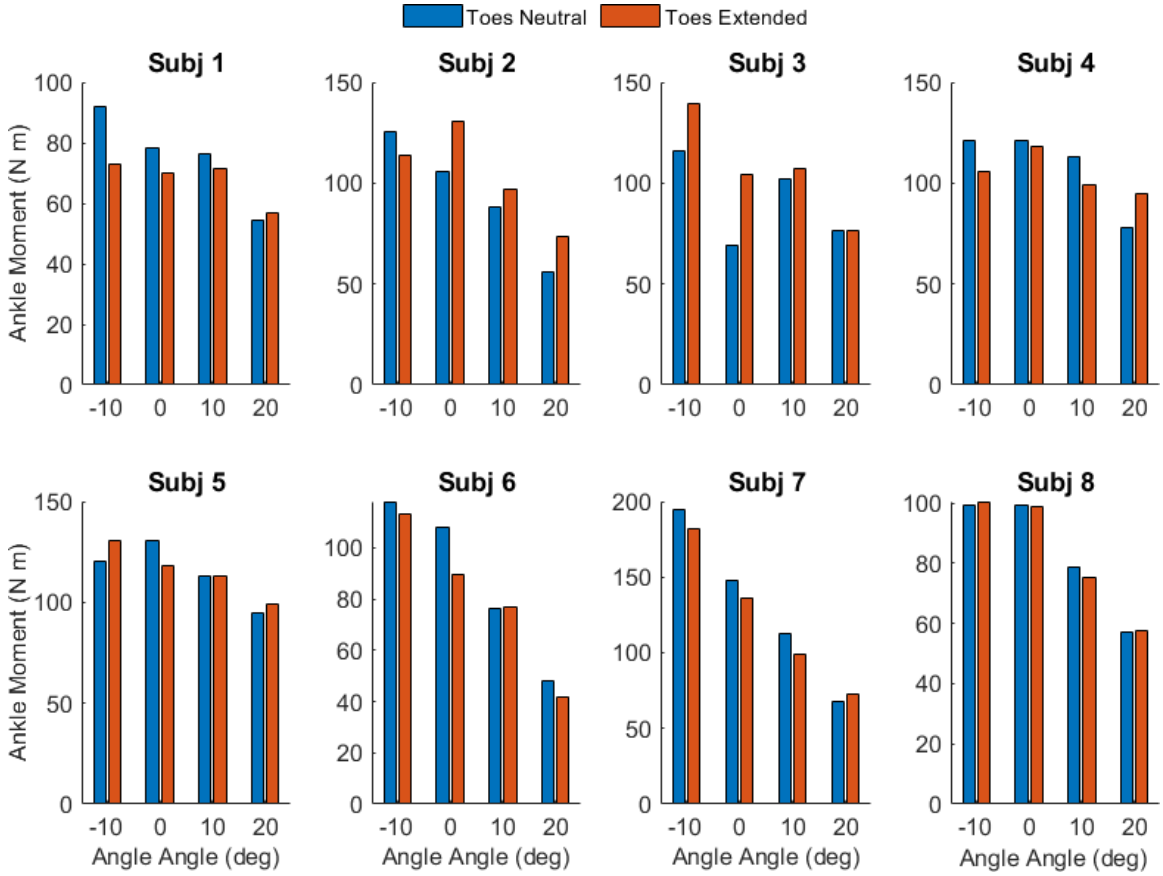

Figure 5-3 With the knee fully extended degrees (0 degree position), no significant effect of MTP joint position on maximum isometric ankle plantarflexion moments was found. Blue bars (left) show data for the MTP joints in a neutral position. Red bars (right) show data for the MTP joints extended to the end of the subject's voluntary range of motion.

With the knee bent to 90 degrees (Figure 5-4), six subjects displayed a reduction in the ankle moment with the MTP joint extended and ankle dorsiflexed to 10 degrees, but two subjects displayed an increase. Of these six, four subjects also displayed a reduction in the ankle moments

with the MTP extended and the ankle joint in the neutral position. Subject 8 was the only subject to exhibit increases in the ankle moment with MTP joint extension across all ankle positions, however, this was not the case with the knee extended (Figure 5-3). Subject 1 is the only other subject to display a trend of increased ankle strength with the MTP extended and ankle joint plantarflexed.

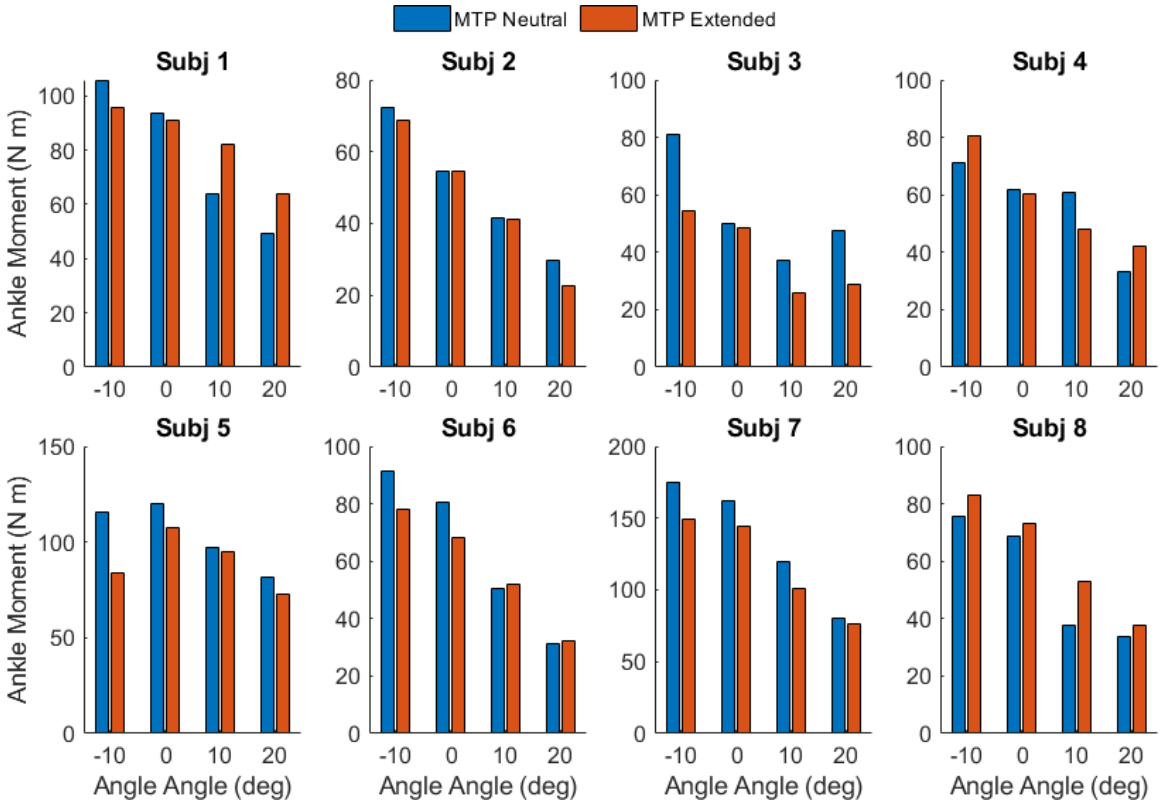

Figure 5-4 With the knee flexed to 90 degrees, no significant effect of MTP joint position on maximum isometric ankle plantarflexion moments was found. Blue bars (left) show data for the MTP joints in a neutral position. Red bars (right) show data for the MTP joints extended to the end of the subject's voluntary range of motion.

5.5 Discussion

This study aimed to determine whether extension of the metatarsophalangeal (MTP) joints altered maximum voluntary isometric ankle plantarflexion moments. It was hypothesized

that passively holding the MTP joints in an extended position would increase the maximum ankle plantarflexion moment. However, this hypothesis was not supported as MTP joint position did not have a significant effect on ankle plantarflexion moments. This suggests that the maximum forces generated by the gastrocnemius, soleus, FHL, and FDL muscles are not substantially affected by the position of the MTP joint.

The MTP joint angle has the potential to alter maximum ankle joint moments due to anatomical and functional relationships with the Achilles tendon, which could subsequently influence the triceps surae. Anatomically, Snow et al. (1995) found a continuous connection of superficial fibers between the PA and the Achilles tendon of young subjects and Stecco et al. (2013) noted a connection between the PA and the paratenon of the Achilles tendon. Functionally, Erdemir et al. (2004) reported a correlation between the Achilles tendon force and PA force during simulated walking with cadaveric specimens. Additionally, Carlson et al. (2000) illustrated that force applied to the Achilles tendon transfers to the PA and that this force transmission is enhanced by MTP joint extension. Thus, the PA force generated by MTP joint extension should elongate the Achilles tendon, which could affect the soleus and gastrocnemius muscles. However, despite these potential connections, the current study suggests that there is no influence of MTP joint extension on the maximum forces generated by the gastrocnemius and soleus.

The absence of an effect on the triceps surae muscles may be due to MTP joint extension generating small PA forces compared to the Achilles tendon forces that arise during maximal contractions. At 500 N of Achilles tendon force, Carlson et al. (2000) reported that extending the MTP joint from 0 degrees (resting position) to 45 degrees increased PA force by 63%, from 314 N to 511 N. Carlson et al. (2000) also reported that the effect of MTP joint extension on PA force decreased with increasing Achilles tendon forces, therefore the effect may be smaller at the larger forces generated during running (e.g., PA force: 765 N or 1.2 BW, Wager and Challis (2016);

Achilles tendon: 3000 – 5000 N during slow running, Komi et al. (1990)). Assuming a 50% increase in PA force at these higher loads, MTP joint extension would create an additional 380 N of PA force. Based on estimated Achilles tendon stiffnesses of 180 – 315 N/mm (Albracht and Arampatzis, 2013; Lichtwark and Wilson, 2007; Maganaris and Paul, 2002; Wren et al., 2001), this force would elongate the Achilles tendon by approximately 1 to 2 mm. Using the equations of Grieve at el. (1978), 1 to 2 mm of triceps surae MTU elongation is equivalent to approximately 2 to 4 degrees of ankle rotation (assumed segment length = 0.42 m). Fitting the maximum ankle moment data from this study with a linear regression model predicts that a 2 degree ankle angle increase would result in a 3.5 N·m increase in the maximum moment generated. Therefore, the additional PA force that arises from MTP joint extension may be too small to have a meaningful effect on the triceps surae's force-generating capacity.

No difference in the maximum ankle plantarflexor moment with maximal MTP joint extension also suggests that the force-generating capacities of the FHL and FDL are unaffected by MTP joint extension. Goldmann & Brüggemann (2012) reported increases of 5-8 N·m in toe flexor moments with changes to ankle and MTP joint angles, with the largest moments generated with the ankle dorsiflexed and MTP joints extended and the smallest moments generated with the ankle plantarflexed and MTP joint in a neutral position. Furthermore, an estimated moment-fascicle length relationship (constructed using estimates of FHL length change from Refshauge et al. (1995)) suggested that the FHL operated on the ascending limb and plateau of the force-length curve (Goldmann and Brüggemann, 2012). However, much of the estimated fascicle length change may have arisen from ankle joint rotation (0.50 mm per degree of rotation) rather than MTP joint rotation (0.22 mm per degree of rotation) (Refshauge et al., 1995). In the present study, the moment arm estimates of Refshauge et al. (1995) produce a mean FHL MTU length change of 10.5 mm with maximal MTP joint extension. No change in the ankle moment across this range indicates that the FHL may operate on the plateau of its force-length curve during MTP

joint extension or that the MTU length change is taken up primarily by the tendon. Alternatively, changes to FDL and FHL forces may have been insubstantial compared to the magnitude of the ankle joint moment. Small changes of 5 – 8 N·m (similar in magnitude to Goldmann & Bruggemann (2012)) would constitute changes of 3 – 25% in the ankle joint moments measured in this study. This is a conservative estimate given that the FHL moment arm is larger at the ankle joint than at the MTP joint (Klein et al., 1996; Hui et al., 2007).

With no effect on the ankle plantarflexor moment, extension of the MTP joints during late stance may serve other functions during locomotion. Stefanyshyn and Nigg (1997) reported that MTP joint extension absorbed energy during running and sprinting, but others (Oh and Park, 2017; Smith et al., 2012) have reported a small period of energy generation or MTP joint flexion during late stance. McDonald et al. (2016) suggested that MTP extension during late stance absorbs energy, but that this energy is transferred through the PA to the arch of the foot where it adds to power generation. Prior to foot contact during walking, Caravaggi et al. (2009) suggested that MTP joint extension pretensions the PA to assist with stiffening the foot earlier in the stance phase, potentially aiding propulsion later in stance. MTP extension may also assist with the modulation of the ankle gear ratio (ratio of the ground reaction force vector moment arm to muscle moment arms) by delaying the anterior movement of the center of pressure and shortening the ground reaction force moment arm. Smith et al. (2014) measured reduced MTP joint motion, increased MTP joint moments, and improved sprint times when subjects sprinted in stiff sprinting footwear compared to barefoot. Willwacher et al. (2014) found that stiffer shoes increased ground reaction force moment arms and modulated changes to ankle moments and push-off times during running. Shortened ground reaction force moment arms may reduce the load required of the plantarflexor muscles and permit faster ankle plantarflexion velocity during push-off (Erdemir and Piazza, 2002). Thus, coordination of MTP joint kinematics could permit the flexibility to select between faster plantarflexion velocity and greater plantarflexor force generation,

potentially contributing to variable gearing at the ankle (Carrier et al., 1994) and locomotor task versatility or optimization.

Limitations to this study primarily relate to the experimental setup. The custom toe plate was effective at maintaining the MTP joint position and isolating MTP joint moments from the dynamometer measurements, but the arch of the foot was unloaded. Therefore, these results may be less relevant to tasks in which the foot is weighted, such as locomotion. Arch elongation and loading has been shown to influence the activation of the intrinsic foot muscles (Kelly et al., 2014), but it is unknown if this also applies to the FDL and FHL, which do not have muscle bellies in the arch of the foot. In addition, the MTP joint was only held in two positions (neutral and fully extended) and there may be an optimal position between these which results in a larger maximum ankle plantarflexion moment. However, if the ankle plantarflexor muscles operate on the ascending limb of their force-length curves (Goldmann and Brüggemann, 2012; Herzog et al., 1991; Maganaris, 2003; Rubenson et al., 2012; Winter and Challis, 2008), this is unlikely. Arampatzis et al. (2005) reported that the compliance of the foot-ankle-dynamometer system can contribute significantly to the measured ankle joint moment. In this study, the foot (and thus, foot-ankle-dynamometer system) compliance may have increased with MTP joint extension, which could have affected the comparisons between the two MTP joint positions. The homogeneity of the subject pool also presents a limitation, as seven of the eight subjects exhibited a "neutral" foot type.

Future work on the interactions between the MTP joints and the ankle plantarflexors should explore the influence of foot type. In this study, the one subject with a "pronated" foot type (Subject 8) displayed a consistent increase in the plantarflexor moment with the MTP joints extended and the knee bent to 90 degrees (Figure 5-4). Angin et al. (2014) measured increased FDL and FHL cross-sectional areas in individuals with *pes planus*, which suggests that the contributions of the FDL and FHL to the ankle moment could be larger in these individuals. This

increased contribution could result in a greater effect of MTP joint extension on the maximum plantarflexion moment. However, the single "pronated foot" subject in this study also displayed the greatest unweighted 1st MTP joint range of motion, which could have produced larger changes in the FHL MTU length than in the other subjects. In addition, future work should attempt to investigate the effects of MTP joint extension on the extrinsic toe flexor muscles and triceps surae separately, as the present study may have missed any equal but opposite effects. As there are three joint angles that could affect the triceps surae (knee, ankle, and MTP) but only two that affect the extrinsic toe flexor muscles (ankle and MTP), the three joints could likely be configured to isolate the effect of MTP joint extension to each muscle group. For example, the hallux could be extended (potentially lengthening both muscle groups) and the knee flexed to maintain constant triceps surae MTU lengths but increase the FDL and FHL MTU lengths. In addition, insights could be gained from repeating the experiments of Carlson et al. (2000) using younger specimens (the connection between the PA and the Achilles tendon may decrease with age; Snow et al. (1995)), applying larger Achilles tendon forces (to better simulate locomotion), and directly measuring the Achilles tendon forces that arise from passive MTP joint extension.

This study proposes that MTP joint extension does not alter the maximum voluntary isometric moment generated at the ankle joint. At each combination of four ankle angles and two knee joint angles, subjects produced statistically similar ankle joint moments with the MTP joints in a neutral position and extended to the end of their range of motion. As MTP joint extension tensions the PA, this study implies that the increased PA force does not influence the force-generating capacity of the gastrocnemius and soleus. Additionally, these results suggest that the force-generating capacity of the extrinsic toe flexor muscles are not greatly influenced by MTP joint extension. Alternatively, the results could suggest that the extrinsic toe flexor muscles have a negligible effect on the ankle joint moment. While MTP joint extension may play an important

role in locomotion, this role does not seem to be related to improving the operating conditions of the ankle plantarflexor muscles.

References

Angin, S., Crofts, G., Mickle, K.J., Nester, C.J., 2014. Ultrasound evaluation of foot muscles and plantar fascia in pes planus. Gait Posture 40, 48–52.

Arampatzis, A., Morey-Klapsing, G., Karamanidis, K., DeMonte, G., Stafilidis, S., Brüggemann, G.-P., 2005. Differences between measured and resultant joint moments during isometric contractions at the ankle joint. J. Biomech. 38, 885–892.

Bojsen-Møller, F., Lamoreux, L., 1979. Significance of free-dorsiflexion of the toes in walking. Acta Orthop. Scand. 50, 471–479.

Caravaggi, P., Pataky, T., Goulermas, J.Y., Savage, R., Crompton, R., 2009. A dynamic model of the windlass mechanism of the foot: evidence for early stance phase preloading of the plantar aponeurosis. J. Exp. Biol. 212, 2491–2499.

Carlson, R.E., Fleming, L.L., Hutton, W.C., 2000. The biomechanical relationship between the tendoachilles, plantar fascia and metatarsophalangeal joint dorsiflexion angle. Foot Ankle Int. 21, 18–25.

Carrier, D.R., Heglund, N.C., Earls, K.D., 1994. Variable gearing during locomotion in the human musculoskeletal system. Science 265, 651–653.

Erdemir, A., Hamel, A.J., Fauth, A.R., Piazza, S.J., Sharkey, N.A., 2004. Dynamic loading of the plantar aponeurosis in walking. J. Bone Jt. Surg. 86, 546–552.

Erdemir, A., Piazza, S.J., 2002. Rotational foot placement specifies the lever arm of the ground reaction force during the push-off phase of walking initiation. Gait Posture 15, 212–219.

Farris, D.J., Sawicki, G.S., 2012. The mechanics and energetics of human walking and running: a joint level perspective. J. R. Soc. Interface 9, 110–118.

Grieve, D.W., Pheasant, S., Cavanagh, P.R., 1978. Prediction of gastrocnemius length from knee and ankle posture, in: Jorgenson, K. (Ed.), Biomechanics VI-A. University Park Press, Baltimore, MD, pp. 405–412.

Herzog, W., Read, L.J., ter Keurs, H.E.D.J., 1991. Experimental determination of force—length relations of intact human gastrocnemius muscles. Clin. Biomech. 6, 230–238.

Hicks, J.H., 1954. The mechanics of the foot. II. The plantar aponeurosis and the arch. J. Anat. 88, 25-30.1.

Hui, H.J., Beals, T.C., Brown, N.A.T., 2007. Influence of tendon transfer site on moment arms of the flexor digitorum longus muscle. Foot Ankle Int. 28, 441–447.

Inman, V.T., 1976. The joints of the ankle. Williams & Wilkins, Baltimore.

Isman, R.E., Inman, V.T., 1969. Anthropometric studies of the foot and ankle. Bull. Prothestics Res.

Iwanuma, S., Akagi, R., Hashizume, S., Kanehisa, H., Yanai, T., Kawakami, Y., 2011. Triceps surae muscle-tendon unit length changes as a function of ankle joint angles and contraction levels: the effect of foot arch deformation. J. Biomech. 44, 2579–2583.

Kelly, L.A., Cresswell, A.G., Racinais, S., Whiteley, R., Lichtwark, G., 2014. Intrinsic foot muscles have the capacity to control deformation of the longitudinal arch. J. R. Soc. Interface 11, 20131188.

Klein, P., Mattys, S., Rooze, M., 1996. Moment arm length variations of selected muscles acting on talocrural and subtalar joints during movement: An In vitro study. J. Biomech. 29, 21–30.

Komi, P.V., 1990. Relevance of in vivo force measurements to human biomechanics. Journal of Biomechanics 23, Supplement 1, 23–34.

Maganaris, C.N., 2003. Force-length characteristics of the in vivo human gastrocnemius muscle. Clin. Anat. N. Y. N 16, 215–223.

McDonald, K.A., Stearne, S.M., Alderson, J.A., North, I., Pires, N.J., Rubenson, J., 2016. The role of arch compression and metatarsophalangeal joint dynamics in modulating plantar fascia strain in running. PLOS ONE 11, e0152602.

Redmond, A.C., Crosbie, J., Ouvrier, R.A., 2006. Development and validation of a novel rating system for scoring standing foot posture: The Foot Posture Index. Clin. Biomech. 21, 89–98.

Refshauge, K.M., Chan, R., Taylor, J.L., McCloskey, D.I., 1995. Detection of movements imposed on human hip, knee, ankle and toe joints. J. Physiol. 488, 231–241.

Rubenson, J., Pires, N.J., Loi, H.O., Pinniger, G.J., Shannon, D.G., 2012. On the ascent: the soleus operating length is conserved to the ascending limb of the force–length curve across gait mechanics in humans. J. Exp. Biol. 215, 3539–3551.

Shaw, H.M., Vázquez, O.T., McGonagle, D., Bydder, G., Santer, R.M., Benjamin, M., 2008. Development of the human Achilles tendon enthesis organ. J. Anat. 213, 718–724.

Smith, G., Lake, M., Lees, A., 2014. Metatarsophalangeal joint function during sprinting: a comparison of barefoot and sprint spike shod foot conditions. J Appl Biomech. 30, 206–212.

Smith, G., Lake, M., Lees, A., Worsfold, P., 2012. Measurement procedures affect the interpretation of metatarsophalangeal joint function during accelerated sprinting. J. Sports Sci. 30, 1521–1527.

Snow, S.W., Bohne, W.H., DiCarlo, E., Chang, V.K., 1995. Anatomy of the Achilles tendon and plantar fascia in relation to the calcaneus in various age groups. Foot Ankle Int. Am. Orthop. Foot Ankle Soc. Swiss Foot Ankle Soc. 16, 418–421.

Stecco, C., Corradin, M., Macchi, V., Morra, A., Porzionato, A., Biz, C., De Caro, R., 2013. Plantar fascia anatomy and its relationship with Achilles tendon and paratenon. J. Anat. 223, 665–676.

Stefanyshyn, D.J., Nigg, B.M., 1997. Mechanical energy contribution of the metatarsophalangeal joint to running and sprinting. J. Biomech. 30, 1081–1085.

Wager, J.C., Challis, J.H., 2016. Elastic energy within the human plantar aponeurosis contributes to arch shortening during the push-off phase of running. Journal of Biomechanics 49, 704–709.

Willwacher, S., König, M., Braunstein, B., Goldmann, J.-P., Brüggemann, G.-P., 2014. The gearing function of running shoe longitudinal bending stiffness. Gait Posture 40, 386–390.

Winter, D.A., 1983. Moments of force and mechanical power in jogging. J. Biomech. 16, 91–97.

Winter, S.L., Challis, J.H., 2008. Reconstruction of the human gastrocnemius force-length curve in vivo: part 2-experimental results. J. Appl. Biomech. 24, 207–214.

Zelik, K.E., Takahashi, K.Z., Sawicki, G.S., 2015. Six degree-of-freedom analysis of hip, knee, ankle and foot provides updated understanding of biomechanical work during human walking. J. Exp. Biol. 218, 876–886.

Chapter 6

Discussion

6.1 Introduction

This chapter contains the conclusions and discussion of the dissertation. Section 6.2 presents a summary of each chapter. Section 6.3 reviews the primary limitations of each study. Section 6.4 outlines future studies that have been motivated by the three studies. Section 6.5 summarizes the dissertation's major conclusions.

6.2 Summary

This dissertation utilized three studies to investigate the interplay between foot mobility and the function of the ankle joint and its musculature during locomotion. Two studies utilized rigid body models of the lower leg and foot to explore how foot model topology influences ankle kinematics, kinetics, and simulated muscle active states during running. The third study altered the metatarsophalangeal (MTP) joint angle *in vivo* to examine its effect on the maximum isometric ankle plantarflexion moment. The first two studies indicated that the foot should be treated as a multi-body system for the analysis of locomotion mechanics, because treating the foot as a single rigid body resulted in overestimated ankle joint power, triceps surae muscle active states, and Achilles tendon elastic energy storage during running. These effects seem to be primarily due to foot joint rotations being erroneously captured as ankle joint rotation. The third study, which experimentally manipulated of the MTP joints during maximal plantarflexions,

indicated that ankle plantarflexion moments are independent of MTP joint position and therefore, the MTP joints do not serve to modulate the ankle moment during locomotion

In Study 1, a kinematic and kinetic analysis of the ankle joint during running was shown to be influenced by the topology of the chosen foot model (Chapter 3). Traditionally, biomechanical analyses have modeled the foot as a single rigid segment, lumping the bones and joints between the ankle and metatarsophalangeal (MTP) joints into one rigid segment and ignoring the toes. Recently, multisegment foot models have been developed which group the foot bones and joints into multiple rigid bodies. These multisegment models attempt to capture and estimate the rotation of foot joints, which may be important for understanding locomotion mechanics. While these models have been previously utilized to study walking, this study was the first application of a multisegment foot model to running. The specific aims of this study were to compare the ankle joint kinematics (angular excursion and velocity) and kinetics (joint moment and power) calculated using a single segment foot and a multisegment foot during running. Ground reaction forces and lower limb segment kinematics of seven subjects were used as inputs to an inverse dynamics analysis using both the single and multisegment foot models. Compared to the single segment foot model, the multisegment foot model computed less total ankle excursion over the stance phase, lower ankle angular velocities during both early and late stance, and less ankle joint power generation during late stance. Little to no change was found in the ankle joint moments between the two models. A second aim of this study was to investigate the function of the medial longitudinal arch of the foot (MLA) using the "midfoot joint" (the joint between the rearfoot and forefoot segments) in the multisegment model. The kinematics and kinetics of the midfoot joint suggested that the MLA functioned in a similar fashion as the ankle joint during running, absorbing energy during early stance and generating energy during late stance. While this is a non-anatomical joint (e.g., it is a representation of the collective motion of the multiple joints within the arch), it suggests that the anatomical joints between the calcaneus

and metatarsals (some of which constitute the MLA) may meaningfully contribute to running energetics. The combined power of the ankle and midfoot joints in the multisegment model was equivalent to the power of the ankle joint in the single segment model, which suggested that the single segment model misallocated foot joint power as ankle joint power.

In Study 2, the two foot models (single and multisegment) were utilized to investigate whether foot model topology altered the simulated active states of the ankle plantarflexor muscles during running (Chapter 4). Similar to traditional inverse dynamics analyses of the ankle, simulations of the ankle plantarflexor muscles are typically performed using a single segment foot model. It was hypothesized that the muscle active states and fiber kinematics would be reduced in the multisegment foot model due to the kinematic differences between the models at the ankle joint. The specific aim of this study was to compare the active state of ankle plantarflexor muscles during simulations driven by the kinematics and kinetics from both a multisegment foot model and a single segment foot model. To achieve this aim, the kinematics and kinetics from Chapter 3 were used to simulate two ankle plantarflexor muscles (representing the gastrocnemius and soleus muscles) using both a single segment foot model and a multisegment foot model. In both modeled muscles, the hypothesis was supported as the multisegment foot model reduced the active state during late stance. This reduction was due to muscle fiber lengths being closer to the optimum length and slower muscle fiber shortening velocities. Sensitivity analyses demonstrated that the reduced active states using the multisegment foot model were robust to changes in the muscle model parameters. Therefore, this study suggests that simulations which utilize a single segment foot model may overestimate the active states, fiber length changes, and fiber velocities of the ankle plantarflexors during running. Thus, foot model topology should be chosen carefully for similar simulations.

In Study 3, the interaction between the MTP joints and the ankle plantarflexor muscles was investigated by changing the MTP joint positions and testing for changes to the maximum

voluntary isometric moment of the ankle plantarflexors (Chapter 5). The connections between the MTP joints, the plantar aponeurosis, and the Achilles tendon suggest that the position of the MTP joints could alter the moment generating capacities of the gastrocnemius and soleus through strain of the triceps surae MTU. Additionally, the flexor digitorum longus (FDL) and flexor hallucis longus (FHL) muscles span the ankle and MTP joints, which could result in changes to their force production with changes to the MTP joint angle. To test the impact of these relationships on the maximum ankle plantarflexion moment, eight healthy volunteers generated maximum isometric plantarflexion moments in 16 different configurations of MTP, ankle, and knee joint angles. While statistically significant effects of knee and ankle joint angles were found, no significant effect of MTP joint angle on ankle plantarflexion moments was found. This suggests that the MTP joints do not play a prominent role in modulating the maximum ankle plantarflexion moment. Further, this implies that neither the connections between the MTP joints and the Achilles tendon, nor the moment-generating capacities of the FDL and FHL at the ankle are influenced by the angle of the MTP joint, or that their effects are equal and opposite such that they cancel.

6.3 Limitations

In Chapter 3, the main limitations were the use of rigid-body components to represent model segments and skin mounted markers to capture foot motion. While the multisegment model was more a comprehensive representation of the human foot than the single segment model, it did not permit deformation of the model's foot segments. Primarily, foot segment deformation would arise from the compression and recoil of the plantar heel pad and the splaying of the forefoot due to motion of the metatarsal bones relative one another during stance (Duerinck et al., 2014; Nester et al., 2010; Okita et al., 2009). The use of skin mounted markers may

introduce errors into tracking the positions of the underlying bones (and therefore, joints). Segment deformation and skin marker artefacts combined have produced changes of up to 4 degrees in intersegment (joint) angles within the foot (Okita et al., 2009). However, these artefacts also existed in the single segment model, which suggests that the comparison between the two models remains valid given similar systematic errors. However, neither model fully captured the motion and energetics of the foot during locomotion.

The primary limitations in Chapter 4 were the simplicity of the muscle model and the estimation of muscle-tendon unit lengths using the equations of Grieve et al. (1978). The simplified muscle model was a Hill-type muscle that did not include the effects of pennation angle or muscle history. Changes in pennation angle (e.g., muscle fiber rotation) occur during both muscle shortening and lengthening as the muscle undergoes shape changes, with the magnitude of fiber rotation proportional to the change in muscle shape (Azizi et al., 2008; Azizi and Roberts, 2014). As the multisegment and single segment foot models exhibited different MTU lengths (and therefore, different shape changes), fiber rotation in the single segment foot model likely would have been greater than in the multisegment foot model, which could have accounted for some of the difference in MTU length if it were included. Utilization of the equations of Grieve et al. (1978) for estimating MTU length limited the analysis to the sagittal plane, but non-sagittal plane kinematic differences between the foot models was statistically insignificant for nearly all of the stance phase. Additionally, Grieve et al. (1978) secured the entire foot on a rigid footplate and measured the ankle angle as the angle between the tibia and the footplate. This likely overestimated the ankle angle by including any motion of the foot joints within the ankle angle, similar to the findings of Study 1. However, this was similar between the multisegment and single segment foot models and therefore, was unlikely to influence the study conclusions.

In Chapter 5, the primary limitation was the inability to completely secure each subject's foot to the dynamometer footplate. The Velcro strapping did not completely prevent the heel from lifting off the footplate, which resulted in additional plantarflexion compared to the ankle angle recorded by the dynamometer. Furthermore, in the MTP extended condition, the heel was slightly more secure due to increased force from the toe plate straps, which pushed backwards on the foot and increased the hold of the heel cup. Thus, in the MTP neutral condition the ankle angle may have been slightly more plantarflexed than the corresponding position in the MTP extended condition. Efforts were made to eliminate this effect by also tightening the toe plate strapping in the MTP neutral condition to generate similar forces on the heel cup. Subjects performed preliminary test contractions to confirm similar heel movement in both conditions. Lastly, holding the MTP joints at the fully extended position for 5 minutes (the approximate time taken to complete all the trials with the MTP joints fully extended) may have introduced some discomfort. However, participants did not report discomfort and did not accept offers to rest midway through any of the conditions.

6.4 Future Work

The findings of these three studies could inform a number of future studies which would build understanding of foot and ankle function.

Studies 1 and 2 demonstrated the use of a multisegment foot model, which could be utilized to study more powerful movements, such as sprinting and jumping. Jumping, in particular, could prove to be a useful motion for understanding how the ankle and foot work together to generate power. As power generation during jumping typically proceeds from the proximal to the distal joints (Gregoire et al., 1984; Hudson, 1986; Van Ingen Schenau, 1989), it could be hypothesized that power generation by the arch of the foot would occur slightly after the

power generation at the ankle in sequence with the rest of the joints of the lower limb. The multisegment foot model could also be used to explore arch function during inline and decline walking & running, which would alter power requirements and illustrate how the ankle and foot work together to generate or absorb the additional energy. Finally, utilizing a multisegment foot model to study the walk-to-run transition could highlight what triggers humans to change gait modes.

Study 3 explored the relationship between the MTP joints and ankle joint which, in part, sheds light on the interaction between the Achilles tendon and plantar aponeurosis. To better isolate this interaction and further explore its potential, the MTP joints could be manipulated while simultaneously estimating Achilles tendon and plantar aponeurosis strain through ultrasound imaging. If Achilles and plantar aponeurosis strains are correlated during simple, passively generated movements, the MTP joints could be manipulated during locomotion using custom footwear while lower limb kinematics and kinetics (motion capture) and Achilles tendon strain (ultrasound imaging) are recorded. If MTP joint manipulations could occur as a function of time, unexpected temporal profiles could be applied to the MTP joint to attempt to disrupt the normal mechanics of the foot and ankle.

6.5 Conclusions

The three studies of this dissertation have generated the following conclusions:

1. Multisegment and single segment foot models produce different ankle kinematics and power during push-off.
2. Single segment foot models overestimate the motion and power of the ankle by combining it with the motion and power of the joints of the foot.

3. The arch of the foot generates meaningful energetic contributions during running, similar to the function of the ankle.
4. Simulating the ankle plantarflexors during running using multisegment and single segment foot models produces different muscle active states, with the single segment foot model overestimating the active state.
5. The angle of the MTP joints does not alter the maximum isometric moment generated by the ankle plantarflexor muscles.

References

Azizi, E., Brainerd, E.L., Roberts, T.J., 2008. Variable gearing in pennate muscles. Proc. Natl. Acad. Sci. 105, 1745–1750.

Azizi, E., Roberts, T.J., 2014. Geared up to stretch: pennate muscle behavior during active lengthening. J. Exp. Biol. 217, 376–381.

Duerinck, S., Hagman, F., Jonkers, I., Van Roy, P., Vaes, P., 2014. Forefoot deformation during stance: Does the forefoot collapse during loading? Gait Posture 39, 40–47.

Gregoire, L., Veeger, H.E., Huijing, P.A., van Ingen Schenau, G.J., 1984. Role of mono- and biarticular muscles in explosive movements. Int. J. Sports Med. 5, 301–305.

Grieve, D.W., Pheasant, S., Cavanagh, P.R., 1978. Prediction of gastrocnemius length from knee and ankle posture, in: Jorgenson, K. (Ed.), Biomechanics VI-A. University Park Press, Baltimore, MD, pp. 405–412.

Hudson, J.L., 1986. Coordination of segments in the vertical jump. Med. Sci. Sports Exerc. 18, 242–251.

Nester, C.J., Liu, A.M., Ward, E., Howard, D., Cocheba, J., Derrick, T., 2010. Error in the description of foot kinematics due to violation of rigid body assumptions. J. Biomech. 43, 666–672.

Okita, N., Meyers, S.A., Challis, J.H., Sharkey, N.A., 2009. An objective evaluation of a segmented foot model. Gait Posture 30, 27–34.

Van Ingen Schenau, G.J., 1989. From rotation to translation: Constraints on multi-joint movements and the unique action of bi-articular muscles. Hum. Mov. Sci. 8, 301–337.

Appendix A

Informed Consent Form

Title of Project: Function of the human foot and ankle during walking, running, and jumping

CONSENT FOR RESEARCH

The Pennsylvania State University

Principal Investigator: Justin C. Wager

Address: 29 Recreation Building, University Park, PA 16802

Telephone Number: 814-365-3445

Advisor: John H. Challis

Advisor Telephone Number: 814-369-3675

Subject's Printed Name: _____

We are asking you to be in a research study. This form gives you information about the research. Whether or not you take part is up to you. You can choose not to take part. You can agree to take part and later change your mind. Your decision will not be held against you. Please ask questions about anything that is unclear to you and take your time to make your choice.

1. Why is this research study being done?

We are asking you to be in this research because you are a runner with no recent injury or history of major injury. This research is being done to find out: 1) how the foot and ankle function during running, walking, and jumping, 2) how the toe joint affects ankle joint strength. Approximately 8 people will take part in this research study here at Penn State University.

2. What will happen in this research study?

You may decide to not participate in this research or to only participate in a portion of this research. The entire research protocol will take approximately 90 minutes. Here is a flow chart of the steps that will occur in your visit.

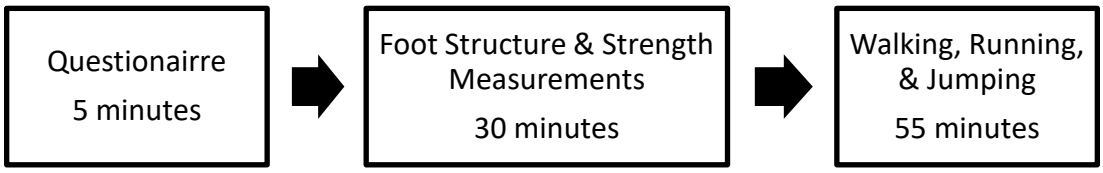

Questionnaire [5 minutes]:

You will complete a questionnaire about your running habits and musculoskeletal injury history.

There are two portions of the study. You may choose to volunteer for both or just one. Please initial next to the portion(s) of the testing that you would like to volunteer for.

_____ *Foot Structure & Strength Measurements [30 minutes]:*
We will ask you to remove your shoes and socks and the dimensions and posture of your lower limb and foot will be measured using a tape measure and the Foot Posture Index (FPI; uses simple visual observations of your foot). Some small marks will be made on your foot and lower leg with permanent marker; these should wash off within a few days. Six to ten photos of your foot and lower leg will be taken and we will not show your face or any identifying information or marks (e.g., tattoos) in the photos. Some photos of your foot will be taken with you standing and then we will ask you to sit and the foot photos will be repeated in the seated position. In two of the photos, we will extend your toes (pull them back towards your shin) to the farthest point that you are comfortable with to estimate your toe joint flexibility.

We will record your height and mass using a standard scale and stadiometer.

We will ask you to sit comfortably in a strength testing device (which is similar to a weight lifting machine at a fitness center) and place your foot on a footplate. Your foot and leg will be secured to the device with Velcro to maintain the leg and foot positions throughout the testing. After securing the Velcro straps, we will ask if the tightness is comfortable and you will be allowed to adjust the tightness if desired. If at any time the straps become uncomfortable, you may choose to stop the testing. A small aluminum plate will be attached to your toes with prewrap and athletic tape. Your toe joint will then be positioned at an angle and the aluminum plate will be attached to a bracket on the footplate using a nylon strap and cam buckle. This will keep your toes at the desired angle throughout each trial. In each trial, a goniometer (similar to a sophisticated protractor) may be used to measure your toe and ankle angles. In addition, a video of the side of your foot and leg may be taken throughout the testing. This video will only be of your foot and leg and will not contain your face.

The strength testing device will be set up so that it cannot move your ankle beyond your range of motion. We will begin the testing by setting these limits on the device. You will be asked to move your ankle voluntarily as far as you can towards your body and away from your body so that we can set the range of motion and ensure your comfort and safety. You can ask to reset these limits at any time if you feel they are uncomfortable.

We will then ask you to complete two maximal voluntary isometric (constant position) ankle plantarflexion contractions against a footplate for 5 seconds each. This will be repeated at 4 different ankle positions, 2 knee joint positions, and 2 different toe joint positions (16 positions total; 32 total trials). We will also ask you to complete 12 maximal voluntary isokinetic (constant speed) ankle plantarflexion contractions. Two trials will be done at each of the 2 toe angles and 2 knee angles for three different speeds of ankle rotation (20°/sec, 60°/sec, 120°/sec). These speeds are within the normal speeds that your ankle rotates during walking and should be comfortable. However, you may choose to skip any portion of the testing. At any time, you may ask to see the footplate rotate without your foot in it to assess the speed. In all portions of the testing, the foot plate will not rotate without you pushing on it. You will be allowed as much rest as desired between trials. The rest period will initially be set at 15 seconds and you may change this as desired. At least 30 seconds rest will be given between angles.

During and/or before testing, parts of your foot and lower leg will be visualized using an ultrasound imaging device. This device is similar to the devices used to visualize the developing embryo or fetus during pregnancy. Various bones and soft tissues in your foot and lower leg will be found and an image of these structures will be recorded for further analysis.

_____ *Walking, Running, and Jumping [55 minutes]:*
Your feet will be wiped down with isopropyl rubbing alcohol to improve the adherence of the motion capture markers to your skin. Markers will be placed on your foot, legs, and upper body. These markers are similar to small solid ping pong balls covered with reflective tape and will be adhered to the skin with hypoallergenic double-sided tape. After the markers are placed, we will ask you to stand on a force plate, which is instrumented similar to a standard bathroom scale. A motion analysis system will then record the location of the markers (no images of you will be recorded, only images of the markers). We will take two photographs of your foot next to a ruler – one from the side and one from the back. These photos will not contain your face or any identifying information. You may choose not to have these photos taken.

We will then ask you to complete the movement portion of testing, which consists of 3 tasks:

1) Walking – we will ask you to walk down a short runway (~20 m) at a speed that is comfortable for you. In the middle of the runway, your foot will land on the force plates to

record the forces that naturally occur between the ground and your foot. Five trials will be collected, and you will be given as much rest as you would like between trials.

2) Running – we will ask you to run down the runway at running paces ranging from 8:39 per mile to 4:28 per mile. The faster speeds will only be used if you feel comfortable running at the desired paces. If you do not feel comfortable with any paces, then you can choose not to complete that portion of the testing. Up to 5 trials will be collected at each speed and you will be given as much rest as you would like between trials. Carpet squares will be placed on the runway to cushion the hard surface of the lab and make it more comfortable for you. However, if at any time you are uncomfortable you can choose to stop and skip any portions of the testing. No more than 4 speeds will be collected.

3) Jumping – we will ask you to stand on the force plates and perform 6 maximal height jumps: 3 using both legs and 3 using only one leg. You will be given as much rest as you would like between jumps.

During each of these tasks, the motion analysis system will record the movement of the markers (no images of the subject will be taken) and the force plate will record the naturally occurring forces between your feet and the force plate.

In total, this study will consist of 1 visit to the Biomechanics Lab, taking about 1.5 hours of your time. The researchers may contact you to participate in future studies related to this research. Your participation in any future research would be voluntary and you would not be penalized for choosing not to participate.

6. How long will you take part in this research study?

This research study will take approximately 90 minutes of your time during your visit to the Biomechanics Lab. Being in this research study does not require any additional time outside of this one session.

7. How will your privacy and confidentiality be protected if you decide to take part in this research study?

Efforts will be made to limit the use and sharing of your personal research information to people who have a need to review this information.

- A subject code number that is linked to this consent form will be kept in a locked file in the offices of the Biomechanics Laboratory and/or in a password protected file on Penn State maintained and secured servers.
- This consent form (which includes your subject code number) will be kept in a locked file in the offices of the Biomechanics Laboratory.

- Your research records will be labeled with your subject code number and will be kept in a password protected file on Penn State maintained and secured servers.

In the event of any publication or presentation resulting from the research, no personally identifiable information will be shared.

We will do our best to keep your participation in this research study confidential to the extent permitted by law. However, it is possible that other people may find out about your participation in this research study. For example, the following people/groups may check and copy records about this research.

- The Office for Human Research Protections in the U. S. Department of Health and Human Services
- The Institutional Review Board (a committee that reviews and approves research studies) and
- The Office for Research Protections.

Some of these records could contain information that personally identifies you. Reasonable efforts will be made to keep the personal information in your research record private. However, absolute confidentiality cannot be guaranteed.

8. What are the costs of taking part in this research study?

8a. What will you have to pay for if you take part in this research study?

There are no costs to you related to this study.

8b. What happens if you are injured as a result of taking part in this research study?

In the unlikely event that you become injured as a result of your participation in this study, medical care is available. It is the policy of this institution to provide neither financial compensation nor free medical treatment for research-related injury. By signing this document, you are not waiving any rights that you have against The Pennsylvania State University for injury resulting from negligence of the University or its investigators.

9. What are your rights if you take part in this research study?

Taking part in this research study is voluntary.

- You do not have to be in this research.
- If you choose to be in this research, you have the right to stop at any time.
- If you decide not to be in this research or if you decide to stop at a later date, there will be no penalty or loss of benefits to which you are entitled.

11. If you have questions or concerns about this research study, whom should you call?

Please call the head of the research study (principal investigator), Justin Wager, at 814-365-3445 if you:

- Have questions, complaints or concerns about the research.
- Believe you may have been harmed by being in the research study.

You may also contact the Office for Research Protections at (814) 865-1775, ORProtections@psu.edu if you:

- Have questions regarding your rights as a person in a research study.
- Have concerns or general questions about the research.
- You may also call this number if you cannot reach the research team or wish to offer input or to talk to someone else about any concerns related to the research.

INFORMED CONSENT TO TAKE PART IN RESEARCH

Signature of Person Obtaining Informed Consent

Your signature below means that you have explained the research to the subject or subject representative and have answered any questions he/she has about the research.

_____ _____ _____

Signature of person who explained this research Date Printed Name

(Only approved investigators for this research may explain the research and obtain informed consent.)

<u>Signature of Person Giving Informed Consent</u>

Before making the decision about being in this research you should have:

- Discussed this research study with an investigator,
- Read the information in this form, and
- Had the opportunity to ask any questions you may have.

Your signature below means that you have received this information, have asked the questions you currently have about the research and those questions have been answered. You will receive a copy of the signed and dated form to keep for future reference.

Signature of Subject

By signing this consent form, you indicate that you voluntarily choose to be in this research and agree to allow your information to be used and shared as described above.

_____ _____ _____

Signature of Subject Date Printed Name

Appendix B

Validity of calculating ankle joint moments without accounting for ground reaction force sharing among foot segments

B.1 Introduction

Two approaches were taken to determine the ground reaction forces and moments (GRF) applied to each foot segment during the stance phase. The first approach was to quantify the GRF acting on each foot segment using multiple force plates and targeted foot strikes over multiple trials, with each segment isolated on a force plate. The second approach was to assign the entire GRF to a single foot segment based on the value of the center of pressure (COP) and the segment endpoints. This appendix details these two approaches and the similarity between the resultant joint moments computed for one subject using these techniques. Due to the similarity, the second approach (assigning the GRF as a function of the COP) was chosen to limit the effect of force plate targeting, avoid inconsistencies arising from combining multiple trials, and reduce the overall number of trials asked of each subject.

B.2 Methods for assigning the GRF to a foot segment

Approach 1: Distribute the GRF among the foot segments using targeted strikes on multiple force plates

To partition the GRF among the foot segments, the subject performed a two walking trials with the foot landing on two adjacent force plates (positioned one after the other in the direction of travel), similar to Bruening et al. (2012). In one trial, the subject landed with the midfoot (at approximately the navicular marker) located on the junction of the two force plates, which measured the GRF acting on the rearfoot (RF) segment. In a second trial, the subject

landed with the MTP joint on the junction of the force plates, which isolated the GRF acting on the TOE segment. The GRF acting on the FF segment (between the midtarsal and MTP joints) was determined by subtracting the known RF and TOE segment GRFs from the resultant GRF computed from both force plates. The center of pressure for the midfoot segment was determined using the force plate COP data and the calculated FF segment GRF (using the method of Zatsiorsky, 2002).

Approach 2: Assign the GRF to a segment based on the location of the center of pressure (COP) from a single force vector

Using the first trial of Approach 1 (a targeted foot strike with the force plate junction at the midfoot), the GRF data from the two force plates were combined into one GRF vector. The COP of this GRF vector was computed as in Zatsiorsky (2002). At each point during the stance phase, segment endpoints were defined by the proximal and distal joint center locations and the combined GRF was assigned to whichever segment contained the COP.

B.3 Results

About the x-axis (inversion/eversion) and z-axis (plantarflexion/dorsiflexion), the two approaches resulted in nearly identical resultant ankle joint moments (Figure B-1). For plantarflexion/dorsiflexion, the root mean square difference (RMSD) between the approaches was 0.50 N·m and the maximum difference was 1.83 N·m. For inversion/eversion, the RMSD was 0.25 N·m and the maximum difference was 1.61 N·m. For abduction/adduction (about the y-axis), the single force plate approach (Approach 2) produced lower resultant ankle joint moments throughout stance, with an RMSD of 2.69 N·m and a maximum of 15.7 N·m.

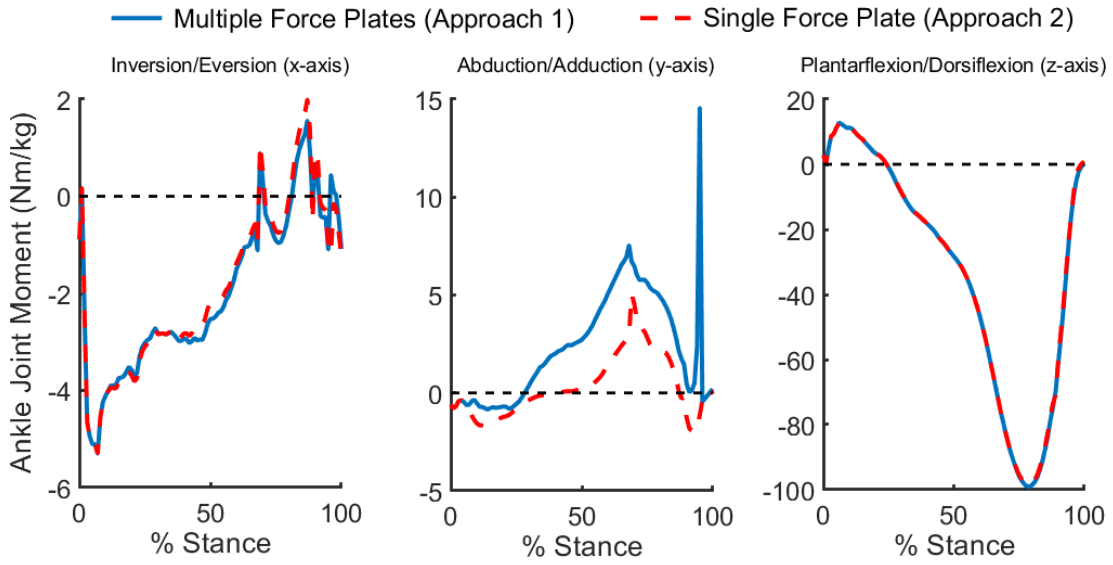

Figure B-1 The resultant ankle joint moments calculated using a multisegment foot model and two different approaches for quantifying the GRF acting on each segment. The solid blue line shows the 'multiple force plate approach', where multiple trials using targeted foot strikes on adjacent force plates isolated the GRF acting on each segment. The dashed red line shows the 'single force plate approach', where a single GRF vector was assigned to a foot segment based on the location of the COP relative to the segments.

References

Bruening, D.A., Cooney, K.M., Buczek, F.L., 2012. Analysis of a kinetic multi-segment foot model part II: Kinetics and clinical implications. Gait & Posture 35, 535–540.

Zatsiorsky, V.M., 2002. Kinetics of Human Motion. Human Kinetics, Champaign, IL.

Appendix C

Muscle model equations and parameters

The general equation used to estimate muscle force was,

$$F_m = q \cdot fl(l_f) \cdot fv(v_f) \cdot F_{max} \quad \text{(A.1)}$$

Where,

F_m is the force output of the muscle model

q is the muscle model active state ($0 \leq q \leq 1$)

fl is the fraction of the maximum isometric force possible by the muscle due to its force-length properties, which are dictated by fiber length (l_f)

fv is the fraction of the maximum isometric force possible by the muscle due to its force-velocity properties, which are dictated by fiber velocity (v_f)

F_{max} is the maximum possible isometric force output for the muscle model

Tendon length was determined by the ratio of the current muscle force to the maximum muscle force,

$$l_t = l_{t0} + \frac{c \cdot F_m}{F_{max}} \cdot l_{t0} \quad \text{(A.2)}$$

Where,

l_t is the current length of the tendon

l_{t0} is the slack length of the tendon

c is the tendon strain due to the maximum isometric muscle force

F_m is the force output of the muscle

F_{max} is the maximum isometric force output of the muscle

The equation for the force-length fraction at a given fiber length, l_f, was,

$$fl = 1 - (\frac{l_f - l_{f0}}{w \cdot l_{f0}})^2 \quad \text{(A.3)}$$

Where,

l_{f0} is the optimal muscle fiber length

w is the width of the force-length curve

The force-velocity fraction was determined by the equation of Hill (1938) during muscle shortening ($vf > 0$),

$$fv = \frac{v_{fmax} - v_f}{v_{fmax} + k \cdot v_f} \quad \text{(A.4)}$$

During muscle lengthening ($vf < 0$), the force-velocity fraction was determined by the equation of Fitzhugh (1977),

$$fv = 1.5 - 0.5\left[\frac{v_{fmax} + v_f}{v_f \cdot (v_{fmax} - 2 \cdot k)}\right] \quad \text{(A.5)}$$

Changes in muscle-tendon unit complex (MTU) length of the uniarticular (soleus) and biarticular (gastrocnemius) used the equations of Grieve et al. (1978), which describe the change in length of the gastrocnemius MTU (as percent of segment length) due to ankle and knee angle changes:

$$L_{MTU\_ANKLE} = A_0 + A_1\theta_A + A_2\theta_A^2 \quad \text{(A.6)}$$

$$L_{MTU_{KNEE}} = A_3 + A_4\theta_K + A_5\theta_K^2 \quad \text{(A.7)}$$

$$L_{MTU} = L_{MTU\_ANKLE} + L_{MTU\_KNEE} \quad \text{(A.8)}$$

Coefficient	Value
A_0	-22.18468
A_1	-0.30141
A_2	-0.00061
A_3	6.46251
A_4	-0.07987
A_5	0.00011

Where,

A_i are coefficients

θ_j are joint angles of the knee (K) and ankle (A)

For the uniarticular muscle, the soleus, the coefficients for the knee angle were set to zero.

The ankle moment arm of the plantarflexor MTU was determined using the first derivative of the length change equations (A.6 - A.8) with respect to the ankle joint angle:

$$r_{MTU} = (A_1 + 2A_2\theta_A)\frac{180}{\pi} \tag{A.9}$$

The moment arm values were expressed as a percentage of segment length; multiplication by the mean shank length of the subjects gave the ankle angle-moment arm relationship (Figure C-1).

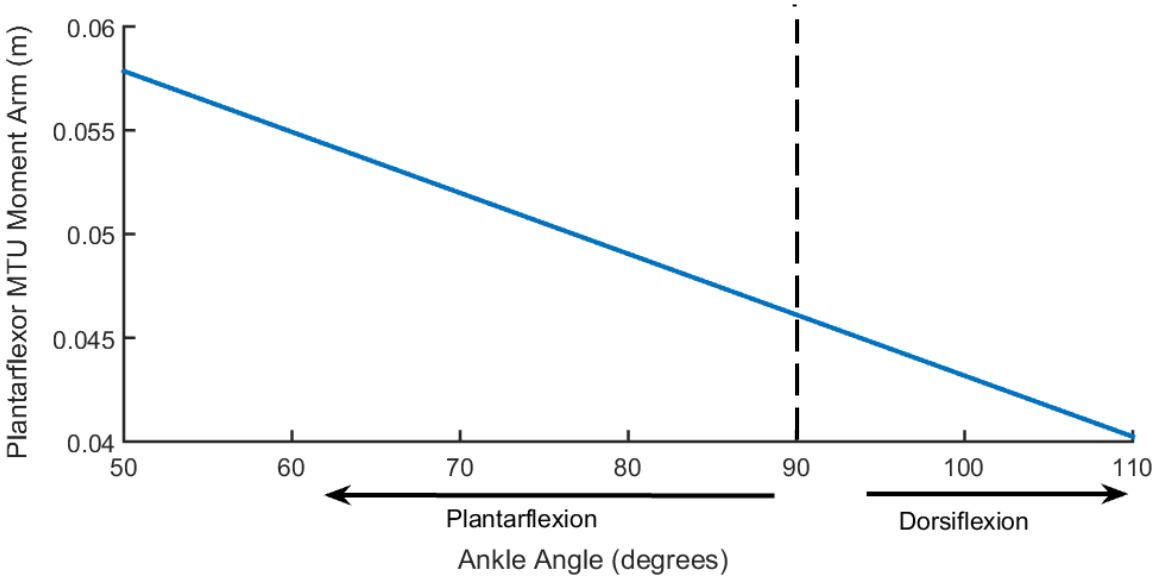

Figure C-1 The relationship between ankle angle and the Achilles tendon moment arm of the simulated muscles, obtained by differentiating the equation of Grieve et al. (1978) with respect to ankle angle.

The sensitivity analysis of the muscle model's parameters used values that spanned a range of values found in the literature. These values and their sources are shown in Table C-1 and Table C-2.

Table C-1 Soleus muscle parameters used in the sensitivity analysis. $l_{f,opt}$ = optimal fiber length, l_{t0} = tendon slack length, w = width of force-length relationship curve, c = tendon strain at maximum isometric muscle force, $v_{f,max}$ = maximum unloaded fiber shortening velocity, k = force-velocity curvature parameter, $F_{m,max}$ = maximum isometric muscle force. Values from Arampatzis et al. (2005); Arnold et al. (2010); Domire and Challis (2007); Pandy et al. (1990); van Soest et al. (1993); Wakeling et al. (2012).

Soleus	**Values used in the sensitivity analysis**			
$\boldsymbol{l_{f,opt}}$ (m)	0.034	0.044	0.055	0.076
$\boldsymbol{l_{t0}}$ (m)	0.226	0.246	0.282	0.360
$\boldsymbol{w}$ (−)	0.336	0.56	0.784	
$\boldsymbol{c}$ (−)	0.04	0.05	0.06	0.08
$\boldsymbol{v_{f,max}}$ $(\boldsymbol{l_{f,opt}/s})$	6	8	10	12.7
$\boldsymbol{k}$ (−)	2.44	4	6.25	6.67
$\boldsymbol{\alpha}$ (−)	1	2	3	4

Table C-2 Gastrocnemius muscle parameters used in the sensitivity analysis. $l_{f,opt}$ = optimal fiber length, l_{t0} = tendon slack length, w = width of force-length relationship curve, c = tendon strain at maximum isometric muscle force, $v_{f,max}$ = maximum unloaded fiber shortening velocity, k = force-velocity curvature parameter, $F_{m,max}$ = maximum isometric muscle force. Values from Anderson & Pandy (1999); Arampatzis et al. (2005); Arnold et al. (2010); Challis (2004); Domire and Challis (2007); Lichtwark and Wilson, (2007); Nagano & Gerritsen (2001); Out et al. (1996); Pandy et al. (1990); van Soest et al. (1993); Wakeling et al. (2012).

Gastrocnemius	**Values used in the sensitivity analysis**			
$\boldsymbol{l_{f,opt}}$ (m)	0.044	0.05	0.055	0.062
$\boldsymbol{l_{t0}}$ (m)	0.237	0.350	0.395	0.401
$\boldsymbol{w}$ (−)	0.336	0.56	0.784	
$\boldsymbol{c}$ (−)	0.04	0.05	0.06	0.08
$\boldsymbol{v_{f,max}}$ $(\boldsymbol{l_{f,opt}/s})$	6	8	10	12.7
$\boldsymbol{k}$ (−)	2.44	4	4.34	5
$\boldsymbol{\alpha}$ (−)	1	2	3	4

References

Anderson, F.C., Pandy, M.G., 1999. A dynamic optimization solution for vertical jumping in three dimensions. Comput Methods Biomech Biomed Engin 2, 201–231.

Arampatzis, A., Stafilidis, S., DeMonte, G., Karamanidis, K., Morey-Klapsing, G., Brüggemann, G.P., 2005. Strain and elongation of the human gastrocnemius tendon and aponeurosis during maximal plantarflexion effort. Journal of Biomechanics 38, 833–841.

Arnold, E.M., Ward, S.R., Lieber, R.L., Delp, S.L., 2010. A model of the lower limb for analysis of human movement. Ann Biomed Eng 38, 269–279.

Challis, J.H., 2004. Examination of the scaling of human jumping. J Strength Cond Res 18, 803–809.

Domire, Z.J., Challis, J.H., 2007. The influence of squat depth on maximal vertical jump performance. J Sports Sci 25, 193–200.

Fitzhugh, R., 1977. A model of optimal voluntary muscular control. J. Math. Biology 4, 203–236.

Hill, A.V., 1938. The Heat of Shortening and the Dynamic Constants of Muscle. Proceedings of the Royal Society of London. Series B, Biological Sciences 126, 136–195.

Grieve, D.W., Pheasant, S., Cavanagh, P.R., 1978. Prediction of gastrocnemius length from knee and ankle posture, in: Jorgenson, K. (Ed.), Biomechanics VI-A. University Park Press, Baltimore, MD, pp. 405–412.

Lichtwark, G.A., Wilson, A.M., 2007. Is Achilles tendon compliance optimised for maximum muscle efficiency during locomotion? J Biomech 40, 1768–1775.

Nagano, A., Gerritsen, K.G., 2001. Effects of neuromuscular strength training on vertical jumping performance—a computer simulation study. J Appl Biomech 17, 113–128.

Out, L., Vrijkotte, T.G.M., van Soest, A.J., Bobbert, M.F., 1996. Influence of the parameters of a human triceps surae muscle model on the isometric torque-angle relationship. J Biomech Eng 118, 17–25.

Pandy, M.G., Zajac, F.E., Sim, E., Levine, W.S., 1990. An optimal control model for maximum-height human jumping. J Biomech 23, 1185–1198.

van Soest, A.J., Schwab, A.L., Bobbert, M.F., van Ingen Schenau, G.J., 1993. The influence of the biarticularity of the gastrocnemius muscle on vertical-jumping achievement. J Biomech 26, 1–8.

Wakeling, J.M., Lee, S.S.M., Arnold, A.S., de Boef Miara, M., Biewener, A.A., 2012. A muscle's force depends on the recruitment patterns of its fibers. Ann Biomed Eng 40, 1708–1720.

Compiled References

Albracht, K., Arampatzis, A., 2013. Exercise-induced changes in triceps surae tendon stiffness and muscle strength affect running economy in humans. Eur. J. Appl. Physiol. 113, 1605–1615.

Alexander, R.M., Bennet-Clark, H.C., 1977. Storage of elastic strain energy in muscle and other tissues. Nature 265, 114–117.

Anderson, F.C., Pandy, M.G., 1999. A dynamic optimization solution for vertical jumping in three dimensions. Comput. Methods Biomech. Biomed. Engin. 2, 201–231.

Arndt, A., Bengtsson, A.-S., Peolsson, M., Thorstensson, A., Movin, T., 2012. Non-uniform displacement within the Achilles tendon during passive ankle joint motion. Knee Surg. Sports Traumatol. Arthrosc. 20, 1868–1874.

Arndt, A., Wolf, P., Liu, A., Nester, C., Stacoff, A., Jones, R., Lundgren, P., Lundberg, A., 2007. Intrinsic foot kinematics measured in vivo during the stance phase of slow running. J. Biomech. 40, 2672–2678.

Arnold, E.M., Delp, S.L., 2011. Fibre operating lengths of human lower limb muscles during walking. Philos. Trans. R. Soc. B Biol. Sci. 366, 1530–1539.

Arnold, J.B., Caravaggi, P., Fraysse, F., Thewlis, D., Leardini, A., 2017. Movement coordination patterns between the foot joints during walking. J. Foot Ankle Res. 10, 47.

Azizi, E., Brainerd, E.L., Roberts, T.J., 2008. Variable gearing in pennate muscles. Proc. Natl. Acad. Sci. 105, 1745–1750.

Azizi, E., Roberts, T.J., 2014. Geared up to stretch: pennate muscle behavior during active lengthening. J. Exp. Biol. 217, 376–381.

Barre, A., Armand, S., 2014. Biomechanical ToolKit: Open-source framework to visualize and process biomechanical data. Comput. Methods Programs Biomed. 114, 80–87.

Bhargava, L.J., Pandy, M.G., Anderson, F.C., 2004. A phenomenological model for estimating metabolic energy consumption in muscle contraction. J. Biomech. 37, 81–88.

Biewener, A.A., Konieczynski, D.D., Baudinette, R.V., 1998. In vivo muscle force-length behavior during steady-speed hopping in tammar wallabies. J. Exp. Biol. 201, 1681–1694.

Blackwood, C.B., Yuen, T.J., Sangeorzan, B.J., Ledoux, W.R., 2005. The Midtarsal Joint Locking Mechanism. Foot Ankle Int. 26, 1074–1080.

Blickhan, R., 1989. The spring-mass model for running and hopping. J. Biomech. 22, 1217–1227.

Bobbert, M.F., van Ingen Schenau, G.J., 1990. Isokinetic plantar flexion: Experimental results and model calculations. J. Biomech. 23, 105–119.

Bojsen-Møller, F., Lamoreux, L., 1979. Significance of free-dorsiflexion of the toes in walking. Acta Orthop. Scand. 50, 471–479.

Bruening, D.A., Cooney, K.M., Buczek, F.L., 2012. Analysis of a kinetic multi-segment foot model part II: Kinetics and clinical implications. Gait Posture 35, 535–540.

Buczek, F.L., Walker, M.R., Rainbow, M.J., Cooney, K.M., Sanders, J.O., 2006. Impact of mediolateral segmentation on a multi-segment foot model. Gait Posture 23, 519–522.

Cappellini, G., Ivanenko, Y.P., Poppele, R.E., Lacquaniti, F., 2006. Motor Patterns in Human Walking and Running. J. Neurophysiol. 95, 3426–3437.

Caravaggi, P., Pataky, T., Goulermas, J.Y., Savage, R., Crompton, R., 2009. A dynamic model of the windlass mechanism of the foot: evidence for early stance phase preloading of the plantar aponeurosis. J. Exp. Biol. 212, 2491–2499.

Caravaggi, P., Pataky, T., Günther, M., Savage, R., Crompton, R., 2010. Dynamics of longitudinal arch support in relation to walking speed: contribution of the plantar aponeurosis. J. Anat. 217, 254–261.

Carlson, R.E., Fleming, L.L., Hutton, W.C., 2000. The biomechanical relationship between the tendoachilles, plantar fascia and metatarsophalangeal joint dorsiflexion angle. Foot Ankle Int. 21, 18–25.

Carrier, D.R., Heglund, N.C., Earls, K.D., 1994. Variable gearing during locomotion in the human musculoskeletal system. Science 265, 651–653.

Carson, M.C., Harrington, M.E., Thompson, N., O'Connor, J.J., Theologis, T.N., 2001. Kinematic analysis of a multi-segment foot model for research and clinical applications: a repeatability analysis. J. Biomech. 34, 1299–1307.

Cavagna, G.A., Saibene, F.P., Margaria, R., 1964. Mechanical work in running. J. Appl. Physiol. 19, 249–256.

Challis, J.H., 2001. The Variability in Running Gait Caused by Force Plate Targeting. J. Appl. Biomech. 17, 77–83.

Challis, J.H., 1995. A procedure for determining rigid body transformation parameters. J. Biomech. 28, 733–737.

Chang, R., Van Emmerik, R., Hamill, J., 2008. Quantifying rearfoot–forefoot coordination in human walking. J. Biomech. 41, 3101–3105.

Delp, S.L., Anderson, F.C., Arnold, A.S., Loan, P., Habib, A., John, C.T., Guendelman, E., Thelen, D.G., 2007. OpenSim: Open-Source Software to Create and Analyze Dynamic Simulations of Movement. IEEE Trans. Biomed. Eng. 54, 1940–1950.

DeVita, P., Helseth, J., Hortobagyi, T., 2007. Muscles do more positive than negative work in human locomotion. J. Exp. Biol. 210, 3361–3373.

Dixon, P.C., Böhm, H., Döderlein, L., 2012. Ankle and midfoot kinetics during normal gait: A multi-segment approach. J. Biomech. 45, 1011–1016.

Duerinck, S., Hagman, F., Jonkers, I., Van Roy, P., Vaes, P., 2014. Forefoot deformation during stance: Does the forefoot collapse during loading? Gait Posture 39, 40–47.

Elftman, H., 1960. The transverse tarsal joint and its control. Clin. Orthop. 16, 41–46.

Elftman, H., 1940. The work done by muscles in running. Am. J. Physiol. 129, 672–684.

Erdemir, A., Hamel, A.J., Fauth, A.R., Piazza, S.J., Sharkey, N.A., 2004. Dynamic loading of the plantar aponeurosis in walking. J. Bone Jt. Surg. 86, 546–552.

Erdemir, A., Piazza, S.J., 2002. Rotational foot placement specifies the lever arm of the ground reaction force during the push-off phase of walking initiation. Gait Posture 15, 212–219.

Farris, D.J., Sawicki, G.S., 2012a. The mechanics and energetics of human walking and running: a joint level perspective. J. R. Soc. Interface 9, 110–118.

Farris, D.J., Sawicki, G.S., 2012b. Human medial gastrocnemius force–velocity behavior shifts with locomotion speed and gait. Proc. Natl. Acad. Sci. 109, 977–982.

Fenn, W.O., 1923. A quantitative comparison between the energy liberated and the work performed by the isolated sartorius muscle of the frog. J. Physiol. 58, 175–203.

Fenn, W.O., Marsh, B.S., 1935. Muscular force at different speeds of shortening. J. Physiol. 85, 277–297.

Fitzhugh, R., 1977. A model of optimal voluntary muscular control. J. Math. Biol. 4, 203–236.

Franz, J.R., Slane, L.C., Rasske, K., Thelen, D.G., 2015. Non-uniform in vivo deformations of the human Achilles tendon during walking. Gait Posture 41, 192–197.

Friederich, J.A., Brand, R.A., 1990. Muscle fiber architecture in the human lower limb. J. Biomech. 23, 91–95.

Fukunaga, T., Roy, R.R., Shellock, F.G., Hodgson, J.A., Day, M.K., Lee, P.L., Kwong-Fu, H., Edgerton, V.R., 1992. Physiological cross-sectional area of human leg muscles based on magnetic resonance imaging. J. Orthop. Res. Off. Publ. Orthop. Res. Soc. 10, 928–934.

Goldmann, J.-P., Brüggemann, G.-P., 2012. The potential of human toe flexor muscles to produce force. J. Anat. 221, 187–194.

Grabiner, M.D., Feuerbach, J.W., Lundin, T.M., Davis, B.L., 1995. Visual guidance to force plates does not influence ground reaction force variability. J. Biomech. 28, 1115–1117.

Gregoire, L., Veeger, H.E., Huijing, P.A., van Ingen Schenau, G.J., 1984. Role of mono- and biarticular muscles in explosive movements. Int. J. Sports Med. 5, 301–305.

Grieve, D.W., Pheasant, S., Cavanagh, P.R., 1978. Prediction of gastrocnemius length from knee and ankle posture, in: Jorgenson, K. (Ed.), Biomechanics VI-A. University Park Press, Baltimore, MD, pp. 405–412.

Grood, E.S., Suntay, W.J., 1983. A Joint Coordinate System for the Clinical Description of Three-Dimensional Motions: Application to the Knee. J. Biomech. Eng. 105, 136–144.

Hamner, S.R., Seth, A., Delp, S.L., 2010. Muscle contributions to propulsion and support during running. J. Biomech. 43, 2709–2716.

Herbert, R.D., Moseley, A.M., Butler, J.E., Gandevia, S.C., 2002. Change in length of relaxed muscle fascicles and tendons with knee and ankle movement in humans. J. Physiol. 539, 637–645.

Herzog, W., Read, L.J., ter Keurs, H.E.D.J., 1991. Experimental determination of force—length relations of intact human gastrocnemius muscles. Clin. Biomech. 6, 230–238.

Hicks, J.H., 1954. The mechanics of the foot. II. The plantar aponeurosis and the arch. J. Anat. 88, 25-30.1.

Hicks, J.L., Uchida, T.K., Seth, A., Rajagopal, A., Delp, S.L., 2015. Is my model good enough? Best practices for verification and validation of musculoskeletal models and simulations of movement. J. Biomech. Eng. 137, 020905.

Hill, A.V., 1938. The Heat of Shortening and the Dynamic Constants of Muscle. Proc. R. Soc. Lond. B Biol. Sci. 126, 136–195.

Hof, A.L., Van Zandwijk, J.P., Bobbert, M.F., 2002. Mechanics of human triceps surae muscle in walking, running and jumping. Acta Physiol. Scand. 174, 17–30.

Hofmann, C.L., Okita, N., Sharkey, N.A., 2013. Experimental evidence supporting isometric functioning of the extrinsic toe flexors during gait. Clin. Biomech. 28, 686–691.

Holt, N.C., Roberts, T.J., Askew, G.N., 2014. The energetic benefits of tendon springs in running: is the reduction of muscle work important? J. Exp. Biol. 217, 4365–4371.

Hudson, J.L., 1986. Coordination of segments in the vertical jump. Med. Sci. Sports Exerc. 18, 242–251.

Hui, H.J., Beals, T.C., Brown, N.A.T., 2007. Influence of tendon transfer site on moment arms of the flexor digitorum longus muscle. Foot Ankle Int. 28, 441–447.

Inman, V.T., 1976. The joints of the ankle. Williams & Wilkins, Baltimore.

Ishikawa, M., Komi, P.V., 2007. The role of the stretch reflex in the gastrocnemius muscle during human locomotion at various speeds. J. Appl. Physiol. 103, 1030–1036.

Ishikawa, M., Komi, P.V., Grey, M.J., Lepola, V., Bruggemann, G.-P., 2005. Muscle-tendon interaction and elastic energy usage in human walking. J. Appl. Physiol. 99, 603–608.

Ishikawa, M., Pakaslahti, J., Komi, P.V., 2007. Medial gastrocnemius muscle behavior during human running and walking. Gait Posture 25, 380–384.

Isman, R.E., Inman, V.T., 1969. Anthropometric studies of the foot and ankle. Bull. Prosthetics Res.

Iwanuma, S., Akagi, R., Hashizume, S., Kanehisa, H., Yanai, T., Kawakami, Y., 2011a. Triceps surae muscle–tendon unit length changes as a function of ankle joint angles and contraction levels: The effect of foot arch deformation. J. Biomech. 44, 2579–2583.

Iwanuma, S., Akagi, R., Hashizume, S., Kanehisa, H., Yanai, T., Kawakami, Y., 2011b. Triceps surae muscle-tendon unit length changes as a function of ankle joint angles and contraction levels: the effect of foot arch deformation. J. Biomech. 44, 2579–2583.

Katz, B., 1939. The relation between force and speed in muscular contraction. J. Physiol. 96, 45–64.

Kelly, L.A., Cresswell, A.G., Racinais, S., Whiteley, R., Lichtwark, G., 2014. Intrinsic foot muscles have the capacity to control deformation of the longitudinal arch. J. R. Soc. Interface 11, 20131188.

Kelly, L.A., Lichtwark, G.A., Farris, D.J., Cresswell, A., 2016. Shoes alter the spring-like function of the human foot during running. J. R. Soc. Interface 13, 20160174.

Ker, R.F., 1996. The time-dependent mechanical properties of the human heel pad in the context of locomotion. J. Exp. Biol. 199, 1501–1508.

Ker, R.F., Bennett, M.B., Bibby, S.R., Kester, R.C., Alexander, R.M., 1987. The spring in the arch of the human foot. Nature 325, 147–149.

Klein, P., Mattys, S., Rooze, M., 1996. Moment arm length variations of selected muscles acting on talocrural and subtalar joints during movement: An In vitro study. J. Biomech. 29, 21–30.

Komi, P.V., 1990. Relevance of in vivo force measurements to human biomechanics. J. Biomech. 23, Supplement 1, 23–34.

Kyrolainen, H., Komi, P.V., Belli, A., 1999. Changes in muscle activity patterns and kinetics with increasing running speed. J. Strength Cond. Res. 13, 400–406.

Lai, A., Lichtwark, G.A., Schache, A.G., Lin, Y.-C., Brown, N.A.T., Pandy, M.G., 2015. In vivo behavior of the human soleus muscle with increasing walking and running speeds. J. Appl. Physiol. 118, 1266–1275.

Lai, A., Schache, A.G., Lin, Y.-C., Pandy, M.G., 2014. Tendon elastic strain energy in the human ankle plantar-flexors and its role with increased running speed. J. Exp. Biol. 217, 3159–3168.

Leardini, A., Benedetti, M.G., Berti, L., Bettinelli, D., Nativo, R., Giannini, S., 2007. Rear-foot, mid-foot and fore-foot motion during the stance phase of gait. Gait Posture 25, 453–462.

Lichtwark, G.A., Wilson, A.M., 2008. Optimal muscle fascicle length and tendon stiffness for maximising gastrocnemius efficiency during human walking and running. J. Theor. Biol. 252, 662–673.

Lichtwark, G.A., Wilson, A.M., 2007. Is Achilles tendon compliance optimised for maximum muscle efficiency during locomotion? J. Biomech. 40, 1768–1775.

Lichtwark, G.A., Wilson, A.M., 2006. Interactions between the human gastrocnemius muscle and the Achilles tendon during incline, level and decline locomotion. J. Exp. Biol. 209, 4379–4388.

Lundgren, P., Nester, C., Liu, A., Arndt, A., Jones, R., Stacoff, A., Wolf, P., Lundberg, A., 2008. Invasive in vivo measurement of rear-, mid- and forefoot motion during walking. Gait Posture 28, 93–100.

MacWilliams, B.A., Cowley, M., Nicholson, D.E., 2003. Foot kinematics and kinetics during adolescent gait. Gait Posture 17, 214–224.

Maganaris, C.N., 2003. Force-length characteristics of the in vivo human gastrocnemius muscle. Clin. Anat. N. Y. N 16, 215–223.

Maganaris, C.N., Paul, J.P., 2002. Tensile properties of the in vivo human gastrocnemius tendon. J. Biomech. 35, 1639–1646.

Mann, R., Inman, V.T., 1964. Phasic Activity of Intrinsic Muscles of the Foot. J. Bone Jt. Surg. 46, 469–481.

McDonald, K.A., Stearne, S.M., Alderson, J.A., North, I., Pires, N.J., Rubenson, J., 2016. The Role of Arch Compression and Metatarsophalangeal Joint Dynamics in Modulating Plantar Fascia Strain in Running. PLOS ONE 11, e0152602.

Miyazaki, S., Yamamoto, S., 1993. Moment acting at the metatarsophalangeal joints during normal barefoot level walking. Gait Posture 1, 133–140.

Nester, C.J., Jones, R.K., Liu, A., Howard, D., Lundberg, A., Arndt, A., Lundgren, P., Stacoff, A., Wolf, P., 2007a. Foot kinematics during walking measured using bone and surface mounted markers. J. Biomech. 40, 3412–3423.

Nester, C.J., Liu, A.M., Ward, E., Howard, D., Cocheba, J., Derrick, T., 2010. Error in the description of foot kinematics due to violation of rigid body assumptions. J. Biomech. 43, 666–672.

Nester, C.J., Liu, A.M., Ward, E., Howard, D., Cocheba, J., Derrick, T., Patterson, P., 2007b. In vitro study of foot kinematics using a dynamic walking cadaver model. J. Biomech. 40, 1927–1937.

Oh, K., Park, S., 2017. The bending stiffness of shoes is beneficial to running energetics if it does not disturb the natural MTP joint flexion. J. Biomech. 53, 127–135.

Okita, N., Meyers, S.A., Challis, J.H., Sharkey, N.A., 2013. Midtarsal joint locking: New perspectives on an old paradigm. J. Orthop. Res. 110–115.

Okita, N., Meyers, S.A., Challis, J.H., Sharkey, N.A., 2009. An objective evaluation of a segmented foot model. Gait Posture 30, 27–34.

Out, L., Vrijkotte, T.G.M., van Soest, A.J., Bobbert, M.F., 1996. Influence of the parameters of a human triceps surae muscle model on the isometric torque-angle relationship. J. Biomech. Eng. 118, 17–25.

Pain, M.T.G., Challis, J.H., 2001. The role of the heel pad and shank soft tissue during impacts: a further resolution of a paradox. J. Biomech. 34, 327–333.

Pataky, T.C., 2012. One-dimensional statistical parametric mapping in Python. Comput. Methods Biomech. Biomed. Engin. 15, 295–301.

Pataky, T.C., 2010. Generalized n-dimensional biomechanical field analysis using statistical parametric mapping. J. Biomech. 43, 1976–1982.

Pataky, T.C., Robinson, M.A., Vanrenterghem, J., 2013. Vector field statistical analysis of kinematic and force trajectories. J. Biomech. 46, 2394–2401.

Pothrat, C., Authier, G., Viehweger, E., Berton, E., Rao, G., 2015. One- and multi-segment foot models lead to opposite results on ankle joint kinematics during gait: Implications for clinical assessment. Clin. Biomech. 30, 493–499.

Prilutsky, B.I., Zatsiorsky, V.M., 1994. Tendon action of two-joint muscles: Transfer of mechanical energy between joints during jumping, landing, and running. J. Biomech. 27, 25–34.

Redmond, A.C., Crosbie, J., Ouvrier, R.A., 2006. Development and validation of a novel rating system for scoring standing foot posture: The Foot Posture Index. Clin. Biomech. 21, 89–98.

Refshauge, K.M., Chan, R., Taylor, J.L., McCloskey, D.I., 1995. Detection of movements imposed on human hip, knee, ankle and toe joints. J. Physiol. 488, 231–241.

Roberts, T.J., Marsh, R.L., Weyand, P.G., Taylor, C.R., 1997. Muscular force in running turkeys: The Economy of minimizing work. Science 275, 1113–5.

Robertson, D.G.E., Winter, D.A., 1980. Mechanical energy generation, absorption and transfer amongst segments during walking. J. Biomech. 13, 845–854.

Rubenson, J., Henry, H.T., Dimoulas, P.M., Marsh, R.L., 2006. The cost of running uphill: linking organismal and muscle energy use in guinea fowl (Numida meleagris). J. Exp. Biol. 209, 2395–2408.

Rubenson, J., Lloyd, D.G., Heliams, D.B., Besier, T.F., Fournier, P.A., 2011. Adaptations for economical bipedal running: the effect of limb structure on three-dimensional joint mechanics. J. R. Soc. Interface 8, 740–755.

Rubenson, J., Pires, N.J., Loi, H.O., Pinniger, G.J., Shannon, D.G., 2012. On the ascent: the soleus operating length is conserved to the ascending limb of the force–length curve across gait mechanics in humans. J. Exp. Biol. 215, 3539–3551.

Scott, S.H., Winter, D.A., 1993. Biomechanical model of the human foot: Kinematics and kinetics during the stance phase of walking. J. Biomech. 26, 1091–1104.

Scovil, C.Y., Ronsky, J.L., 2006. Sensitivity of a Hill-based muscle model to perturbations in model parameters. J. Biomech. 39, 2055–2063.

Shaw, H.M., Vázquez, O.T., McGonagle, D., Bydder, G., Santer, R.M., Benjamin, M., 2008. Development of the human Achilles tendon enthesis organ. J. Anat. 213, 718–724.

Siegel, K.L., Kepple, T.M., Caldwell, G.E., 1996. Improved agreement of foot segmental power and rate of energy change during gait: Inclusion of distal power terms and use of three-dimensional models. J. Biomech. 29, 823–827.

Slane, L.C., Thelen, D.G., 2014. Non-uniform displacements within the Achilles tendon observed during passive and eccentric loading. J. Biomech. 47, 2831–2835.

Smith, G., Lake, M., Lees, A., Worsfold, P., 2012. Measurement procedures affect the interpretation of metatarsophalangeal joint function during accelerated sprinting. J. Sports Sci. 30, 1521–1527.

Snow, S.W., Bohne, W.H., DiCarlo, E., Chang, V.K., 1995. Anatomy of the Achilles tendon and plantar fascia in relation to the calcaneus in various age groups. Foot Ankle Int. Am. Orthop. Foot Ankle Soc. Swiss Foot Ankle Soc. 16, 418–421.

Stearne, S.M., Alderson, J.A., Green, B.A., Donnelly, C.J., Rubenson, J., 2014. Joint kinetics in rearfoot versus forefoot running: implications of switching technique. Med. Sci. Sports Exerc. 46, 1578–1587.

Stearne, S.M., McDonald, K.A., Alderson, J.A., North, I., Oxnard, C.E., Rubenson, J., 2016. The Foot's Arch and the Energetics of Human Locomotion. Sci. Rep. 6, 19403.

Stecco, C., Corradin, M., Macchi, V., Morra, A., Porzionato, A., Biz, C., De Caro, R., 2013. Plantar fascia anatomy and its relationship with Achilles tendon and paratenon. J. Anat. 223, 665–676.

Stefanyshyn, D.J., Nigg, B.M., 1997. Mechanical energy contribution of the metatarsophalangeal joint to running and sprinting. J. Biomech. 30, 1081–1085.

Takahashi, K.Z., Kepple, T.M., Stanhope, S.J., 2012. A unified deformable (UD) segment model for quantifying total power of anatomical and prosthetic below-knee structures during stance in gait. J. Biomech. 45, 2662–2667.

Takahashi, K.Z., Stanhope, S.J., 2013. Mechanical energy profiles of the combined ankle–foot system in normal gait: Insights for prosthetic designs. Gait Posture 38, 818–823.

Takahashi, K.Z., Worster, K., Bruening, D.A., 2017. Energy neutral: the human foot and ankle subsections combine to produce near zero net mechanical work during walking. Sci. Rep. 7, 15404.

Tulchin, K., Orendurff, M., Adolfsen, S., Karol, L., 2009. The Effects of Walking Speed on Multisegment Foot Kinematics in Adults. J. Appl. Biomech. 25, 377–386.

Tulchin, K., Orendurff, M., Karol, L., 2010. The effects of surface slope on multi-segment foot kinematics in healthy adults. Gait Posture 32, 446–450.

Umberger, B.R., 2010. Stance and swing phase costs in human walking. J. R. Soc. Interface 7, 1329–1340.

Umberger, B.R., Gerritsen, K.G.M., Martin, P.E., 2003. A model of human muscle energy expenditure. Comput. Methods Biomech. Biomed. Engin. 6, 99–111.

Van Ingen Schenau, G.J., 1989. From rotation to translation: Constraints on multi-joint movements and the unique action of bi-articular muscles. Hum. Mov. Sci. 8, 301–337.

Wager, J.C., Challis, J.H., 2016. Elastic energy within the human plantar aponeurosis contributes to arch shortening during the push-off phase of running. J. Biomech. 49, 704–709.

Ward, S.R., Eng, C.M., Smallwood, L.H., Lieber, R.L., 2009. Are Current Measurements of Lower Extremity Muscle Architecture Accurate? Clin. Orthop. Relat. Res. Rosemt. 467, 1074–82.

Wearing, S.C., Hooper, S.L., Dubois, P., Smeathers, J.E., Dietze, A., 2014. Force-deformation properties of the human heel pad during barefoot walking. Med. Sci. Sports Exerc. 46, 1588–1594.

Wearing, S.C., Urry, S.R., Smeathers, J.E., 2000. The effect of visual targeting on ground reaction force and temporospatial parameters of gait. Clin. Biomech. 15, 583–591.

Wickiewicz, T.L., Roy, R.R., Powell, P.L., Edgerton, V.R., 1983. Muscle architecture of the human lower limb. Clin. Orthop. 275–283.

Wickiewicz, T.L., Roy, R.R., Powell, P.L., Perrine, J.J., Edgerton, V.R., 1984. Muscle architecture and force-velocity relationships in humans. J. Appl. Physiol. 57, 435–443.

Winter, D.A., 2009. Biomechanics and Motor Control of Human Movement, 4th ed. John Wiley & Sons, Inc., Hoboken, NJ.

Winter, D.A., 1983. Moments of force and mechanical power in jogging. J. Biomech. 16, 91–97.

Winter, S.L., Challis, J.H., 2008. Reconstruction of the human gastrocnemius force-length curve in vivo: part 2-experimental results. J. Appl. Biomech. 24, 207–214.

Wolf, P., Stacoff, A., Liu, A., Nester, C., Arndt, A., Lundberg, A., Stuessi, E., 2008. Functional units of the human foot. Gait Posture 28, 434–441.

Wren, T.A.L., Yerby, S.A., Beaupré, G.S., Carter, D.R., 2001. Mechanical properties of the human achilles tendon. Clin. Biomech. 16, 245–251.

Zatsiorsky, V.M., 2002. Kinetics of Human Motion. Human Kinetics, Champaign, IL.

Zelik, K.E., Adamczyk, P.G., 2016. A unified perspective on ankle push-off in human walking. J. Exp. Biol. 219, 3676–3683.

Zelik, K.E., Honert, E.C., 2018. Ankle and foot power in gait analysis: Implications for science, technology and clinical assessment. J. Biomech. 75, 1–12.

Zelik, K.E., Takahashi, K.Z., Sawicki, G.S., 2015. Six degree-of-freedom analysis of hip, knee, ankle and foot provides updated understanding of biomechanical work during human walking. J. Exp. Biol. 218, 876–886.

Vita

EDUCATION

2019 **The Pennsylvania State University**, Ph.D. Kinesiology
Emphasis: Biomechanics
Advisor: Dr. John H. Challis

2015 **The Pennsylvania State University**, M.S. Kinesiology

2010 **State University of New York College at Cortland**, B.S. Kinesiology

PUBLICATIONS

Refereed journal articles

Wager, J.C., & Challis, J. H. (2016). Elastic energy within the human plantar aponeurosis contributes to arch shortening during the push-off phase of running. Journal of Biomechanics, 49(5), 704–709.

Selected conference proceedings

Knausenberger, A., **Wager, J.C.**, Moran, M.F. (2019). Immediate effects of a textured insole on running biomechanics. 66th Annual Meeting of the American College of Sports Medicine.

Wager, J.C., & Challis J.H. (2017). Differences in the active state of a simulated ankle muscle using two foot models. 41st Annual Meeting of the American Society of Biomechanics.

Wager, J.C., & Challis J.H. (2016). Multisegment and single segment foot models produce different ankle joint power during running. 40th Annual Meeting of the American Society of Biomechanics.

Wager, J.C., & Challis J.H. (2015). Assessment of the contributions of elastic energy in the human plantar aponeurosis. 39th Annual Meeting of the American Society of Biomechanics. [Journal of Biomechanics Award]

RESEARCH AWARDS

Journal of Biomechanics Award
2015 Meeting of the American Society of Biomechanics
Awarded for "substantive and conceptually novel mechanics approaches explaining how biological systems function"

Runner-up, Best Poster Presentation - Health & Life Sciences
2015 Graduate Exhibition, The Pennsylvania State University
Awarded for communication of research to a general audience